

Lappeenrannan teknillinen yliopisto
Teknillinen tiedekunta. Konetekniikan osasto
Tutkimusraportti 74

Lappeenranta University of Technology
Faculty of Technology. Department of Mechanical Engineering.
Research report 74

Rahamathunnisa Muhammad Azam
Mari Tanttari
Tommi Kääriäinen
David Cameron

Coatings on Composites

Lappeenranta University of Technology
Faculty of Technology. Department of Mechanical Engineering
Advanced Surface Technology Research Laboratory
Prikaatinkatu 3 E
50100 Mikkeli

ISBN 978-952-214-504-8
ISSN 1459-2932

Mikkeli 2007

PREFACE

Coatings on composites (COATCOM) –project has been carried out during the years 2004 – 2007 by Advanced Surface Technology Research Laboratory (ASTRaL) in the Lappeenranta University of Technology. The project was carried out by researchers Rahamathunnisa Muhammad Azam and Mari Tanttari, project manager Tommi Kääriäinen and project director professor David Cameron.

The goal of the project was to study the application of magnetron sputtered thin film coatings on to carbon and glass fibre composite materials. The work was distributed into two themes. In the basic research part, the general aspects of magnetron sputtered coatings on composite materials have been investigated whereas in the specific studies these coatings have been applied to the specific composite products and their performance has been tested.

The project was funded through the European regional development fund (EAKR) and coordinated by Finnish technology agency (TEKES).The project was also funded by Exel Oyj, Fibrocom Oy, Metso Paper Oy and Savcor Coatings Oy. Mikkeli technology center Miktech Oy supported the project as a limited partner.

ASTRaL acknowledges the project steering group who followed up the project work and progress. Steering group consisted of the following members: Technology expert Timo Alasuvanto Tekes, Senior Vice President R&D Jukka Juselius and product manager Harri Matilainen from Exel Oyj, managing director Mauri Laitinen from Fibrocom Oy, R&D manager Samppa Ahmaniemi and R&D engineer Ville Eronen from Metso Paper Oyj, Senior Vice President Kaj Pischow and researcher T.K. Subramanyam from Savcor Coatings Oy, and managing director Vesa Sorasahi, development director Jouko Lassila, project engineer Anne-Mari Mattila, development manager Harri Hinttala, development manager Tommi Luhtanen, development manager Pekka Peltomäki and development manager Juha Kauppinen from Mikkeli technology centre Oy.

ABSTRACT

Rahamathunnisa Muhammad Azam, Mari Tanttari, Tommi Kääriäinen and David Cameron:
Coatings on Composites.

Lappeenranta University of Technology
Faculty of Technology, Department of Mechanical Engineering
Research Report 74
November 2007

ISBN 978-952-214-504-8
ISSN 1459-2932

Keywords: Magnetron sputtering, thin film coatings, carbon fibre reinforced plastics, polymers

Polymer based composite materials coated with thin layers of wear resistant materials have been proposed as replacements for steel components for certain applications with the advantage of reduced mass. Magnetron sputtered coatings can be successfully deposited on composite materials. Nevertheless there are number of issues which must be addressed such as limited temperature, which the composite can withstand because of the epoxy binder which is used, the adhesion of the coating to the composite and the limited mechanical support, the hard coating can obtain from the relatively soft epoxy. We have investigated the deposition of chromium nitride, titanium carbide and titanium doped DLC coatings on carbon fibre reinforced composites and various polymers. The adhesion of the coatings has been studied by the pull-off adhesion tester. In general, the failure mechanism has been noticed to be due to the cohesive failure for a wide range of conditions. The wear behavior of the coatings has been noticed to be complicated. Wear tests on coated composites have shown that where the reinforcing fibres are near the surface, the composite samples do not perform well due to breakage of the fibres from the polymer matrix. A fibre free surface has been noticed to improve the wear resistance.

Table of content

PREFACE.....	2
ABSTRACT	3
Table of content	4
1 Introduction.....	6
2 Substrates.....	7
2.1 Carbon-fibre reinforced polymer composites (CFRP).....	7
2.2 Polymers.....	7
3 Vacuum Deposition Process	7
3.1 Physical Vapor Deposition Process	8
3.2 Sputter Deposition	8
3.2.1 Disadvantages of Sputter Deposition	9
3.3 Magnetron Sputtering	10
3.3.1 Balanced Magnetrons.....	10
3.3.2 Unbalanced Magnetrons.....	12
3.3.3 Reactive Magnetron Sputtering	13
3.3.4 Pulsed DC Magnetron Sputtering	13
4 Sputtering equipments	14
5 Wear resistant coatings.....	16
5.1 Chromium nitride coating.....	16
5.2 TiC and Ti doped DLC	17
6 Characterization techniques	18
6.1 X-Ray Diffraction (XRD).....	18
6.2 Raman spectroscopy	19
7 Mass spectrometer.....	20
7.1 Principle	20
7.2 Quadrupole Mass Analyzer.....	20
8 Adhesion of the films on carbon fibre composites and polymers.....	21
8.1 Adhesion as a phenomenon.....	21
8.2 The aim of the adhesion testing.....	22
8.3 Preparation of the Testing	22
8.4 Apparatus	22
8.5 The test method	23
8.6 Testing parameters.....	23
8.7 Adhesion tests for the plain substrates.....	24
8.8 Examination of the failures	25
8.9 Examination of parameters	27
9 Influence of different pre-treatments on substrate properties	31
9.1 Effect of ex-situ substrate pre-treatment.....	31
9.1.1 Contact angle and surface energy measurements	31
9.1.2 DMA studies - Effect of substrate chemical cleaning on bulk properties.....	32
9.2 Effect of in-situ substrate pre-treatment	34
9.2.1 Pre-treatment of substrates with different plasmas.....	35
9.2.2 Ion cleaning and bias voltage	36

9.3	Effect of substrate temperature.....	37
10	Effect of flux of ion energy bombardment on structure and mechanical properties of CrN.....	39
10.1	Experimental	39
10.2	Energy and flux of ions.....	41
10.3	Film structure and morphology	47
10.4	Film stress and mechanical properties.....	51
11	Characterization of films	52
11.1	Chromium nitride Coating on CFRP	52
11.2	Structural analysis.....	54
11.3	Determination of mechanical properties.....	55
11.4	Chromium nitride coating on polymers	55
11.4.1	Determination of Hardness and Young's modulus	57
11.5	DLC and Ti doped DLC coatings.....	58
11.5.1	Deposition Parameters – Frequency and Off-time of Pulse	58
11.5.2	Deposition Parameters – BIAS Voltage and Titanium Proportion	59
12	Wear-resistant behaviour of coating-composite combination	64
12.1	Abrasive wear performance of coated composites	64
12.2	Wear performance of polymers	66
12.3	Wear performance of single side coated CFRP component	66
13	Summary	72
	References	74

Appendix 1. Literature study

1 Introduction

Carbon and glass fibre composites are used for a wide range of industrial products. These materials can be fabricated into complex components but their performance in terms of abrasion and impact resistance is limited. In order to enhance their performance and thus extend their use into more products and other fields of use, their surface properties need to be enhanced.

Carbon Fibre Reinforced Plastics (CFRP) and Glass Fibre Reinforced Plastics (GFRP) are the composite materials where the thermoplastics such as polyamide, polypropylene and polycarbonate and thermosetting plastics such as epoxy, polyester, vinyl ester and phenol have been reinforced by carbon and glass fibres (reinforcements) in order to improve their properties such as mechanical strength and stiffness. Furthermore the small particles so called additives are added to the composites for further improvements of their properties and facilitate their manufacturing. Usually the total amount of reinforcements and additives in composite is between the 30-70 weight percent.

Polymer based composite materials have relatively low temperature resistance. Due to this there are only a few suitable coating methods that can be used for metal and ceramic deposition on composite materials. The size and the shape of the product will also put a limitation on the coating methods. The functional parts in the paper machine which need tribological improvements can be over 10 meters long and might have very complex shapes (scraper blade holder). The coating methods mainly used for the composite materials are lamination and profiling (adhesive bonding), lacquering, thermal spraying, physical vapor deposition and electroless-electrolytic plating[1]All of these methods can be divided to the sub categories where the coating methods have their own features and effects on the substrate and coating performance.

Magnetron sputtering of wear and erosion resistant thin surface coatings is a technique which has widespread application to a range of products. However deposition on to composite materials brings with it a number of new problems. In particular, the adhesion of the coating on to the resin-bound fibrous composite brings challenges in the mechanical and chemical mismatch between them. In this study the magnetron sputtering as a thin film deposition method and its capability for enhancing the properties of polymer based composites have been investigated.

2 Substrates

2.1 Carbon-fibre reinforced polymer composites (CFRP)

Carbon and glass fibre composites are used for a wide range of industrial products. These materials can be fabricated into complex shapes and components but their performance in terms of abrasion and impact resistance is limited. In recent studies, it has been observed that adding the fibers to the polymer matrix can deteriorate the tribological properties of the parent polymer [2]. In order to enhance their performance and thus extend their use into more products and other fields of use, their surface properties need to be enhanced.

The surface properties of a material can be enhanced by depositing a material over it having improved surface properties. Hard chrome plating was used in industry for many decades in applications requiring abrasive wear resistance, hardness and sliding properties. The high toxicity of galvanic bath and hexavalent chromium involved in this process are not environment friendly and the waste disposal costs a lot. The process might also require post baking of the plating and grinding of the uneven thick chrome layer that increases the cost further. Furthermore, during the chromium plating mainly chromium hydride is formed and at dissociation of the chromium-hydride (hexagonal structure), the body-centered cubic chromium is formed with a smaller volume than the chromium-hydride. As a result of the volume reduction, there are very high internal tensions in the deposit and from a certain layer thickness the deposit cracks. The low deposition rate and limited corrosion resistance also adds up to the disadvantages of chrome plating. Nitride coatings are found to replace hard chrome plating and have been deposited using vacuum deposition processes.

2.2 Polymers

Polymers like polymethyl methacrylate (PMMA), vinyl ester, polycarbonate (PC) and polyamide (PA) has also been analyzed in pursuit of better understanding film properties on different polymers that are very widely used in industries in various applications. Polycarbonate (PC) is thermally stable up to 190°C. However, PC demonstrates low hardness, low resistance to abrasion and poor chemical attack. Coated with amorphous carbon films, PC could improve in its mechanical, chemical properties and compatibility.

3 Vacuum Deposition Process

In a vacuum, gas pressure is less than the ambient atmospheric pressure. Plasma is a gaseous environment where there are enough ions and electrons for there to be appreciable electrical conductivity. Vacuum deposition is the deposition of a film or coating in a vacuum (or low pressure plasma) environment. Generally, the term is applied to processes that deposit atoms or molecules one at a time, such as in PVD or low pressure chemical vapor deposition (LPCVD)

processes. It can also be applied to other deposition processes such as low pressure plasma spraying (LPPS).

The vacuum in deposition processing increases the “mean free path” for collisions of atoms and high energy ions and helps reduce contamination to an acceptable level. When establishing plasma in a vacuum, the gas pressure plays an important role in the enthalpy, the density of charged and uncharged particles and the energy distribution of particles in the plasma. Plasma in a “good vacuum” provides a source of ions and electrons that may be accelerated to high energies in an electric field.

3.1 Physical Vapor Deposition Process

In PVD processing, these high energy ions can be used to sputter a surface as a source of deposition material (target) and/or bombard a growing film to modify the film properties. PVD processes are atomistic, where material vaporized from a solid or liquid source is transported as a vapor through a vacuum or low pressure gaseous or plasma environment. When it contacts the part, it condenses.

The vaporized material may be an element, alloy or compound. Some PVD processes can be used to deposit films of compound materials (reactive deposition) by the reaction of depositing material with the gas in the deposition environment (e.g., TiN, CrN) or with a co-depositing material such as TiC or even a combination of the two.

Typically, PVD processes are used to deposit films with thicknesses in the range of few nanometers to thousands of nanometers; however, they can be used to form multilayer coatings, thick deposits and free-standing structures.

3.2 Sputter Deposition

Sputter deposition is the deposition of particles vaporized from a surface (sputter target) by the physical sputtering process. Physical sputtering is a non-thermal vaporization process where surface atoms are physically ejected by a momentum transfer from an energetic bombarding particle that is usually a gaseous ion accelerated from plasma or an “ion gun.” This PVD process is often called sputtering.

Sputter deposition can be performed in a vacuum or low pressure gas (< 5 mTorr) where energetic particles that are sputtered or reflected from the sputtering target are “thermalized” by gas-phase collisions before they reach the substrate.

Depending on the ion source used, two techniques have been developed namely ion beam sputtering and glow discharge sputtering. Glow discharge sputtering is most convenient because of the precise control of the chemical composition and physical properties of the films using a large number of sputtering parameters. The glow discharge can be set up by applying dc or RF voltage between the sputter target and the substrate.

In dc sputtering, the target must be electrically conducting. Insulating targets being non-conductors, develop a space charge around themselves during dc sputtering leading to a drop in the sputtering yield (i.e., the ratio of atoms ejected from the target surface per incident ion) since no atoms can get through the target. As the time available is insufficient to form a space charge on the target in RF sputtering, insulating as well as electrically conducting surfaces can be easily sputtered.

Advantages of Sputter Deposition

- Elements, alloys and compounds can be sputtered and deposited
- The sputtering target provides a stable, long-lived vaporization source
- In some configurations, the sputtering source can be a defined shape such as a line or the surface of a rod or a cylinder
- In some configurations, reactive deposition can be easily accomplished using reactive gaseous species that are activated in plasma
- There is very little heat in the deposition process
- The source and the substrate can be spaced close together
- The sputter deposition chamber can have a small volume
- The average arrival energy at the substrate surface is higher for sputtered atoms (about 10 eV) than for evaporated atoms (about 0.25 eV at 3000K) and there is an enhanced adhesion of the sputtered deposited films on the surface of the substrate

3.2.1 *Disadvantages of Sputter Deposition*

- In many configurations, the deposition flux distribution is non-uniform, requiring moving fixturing to obtain films of uniform thickness
- Sputtering targets are often expensive and material use may be poor
- Most of the energy incident on the target becomes heat, which must be removed
- In some cases, gaseous contaminants are “activated” in the plasma, making film contamination
- In reactive sputter deposition, the gas composition must be carefully controlled to prevent poisoning the sputtering target

Sputter deposition is widely used to deposit thin film metallization on semi-conductor material, coatings on architectural glass, reflective coating on polymers, magnetic films for storage media, transparent electrically conductive films on glass and flexible webs, dry-film lubricants, wear resistant coating on tools and decorative coatings.

3.3 Magnetron Sputtering

3.3.1 *Balanced Magnetrons*

Magnetron sputtering is the most widely used variant of DC sputtering. In a dc glow discharge, the secondary electrons leaving the cathode travel straight to the anode (generally the substrate) taking the shortest path. If it undergoes collisions with the gas molecules during the traverse, ionization results. Due to the high energy of the electrons in such a system, the possibility of ionization is less. Most of the electrons bombard the substrate during the film deposition resulting in substrate heating. In normal dc glow discharge, the sputtering rate depends directly on the ion flux, which in turn depends on the density of the ions in the plasma. The major limitation on the ion density is the recombination of ions with electrons. This commonly happens on the inner walls of the vacuum vessel.

The introduction of the magnetic field confines the electrons to the cathode surface, thereby reducing the substrate heating. The use of magnetic field is primarily to trap the electrons close to the sputtering target, so as to prevent them from escaping to the walls where they will cause ion loss by recombination and also to enable them to create ions by electron impact close to the sputtering target where they are most useful. Lower magnetic fields (up to a few hundred Gauss) affects the motion of the electrons but doesn't have much influence over the heavier ions.

The magnets used may be either permanent having high retentivity and coercivity or electromagnets. Permanent magnets have the advantage that they may be placed so as to position the field lines in a desirable manner and this is harder to do with electromagnets. The design of the magnetron sputtering target involves the optimization of the magnetic field geometry to satisfy the condition that the magnetic field lines should be parallel to the target surface and perpendicular to the electric field. This condition can be achieved by placing the bar/horse shoe ring magnets behind the target.

The magnetic field lines first emanate normal to the target surface, then bend with a component parallel to the target surface (this component is useful for the confinement of the electrons) and finally return, completing the magnetic circuit.

When a magnetic field of strength B is superimposed on the electric field E between the target and the substrate, electrons within the dual field environment experience the well known Lorentz force (F) in addition to the electric field i.e.,

$$F = m \frac{dv}{dt} = -e(E + V \times B)$$

Where e , m and v are the charge, mass and velocity of the electron respectively.

When the electric field is neglected ($E=0$) and the magnetic field is uniform, the electrons drift along the field lines with velocity v which is unaffected by the magnetic field. When the electric

field is applied, these electrons orbit the field lines with a cyclotron frequency and the radius of gyration (r) is given by

$$r = \frac{mv}{Be}$$

This is the equation of the helix. When the electric and magnetic fields are at an angle Θ , then the resulting radius of gyration is

$$r = \frac{mv \sin\Theta}{Be}$$

This equation indicates that the radius of the helix decreases with increasing B and there is maximum radius when the electric and magnetic fields are mutually perpendicular.

During the orbit, the electron energy increases from 0 to 500 eV at its maximum distance from the target and begins to decrease as it approaches the target to make an ionizing collision with an argon atom. i.e., $e^- + \text{Ar} = \text{Ar}^+ + e^-$

The resultant electrons are subjected to the $E \times B$ field. Since the ionization potential of Ar is 15.75 eV, a single $E \times B$ subjected electron provides up to 30 Ar ions before it loses all of its energy and escapes the magnetic trap. Electrons may lose their energy through other processes like excitation of argon atoms and relaxation of these excited atoms by photon emission. This is mainly responsible for glow discharge.

The advantage of the magnetic field is the repeated collision resulting in the generation of high density positive ions and low energy electrons at a distance of few millimeters from the target within the region of the magnetic trap. As there are equal number of electrons and ions, there is no electric field in the plasma region. This plasma region has the properties of a perfect conductor.

The electric field in front of the magnetron is greatly altered by the presence of the conducting plasma such that the bulk of the negative potential applied to the target appears across a thin region between the target and the plasma. In typical magnetrons systems, this thickness (which is also called as the cathode dark space) is about one millimeter. Generally the radius of gyration of the electrons is larger than the dark space thickness. The moving electrons gains a velocity v which can be expressed as

$$v = \left[\frac{2eP}{m} \right]^{1/2}$$

The electric field is normal to the target surface and accelerates the ions from the plasma to the target. Because of their much greater mass, the ions are unaffected by the magnetic field. The use of a magnetic field also allows the formation of plasma at low chamber pressures (10^{-5} to 10^{-2} mbar).

3.3.2 Unbalanced Magnetrons

Unbalanced magnetron is the term given to magnetic configurations where some of the electrons are allowed to escape. Most magnetrons have some degree of unbalance but in the application of unbalanced magnetrons, the magnetic fields are deliberately arranged to allow electrons to escape. These electrons create plasma away from the magnetron surface. This plasma can then provide the ions for bombardment of the substrate and/or can activate a reactive gas of reactive deposition processes. The magnetron configuration for unbalancing the magnetron configuration can be supplied either by permanent magnets or by electromagnets.

Unbalanced magnetrons are often used in a dual arrangement where the escaping of the north pole of one magnetron is opposite the south pole of the other magnetron. This aids in trapping the escaping electrons. The escaping electrons are further trapped by having a negatively biased plate above and below the magnetrons.

There are two types of unbalanced magnetron configuration Type-1 and Type-2 as shown in Figure 1.

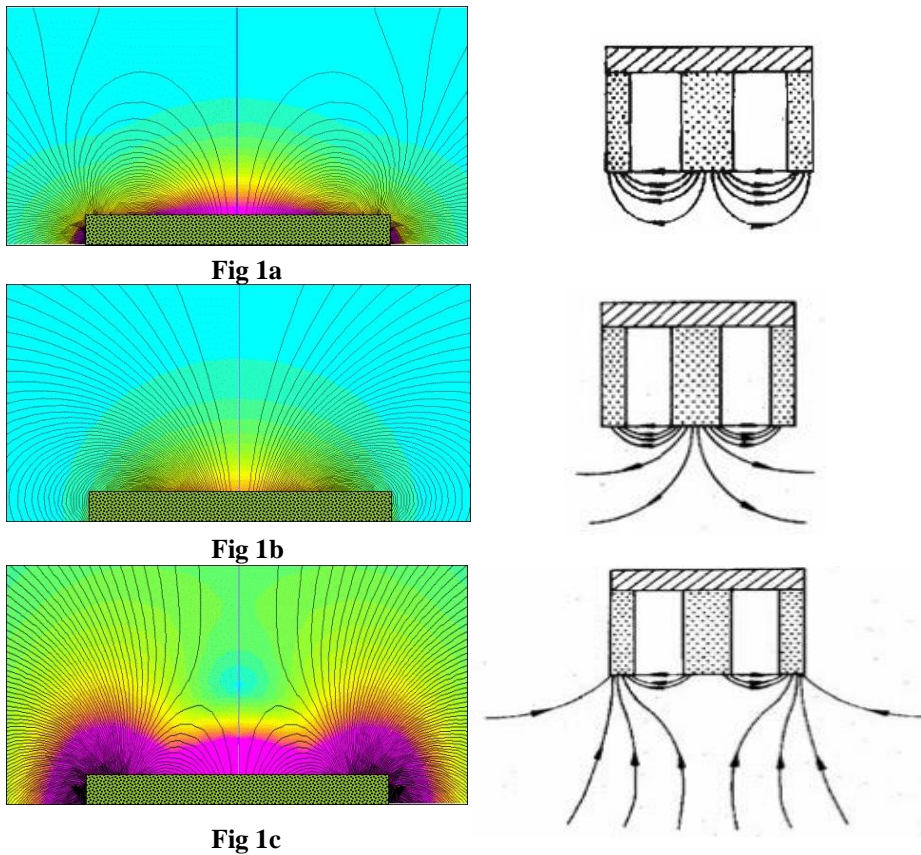


Figure 1. Showing different magnetron configuration: Balanced magnetron configuration (1a), Unbalanced magnetron configuration: Type-1 (1b) and Type-2 (1c)

3.3.3 *Reactive Magnetron Sputtering*

Compound materials are commonly reactively sputter deposited by using a reactive gas in the plasma. The plasma activates the reactive gas making it more chemically reactive. The target atoms react with the reactive gas to form a compound on the substrate.

3.3.4 *Pulsed DC Magnetron Sputtering*

The main problem encountered in reactive magnetron sputtering using DC potential is reduced deposition rate due to the reaction of reactive gas with the target surface forming compound referred to as 'target poisoning'. As the secondary electron emission coefficient of compound is higher than the pure metal films, the sputtering rate of target decreases leading to decrease in deposition rate affecting the film stoichiometry. Also in deposition of dielectric films, the target poisoning results in charge build up of positive ions resulting in dielectric breakdown forming an arc. Consequently, the arc ejects droplets of target material that will affect the film quality. The arcing also reduces deposition rate and the stoichiometry of the growing film.

The above problems could be overcome by applying pulsed DC to the target in the range 10 to 400 kHz that reduces arcing and defects in the film. The deposition rate may also approach those for pure metal films and hence the stoichiometry is controlled. In pulse DC sputtering, the electrons from plasma move to the target surface during positive bias (pulse-off time) and neutralize charge build-up generated during negative cycle.

The pulse can be unipolar or bipolar. The bipolar pulse can be symmetric, where the positive and negative pulse heights are equal and the pulse duration can be varied or asymmetric with the relative voltages and the duration time being variable.

4 Sputtering equipments

Three types of sputtering equipments have been used for deposition of films.

1. Figure 2. Closed field magnetron sputtering system.

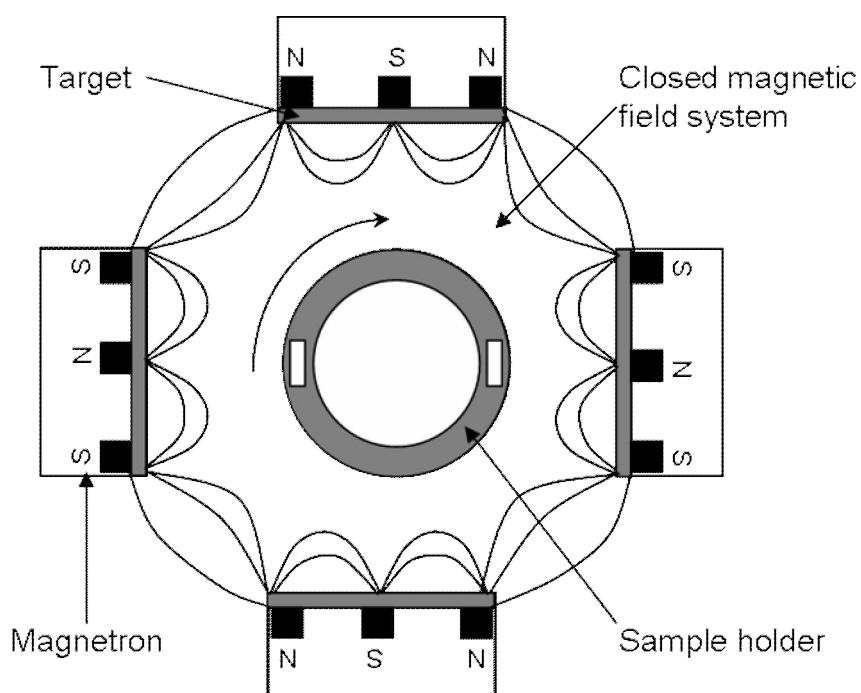


Figure 2. The schematic diagram of closed field magnetron deposition system. [3]

2. Custom built system “Ganesh”: The equipment Ganesh has two planar Type-II unbalanced magnetrons placed side by side with substrate holder in front of targets about 6.5 cm from the target. The substrate has the provision to be scanned along two targets. The picture of the chamber of Ganesh is shown Figure 3.

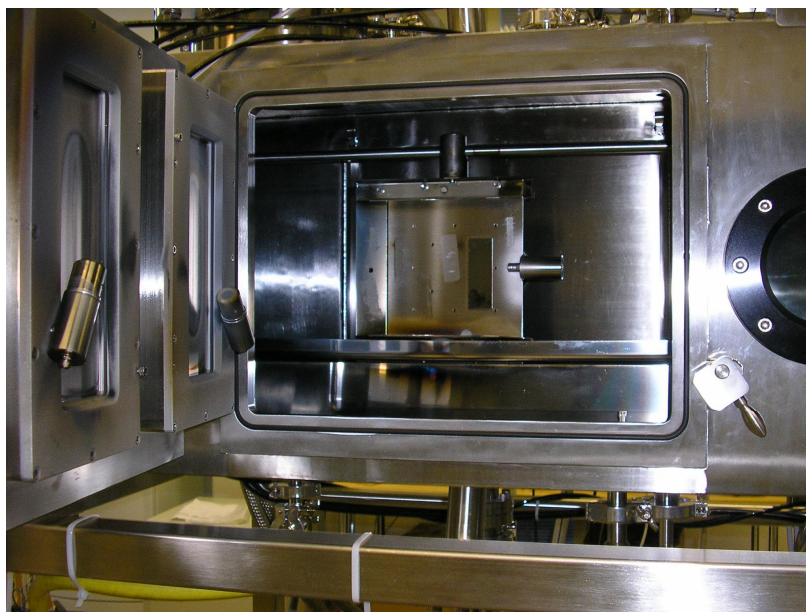


Figure 3. The image of custom built system “Ganesh”.

3. SLOAN: SLOAN SL 1800 sputtering system is a cylindrical system but with two magnetrons, not in a closed field arrangement. The magnetrons are equipped with a moving magnet system to increase target utilization. The substrates were placed on the drum which rotates. Diamond like carbon (DLC) and titanium doped DLC films were prepared using a high purity, 99.5 %, metallic titanium target. Advanced Energy Pinnacle plus d.c. power supply was used as a power source. Initially the sputter chamber was pumped down by cryo-pump to a background pressure of the order of 10^{-7} mbar before deposition. Pressure in the chamber was measured by Pfeiffer vacuum single gauge. The titanium target was sputtered by Ar gas. Methane gas of 99.999 % purity was used as a precursor for the DLC and Ti-DLC generation and as a reactive gas. Methane was connected through a piezovalve, which was controlled by an optical emission spectrometry system.

5 Wear resistant coatings

5.1 Chromium nitride coating

Nitride coatings such as titanium nitride and chromium nitride are widely used in industry for cutting tool industries and other applications. Though both titanium nitride and chromium nitride possess good mechanical properties, chromium nitride is found to possess good wear resistance, abrasion resistance, corrosion resistance and thermal stability. Thus chromium nitride has been chosen as the coating material to enhance the surface mechanical properties of the carbon fibre reinforced polymer composites (CFRP), the substrate material. The matrix material in the CFRP, the substrate material in the present study is vinyl ester. Chromium nitride coatings on polymers like polymethyl methacrylate (PMMA), vinyl ester, polycarbonate (PC) and polyamide (PA) have also been analyzed in pursuit of better understanding of film properties on different polymers that are very widely used in industries in various applications. These polymers are also mainly used as matrix material in CFRP composites.

The report is based on step by step procedure in analyzing film. First, as the film is coated on polymers, the adhesion is of main concern, which in fact is challenging because good adhesion is mainly obtained by high deposition temperature. As polymers cannot withstand high temperature, good adhesion has to be obtained by low temperature means which is brought about by in-situ and ex-situ cleaning. The adhesion analysis was then broadly based on these two cleaning methods. Ex-situ cleaning involves cleaning of substrates prior to deposition in ultrasonic bath with acetone, iso propyl alcohol, ethanol and detergent solution in addition to de-ionized water or just mere wiping of substrates with one or more of above solutions. This cleaning also involved baking in oven at different temperature. The film adhesion was then examined with the above parameters, compared and brought to a solution. In situ cleaning is ion cleaning where substrates are bombarded with neutral Argon ions by applying negative potential to the substrate to accelerate the positive Ar ions towards it. The adhesion was examined for different substrate bias voltage and different bias timing.

The films were then characterized for its structure by XRD and SEM explained in the following section for different applied current to the target, number of targets used, different bias voltage on substrate during deposition, using different pulse frequency, different flow of reactive gas, different pressure of the chamber and so on. The chromium nitride films were also studied for ion energy effect of various ions of chromium, nitrogen and argon species on structure and mechanical properties of films. The neutrals of above species were also determined to know their effect. The flux and energy of ions and neutrals were determined with Hiden EQP 300 mass spectrometer. The films were characterized for different DC pulse frequencies, applied to the target and found to have significant effect on structure and mechanical properties. This gives an insight to modify the film properties accordingly with different pulse frequencies. All the above studies are done to optimize the film properties.

5.2 TiC and Ti doped DLC

Diamond-like carbon (DLC) deposited by plasma enhanced CVD is an amorphous, in most cases hydrogenated, metastable material characterized by attractive optical, electrical, chemical, and tribological properties. Amorphous carbon coatings have lots of interesting properties such as very high hardness and elastic modulus, high electric resistivity, high optical transparency and chemical inertness, which are close to those of diamond. These coatings have a wide range of uses including optical, electronic, thermal management, biomedical and tribological applications. In certain applications, there is a need for thin coatings to improve friction and wear performance. [4,5]

DLC coatings typically have an extremely high intrinsic, compressive stresses, which usually lead to delamination of the films as an effect on a high shear stress induced on the film-substrate interface. It is known that in the multilayered coating by using an appropriate interleaving material the compressive stress can be reduced [6]. The stress distribution through the coating thickness can also affect significantly in tribological properties. Thus, stress reduction and increased toughness of film is possible to achieve by functionally gradient microstructures [7].

In order to develop the properties of DLC films, the composition has been modified by metal doping. The structure of the materials is somewhat similar to DLC but metal containing DLC (Me-DLC) films with properties intermediate between DLC and metal carbides are achieved. Lower internal compressive stresses, a small friction coefficient, low abrasive wear rate and good adhesion to the substrate were achieved [8]. Metal containing diamond-like amorphous carbon coatings have been found to have the combination of hardness and toughness needed to resist impact conditions [9].

The technique used for doped DLC-films, i.e. Ti doped DLC, is based on magnetron sputtering combined with plasma assisted chemical vapor deposition. This has the advantage of being able to deposit high quality coatings at low temperatures. The disadvantage is that the deposition rate is low (1 μ m/hr maximum).

DLC films have been produced by ion-assisted chemical vapor deposition [10], plasma-enhanced chemical vapor deposition (PECVD) [11] and r.f. magnetron sputtering [12]. Among these methods, PECVD is more suitable for amorphous film deposition on polymers due to its processing performed at low temperature, avoiding any degradation of polymer substrates. Also recent studies showed [13] that with these thin PVD and PACVD films, high elastic recovery was achieved and thus, soft plastic surfaces are possible protect with both hard and elastic coatings.

6 Characterization techniques

6.1 X-Ray Diffraction (XRD)

X-ray diffraction has very convincingly demonstrated the crystallinity of solids by exploiting the fact that the spacing between atoms is comparable to the wavelength of X-rays. This results in easily detected emitted beams of high intensity along certain directions when incident X-rays impinge at critical diffraction angles (θ). Under these conditions, the well known Bragg relation $n\lambda = 2d \sin \theta$ holds, where n is an integer.

Diffraction treats each atom as a scattering center and if the scattered radiation from the points is in phase, there is constructive interference and a strong signal. This signal position and its intensity is dependant on the separation between diffraction points and the number of points on a particular plane.

As an X-ray beam travels through any substance, its intensity decreases with the distance traveled through the substance. The mathematical definition for this is expanded as flows:

$$-\frac{dI}{I} = \mu dx$$

where μ is the linear absorption coefficient. This constant is dependent on the material properties, its density and the wavelength of x-rays. Integrating this equation gives:

$$I_x = I_o \exp(-\mu x)$$

where I_0 = intensity of incident beam, and I_x = intensity of transmitted beam after passing through distance x . The linear absorption constant coefficient is linearly proportional to the density of the material ρ and is usually tabulated as the mass absorption coefficient (μ / ρ). This gives:

$$I_x = I_o \exp(-\rho \frac{\mu}{\rho} x)$$

When a material is interacted with an accelerated electron having sufficient energy, an electron from an inner energy shell is excited in to an outer energy level. To restore equilibrium, the empty inner level is filled by electrons from a high energy level.

There are discrete energy differences between two energy levels. When an electron drops from one level to a second level, a photon having that particular energy and wavelength is emitted. Photons with his energy and wavelength comprise the characteristic spectrum and are X- rays.

If an electron is excited from the K shell, electrons may fill that vacancy from any outer shell. Normally, electrons in the next closest shell fill the vacancies. Thus photons with energies $\Delta E = E_K - E_L$ (K_α X rays) or $\Delta E = E_K - E_M$ (K_β X rays) are emitted. If an electron from the L shell fills the K shell, then an electron from the M shell may fill the L shell, giving a photon with

energy $\Delta E = E_L - E_M$ (L_α X rays) which has a longer wavelength or lower energy. We need a more energetic stimulus to produce K_α X rays compared to L_α X rays.

Only a small range of characteristic x-rays are widely used for diffraction. Their K_α lines are used. The K_β line which is always present with K_α , at a slightly shorter wavelength, is filtered out using an absorbing film.

The most useful of the X rays are the most energetic, shortest wavelength photons produced by filling the K and L shells. These X-rays can be used to determine the composition of the material.

When an unknown material is bombarded with high energy photons, the material emits both the characteristic and the continuous spectra. If the emitted characteristic wavelengths matches with those expected for various materials, the identity of the material can be determined.

The intensity of the characteristic peaks can also be measured. By comparing measured intensities to standard intensities, the amount of each emitting atom can be estimated and the composition of the material can be determined using X-ray fluorescent analysis or on a microscopic scale using the electron microprobe or the scanning electron microscope, permitting to identify individual phases or even inclusions in the microstructure.

6.2 Raman spectroscopy

Raman scattering is a fundamental form of molecular spectroscopy. Together with infrared absorption, Raman scattering is used to obtain information about the structure and properties of molecules from their vibrational transitions.

The Raman effect occurs when light impinges upon a molecule and interacts with the electron cloud of the bonds of that molecule. A molecular polarisability change, or amount of deformation of the electron cloud, with respect to the vibrational coordinate is required for the molecule to exhibit the Raman effect. The amount of the polarisability change will determine the intensity, whereas the Raman shift is equal to the vibrational level that is involved. The incident photon (light quantum), excites one of the electrons into a virtual state (Figure 4). For the spontaneous Raman effect, the molecule will be excited from the ground state to a virtual energy state, and relax into a vibrational excited state, and which generates Stokes Raman scattering. If the molecule was already in an elevated vibrational energy state, the Raman scattering is then called anti-Stokes Raman scattering.[14]

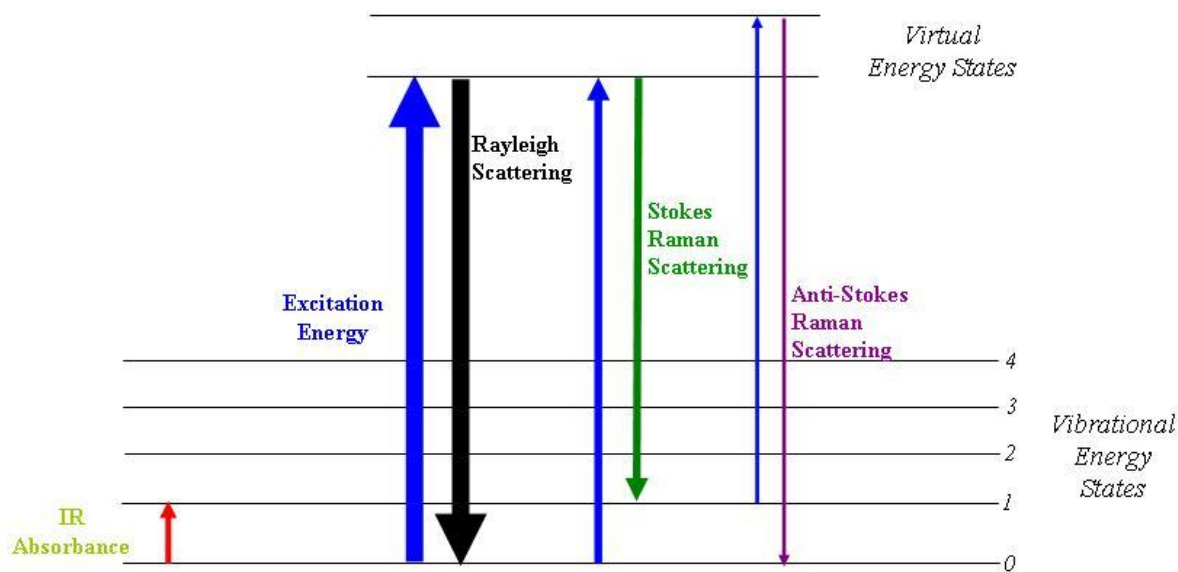


Figure 4. A description of the vibrational Raman effect based upon an energy level approach. [14]

7 Mass spectrometer

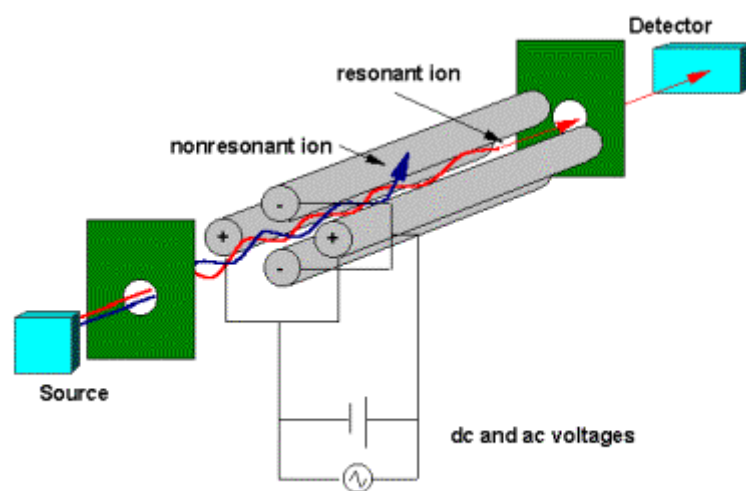
7.1 Principle

Mass spectrometry is an analytical technique that identifies the chemical composition of a compound or sample on the basis of the mass-to-charge ratio of charged particles. The method employs chemical fragmentation of a sample into charged particles (ions) and measurements of two properties, charge and mass, of the resulting particles, the ratio of which is deduced by passing the particles through electric and magnetic fields in a mass spectrometer. The design of a mass spectrometer has three essential modules: an ion source, which transforms the molecules in a sample into ionized fragments; a mass analyzer, which sorts the ions by their masses by applying electric and magnetic fields; and a detector, which measures the value of some indicator quantity and thus provides data for calculating the abundances each ion fragment present. The technique has both qualitative and quantitative uses, such as identifying unknown compounds, determining the isotopic composition of elements in a compound, determining the structure of a compound by observing its fragmentation, quantifying the amount of a compound in a sample using carefully designed methods (e.g., by comparison with known quantities of heavy isotopes), studying the fundamentals of gas phase ion chemistry (the chemistry of ions and neutrals in vacuum), and determining other physical, chemical, or biological properties of compounds.

7.2 Quadrupole Mass Analyzer

Mass analyzers separate the ions according to their mass-to-charge ratio. There are different types of mass analyzers. The quadrupole mass analyzer is one type of mass analyzer used in mass spectrometry. As the name implies, it consists of 4 circular rods, set perfectly parallel to each other. In a quadrupole mass spectrometer the quadrupole mass analyzer is the component of

the instrument responsible for filtering sample ions, based on their mass-to-charge ratio (m/z). Ions are separated in a quadrupole based on the stability of their trajectories in the oscillating electric fields that are applied to the rods. The quadrupole consists of four parallel metal rods. Each opposing rod pair is connected together electrically and a radio frequency voltage is applied between one pair of rods, and the other. A direct current voltage is then superimposed on the R.F. voltage. Ions travel down the quadrupole in between the rods. Only ions of a certain m/z will reach the detector for a given ratio of voltages: other ions have unstable trajectories and will collide with the rods. This allows selection of a particular ion, or scanning by varying the voltages.



http://www.mcb.mcgill.ca/~hallett/GEP/PLecture1/MassSpe_files/image011.gif

8 Adhesion of the films on carbon fibre composites and polymers

8.1 Adhesion as a phenomenon

Cohesion is the strength in a single material due to inter-atomic or inter-molecular forces. Adhesion is the mechanical strength joining two different objects or materials. Adhesion is generally a fundamental requirement of most deposited film/substrate systems. In PVD technology, adhesion occurs on the atomic level between atoms and on the macroscopic level between the substrate surface and the deposited film. [15]

Deformation of a material requires the input of energy. At some level of deformation, the material will fail. The amount of energy that must be put into the system to cause this failure is a measure of the cohesive or adhesive strength.

8.2 The aim of the adhesion testing

Adhesion testing is used to monitor process and product reproducibility as well as for product acceptance. Adhesion tests are commonly very difficult to analyze analytically, thus tests are often used as comparative tests and they have been found useful in comparing the adhesion behaviour of different coatings.

The practical adhesion is usually measured by applying an external force to the thin film structure to a level that causes failure between the film and substrate. There are number of different adhesion tests and test variations. The adhesion must be good after the film deposition processing, after subsequent processing and throughout its service life.

The purpose of this test is to measure the mechanical tensile strength of a coating. The sample will be subjected to increasing tensile stresses until the weakest path through the material fractures. The weakest path could be along an interface between two coatings, a cohesive fracture within one coating, a cohesive fracture of the substrate or a combination of these.

In our project we are interested in the force which is required to break the bond between the coating and substrate. The pull-off tensile test is performed by bonding a stud to the surface of the coating using glue and then pulling the stud to failure.

8.3 Preparation of the Testing

The test element should be glued on the surface with a suitable adhesive. A major factor in the reproducibility of pull-off test is the amount of adhesive on the surface [15]. If there is too much adhesive, a peeling stress around the edges is found. The glue only needs to be stronger than the coating not twice as strong. In our case two-component epoxy adhesive, Loctite Hysol 9466, is used. The epoxy has the tensile strength value 32 MPa.

8.4 Apparatus

In experimental procedures, we are using the PAT adhesion tester of DFD® INSTRUMENTS, which is high precision pull-off type measuring instrument for adhesion [16]. The testing machine is dimensioned for measuring of bond strength of all types of paints, thermal sprayed coatings, thin films, concrete coatings, ceramics, etc. Different test ranges are achieved by using different test element sizes. In our case, it was presumed that with the micro-testing head 1 kN and the test element area 12.6 mm² we are achieving suitable testing range. This was based on the earlier literature survey.

The automatic adhesion tester is very simple to use. The micro testing head is connected to the test element, which has been glued to the coating. The servo motor is started by pressing the button that will force hydraulic fluid into the system and pressurizing the circuit. After test specimen fracture has occurred, the value is readable on the precision gauge. The actual test

result is calculated by the ratio 4:1, which is based on the maximum indicated load, the instrument calibration data and the original surface area stressed.

8.5 The test method

ASTM D4541 and ISO 4624 both define the method and procedures for carrying out pull-off adhesion testing of paints, varnishes and other coatings [17, 18, 19]. These standard test methods use a class of apparatus known as portable pull-off adhesion testers. Variations in results obtained using different devices with the same coating are possible. Therefore, it is recommended that the type of apparatus is reported in the test report. PAT adhesion tester used in our adhesion tests is in accordance with these standards. A schematic presentation of the test method is shown in Figure 5.

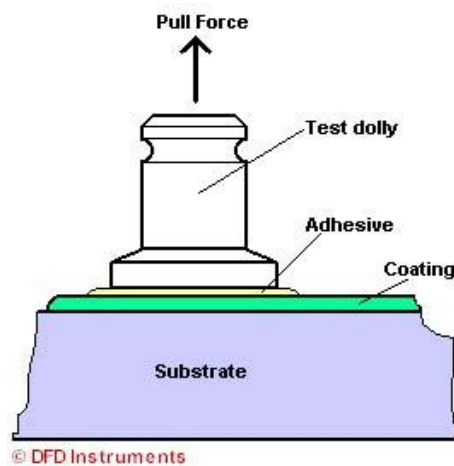


Figure 5. Schematic presentation of the adhesion test [16].

The key issues of the standards are [18, 19]:

- § The test elements must be cleaned sufficiently to prevent “glue failure” during testing.
- § The tensile stress shall be applied in a direction perpendicular to the plane of the coated substrate and shall be increased at a substantially uniform rate.
- § Special attention is required in selecting suitable adhesives. The bonding properties of the adhesive should be greater than the coating and adhesive is not allowed to alter the coating chemically.

8.6 Testing parameters

Adhesion tests were carried out with six determinations per each coated sample. Sample-5 consists of vinyl ester resin with carbon fibre reinforcements and is reference sample. Sample-2

consists of vinyl ester resin with carbon fibre reinforcements and in addition there is carbon black powder in the resin.

An ultra-sonic bath with detergent solution, isopropyl alcohol and acetone were used to clean studs before test. Studs were baked in an oven at +40°C for 1 h.

The first step was to find out how to apply a sufficient amount of adhesive in the centre of the test area. Even small air pores in the adhesive may affect the test results significantly. Different curing times and temperatures have been studied to find out which is suitable for our purposes.

8.7 Adhesion tests for the plain substrates

Adhesion tests were carried out on uncoated samples, which have the same pre-treatment as the coated samples. In addition, effects of different heat treatments were studied.

Samples were pre-cleaned in ultra-sonic bath with detergent solution, isopropyl alcohol and acetone for ten minutes in each solution. The samples were then annealed in an oven at different temperatures and different times. There were also reference samples without pre-cleaning and without annealing. The results are shown in Figure 6.

In the case of the Sample-5 there are some scattering with the strength values. Some removed fibres from the substrate were observed on the surface of the stud with the samples pre-cleaned and both pre-cleaned and annealed at +50°C for 1h. In the case of the Sample-2 all the failures were between glue and surface.

In summary, the adhesion results do not represent absolute values for the adhesion but only relative values. However, since two samples of Sample-5 exhibited higher adhesion strengths with failure of substrate, it is presumed that strength values over 20 MPa is needed to reach cohesive failure of substrate or adhesive failure at substrate/coating interface. Different heat treatments have not been shown to affect strength values of uncoated samples.

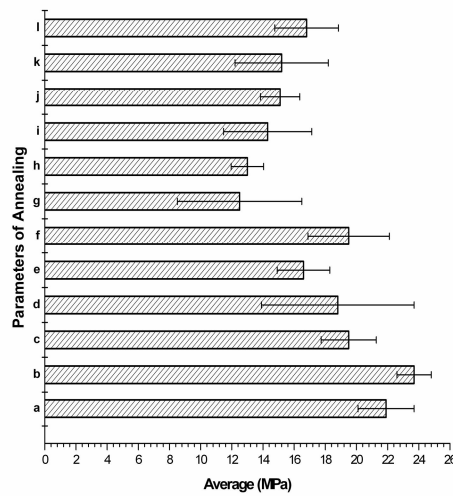


Figure 6. Adhesion values of uncoated Sample-5 and Sample-2 as a function of different annealing treatments. a) pre-cleaned sample-2, +80°/18h b) not pre-cleaned sample-2 c) pre-cleaned sample-2, +150°/1h d) pre-cleaned sample-2, +100°/1h e) pre-cleaned sample-2, +50°/1h f) pre-cleaned sample-2, no heat treatments g) pre-cleaned sample-5, +80°/18h h) not pre-cleaned sample-5 i) pre-cleaned sample-5, +150°/1h j) pre-cleaned sample-5, +100°/1h k) pre-cleaned sample-5, +50°/1h l) pre-cleaned sample-5, no heat treatments

8.8 Examination of the failures

According to standard [18] the nature of the failure for all tests should be qualified. The fracture surfaces are inspected in accordance with the percent of adhesive and cohesive failures and the actual interfaces and layers involved.

It has been quite complex to examine the different surfaces and nature of failures in our studies. Figure 7 shows the description of the specimen split to different layers. The original sample consisted of substrate with the outermost layer of resin. The reason to separate these layers is to ascertain the connection between different type of fractures and strength values. Also the coating is composed of Cr- and CrN-layers. However, no fracture at Cr/CrN interface was observed.

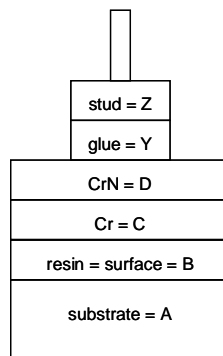


Figure 7. Schematic presentation of the layers and symbols used in examination of failures.

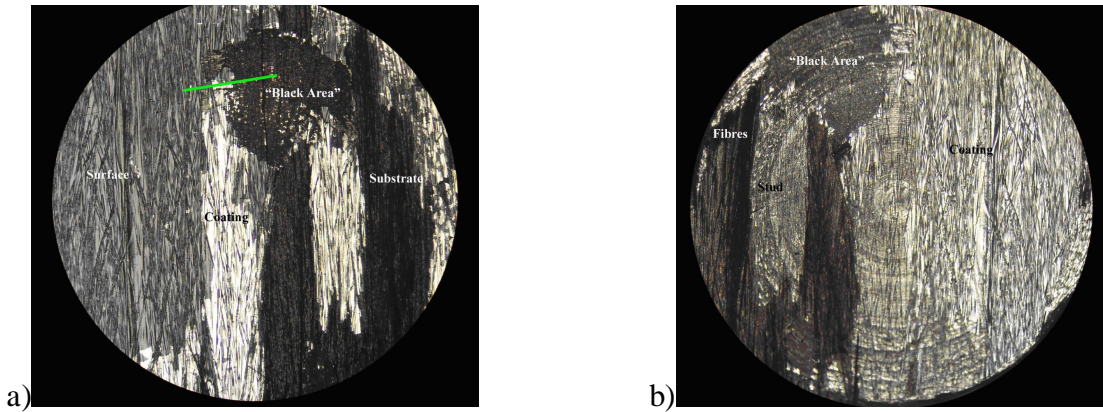


Figure 8. Failure surfaces of the sample (a) and stud (b) taken by optical microscope. 4 mm in diameter.

Figure 8 shows different layers from the surface of the stud and sample. (0305029-2 – parameters of coating: 1 Target, OEM 70%, +104°C). The area of the each type of fracture is estimated visually by optical microscope.

Also some surfaces of the failures were examined with a scanning electron microscope (SEM) and energy dispersive spectroscopy (EDS). It was ensured the layers of fractures by comparing spectra from different areas. Linescan was used to select an area of interest which includes three different layers. Figure 9 shows SEM micrograph and EDS spectra. Identification of the peaks in the spectrum indicates that Cr, O, H and Fe are present in different areas in the line of interest. Thus, the earlier estimations of the nature of the fracture made by optical microscope were confirmed.

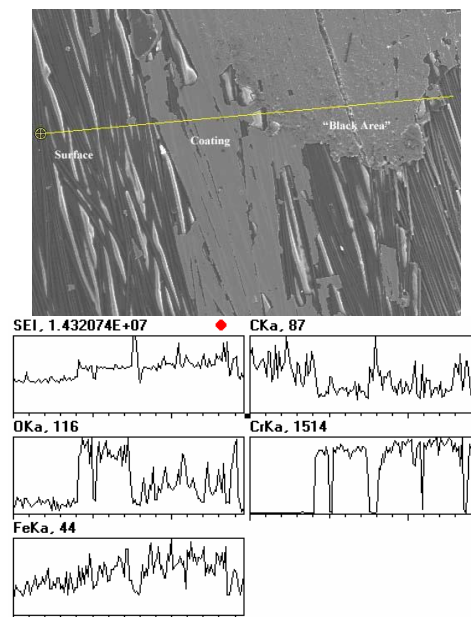


Figure 9. SEM micrographs of the surface of the stud and EDS spectrum from the yellow line.

8.9 Examination of parameters

Different parameters have been taken into consideration in order to exam effects on adhesion strength values. Table 1 presents the summary concerning of different parameters and observed effects. In addition the following steps for future are mentioned.

Table 1. Consideration of different parameters

PARAMETER		OBSERVED EFFECT
<i>pre-cleaning</i>	un-cleaned vs. 3-steps cleaned	cleaning gives better adhesion
<i>baking time</i>	18 h vs. 3 h	both gives the same average values but a sort of failure 3 h looks more consistent
<i>ion cleaning</i>	10 min vs. 15 min and 20 min	initial indications suggest that longer ion cleaning time gives better adhesion
<i>curing conditions for studs</i>	room temperature/72h vs. +40°C/4 h in the oven	curing in the oven shorten the time of test procedure, minimize the variation of strength value
<i>substrate temperature</i>	+85 - +125°C	no consistent difference noticed
<i>OEM-value</i>	70% vs. 65%, 60%	no significant difference noticed

There are two problems that have to be dealt with in order to understand the behaviour of failure. First, in some cases measurements are limited by the strength of adhesion bonds between the loading fixture and the specimen surface. Secondly, it is observed that even among the same sample the type of failures and also the values of strength varied a lot.

It is noticed that the curing of the glue in the oven has effects on test process and values. The strength value does not depend on the portion of the fracture since with the 20% and $\geq 50\%$ fractures the same value range is obtained. This phenomenon is reported in Table 2 which presents the adhesion tests and different parameters during coating.

The criterion for the entry to this comparison between different coatings was that the temperature of the deposition shall be less than +105°C. However, one example of higher temperature deposition is involved. Samples cured in the oven are separated by *-mark in the end of coating number. The values of adhesion are in same level even though the mean percentage area of fracture is smaller with the oven cured samples. Figure 10 shows different coatings as a function of percentage area of fracture and breaking strength.

If tests where glue failure represents more than 45% of the area are disregarded the case is shown in Figure 11. The line of strength values is relatively smooth. The variation of breaking strength value is between 19.6 – 22.4 MPa. The fractures in our studies took place in the bulk material and it gives the assumption that the adhesive forces acting between coating and substrate are stronger than the cohesive forces of the substrate. 22-23 MPa strength is needed to break substrate. So the adhesion between substrate and coating is assumed to be higher.

Table 2 Results of adhesion tests including different parameters of depositions.

Sample ID	Baking Parameters		Ion Cleaning Parameters			Coating Parameters			Breaking Strength	Area Of Fracture As %
	Time [h]	Temp [°C]	Time [min]	Voltages [V]	Total Time [min]	OEM [%]	Target	Temp [°C]	[MPa]	Average (no of studs)
0305019-5 (a)	3	+80	10	400	36	65	1	+85	22,4 ± 3,2	99% (6)
0305019-2 (b)	3	+80	10	400	36	65	1	+85	21,4 ± 0,4	77% (4)
0305027-5 (c)	18	+80	10	400	34	65	1	+95	20,8 ± 2,4	47% (3)
0305027-5* (d)									21,1 ± 2,3*	32% (3)
0305027-2 (e)	18	+80	10	400	34	65	1	+95	20,4 ± 2,7	77% (4)
0305027-2* (f)									21,6 ± 1,5*	59%(4)
0305029-5 (g)	18	+80	10	400	22	70	1	+104	19,6 ± 0,4*	46%(2)
0305029-2 (h)	18	+80	10	400	22	70	1	+104	20,7 ± 3,1	77% (8)
0305029-2* (i)									25,6 ± 2,2*	35% (5)
0305030-5 (j)	18	+80	10	400	25	60	1	+104	21,9 ± 3,0	67% (3)
0305030-5* (k)									21,2 ± 2,8*	52% (4)
0305030-2 (l)	18	+80	10	400	25	60	1	+104	22,3 ± 2,9	75% (8)
0305030-2* (m)									23,5 ± 2,9*	55% (6)
0305045-2* uc (n)	18	+80	20	400	38	70	1	+125	32,9 ± 5,7*	60% (5)

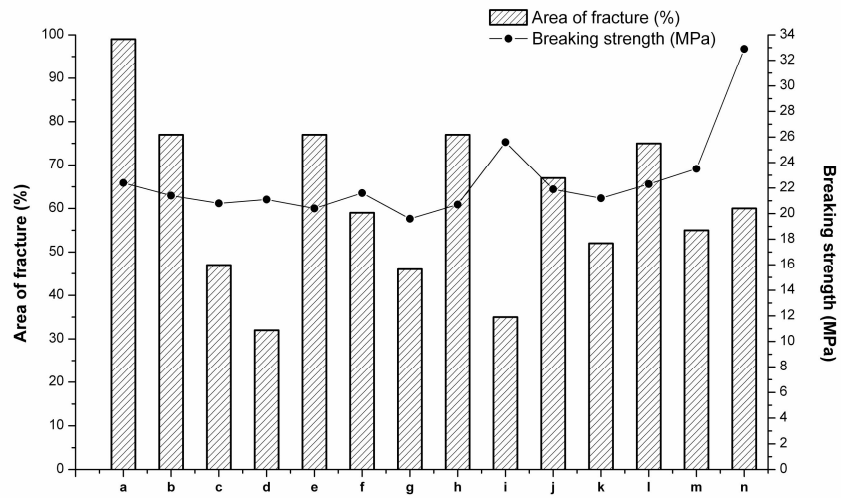


Figure 10. Different coatings as a function of percentage area of fracture (columns) and breaking strength (line).

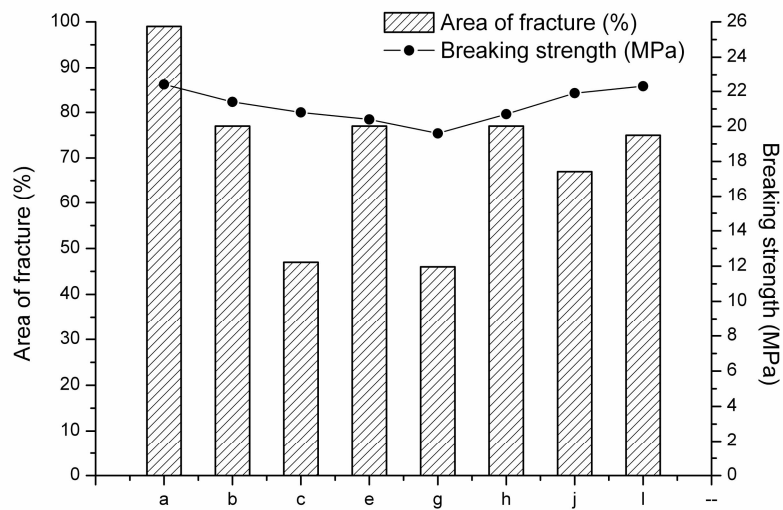


Figure 11. Reliable coatings as a function of percentage area of fracture and breaking strength.

The initial measurements with titanium doped DLC showed that the fracture strength was significantly better compared to chromium nitride coated CFRP-2 and CFRP-5.

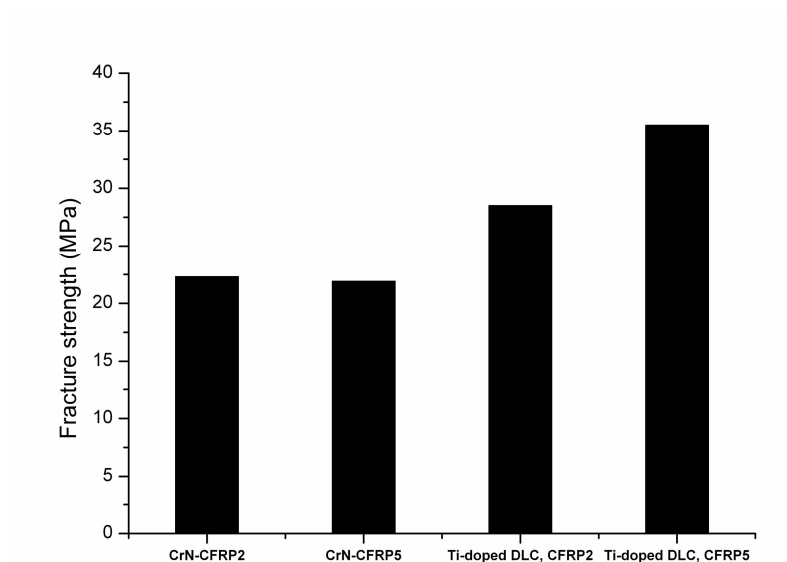


Figure 12. Adhesion tests for CrN and Ti-doped DLC coatings.

9 Influence of different pre-treatments on substrate properties

9.1 Effect of ex-situ substrate pre-treatment

9.1.1 Contact angle and surface energy measurements

It is well known that the adhesion should be increasing as a function of decreasing contact angle and increasing surface energy. The effect of different cleaning procedures on contact angle and surface energy were studied.

The polycarbonate (PC), vinylester, glass and carbon fibre reinforced polymer (CFRP) materials were cleaned using three different procedures:

1. Ethanol wiped
2. 2-step + baked: detergent solution (4%) + isopropyl alcohol (IPA), in an ultrasonic bath for 5 min in each, baking at 80°C for 3 h
3. 3-step + baked: detergent solution (4%) + IPA + acetone, 5 min in an ultrasonic bath, baking at 80°C for 3 h

Note: Acetone was noticed to degrade the PC and vinyl ester substrate during the cleaning procedure and was therefore not used for them.

Contact angles were measured from three different liquids: water, glycerol and ethylene glycol by using circle-fitting method. The Owens-Wendt –method was used to determine the surface energy.

Different values of contact angles and surface energies are shown in the Figure 13 and Figure 14. PC achieved highest surface energy after 2-step cleaning and baking but it could be also due to roughening effect of cleaning. The interesting phenomenon was between vinyl ester and CFRP. Vinyl ester had obviously higher surface energy after 3-step cleaning and baking while CFRP achieved lowest surface energy.

The conclusion was that with these materials ethanol wiping is enough for cleaning process. Except vinyl ester that both ethanol wiping and 3-step cleaning would be included.

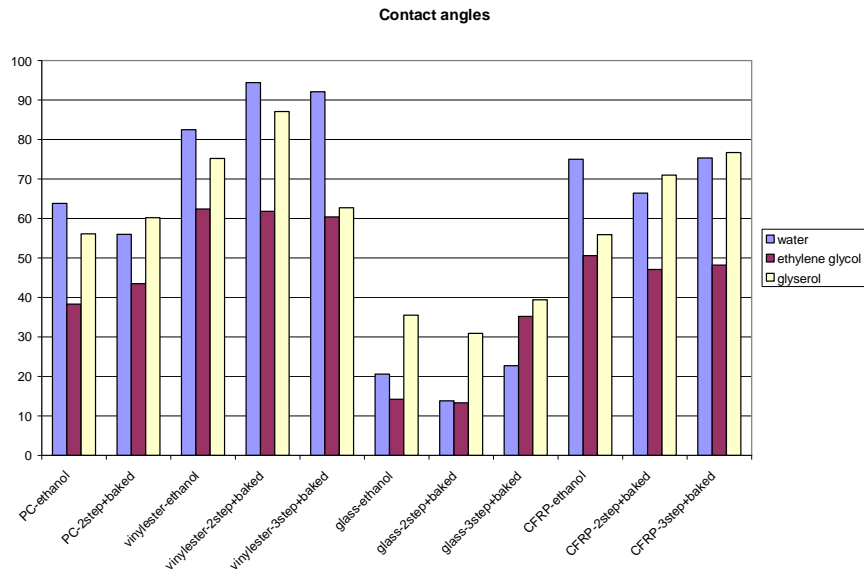


Figure 13. Contact angles for different materials after pre-cleaning.

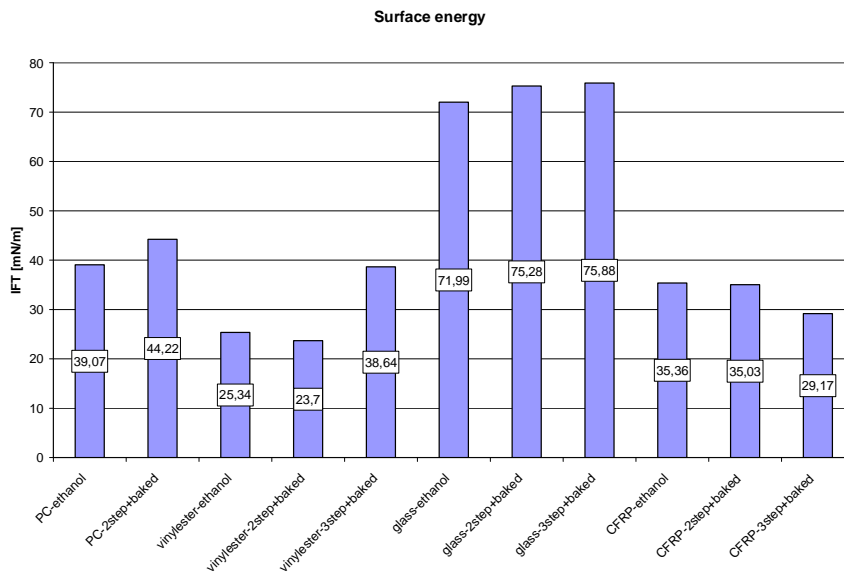


Figure 14. Different surface energies for different materials after pre-cleaning.

9.1.2 DMA studies - Effect of substrate chemical cleaning on bulk properties

The influence of different pre-treatments on strength and glass transition temperature (T_g) were studied by dynamic mechanical analysis (DMA). The determination of glass transition is important as it characterizes the thermal limits of a material. The used method was three-point bending which is ideal for materials with a high storage modulus.

The DMA process included dynamic heating from the room temperature up to 200°C, heating rate was 3K/min, cooling by the rate -3K/min back to room temperature, stabilizing by 15 min and then heating again up to 200°C. Initial strength values were noticed in the beginning of run and during the isothermal stage. Glass transition temperatures were determined from the storage and loss modulus (E' and E'') as well as from the dynamic loss factor ($\tan \delta$). Values of T_g and initial strength can be seen from the Fig. 15 and Fig. 16 No significant differences can be noticed between different pre-treatments. For CFRP-samples the storage modulus value was increasing after first heating and also the baking was slightly increasing the value comparing to other pre-treatments. The conclusion was that different pre-treatments do not have a significant influence on the substrate material.

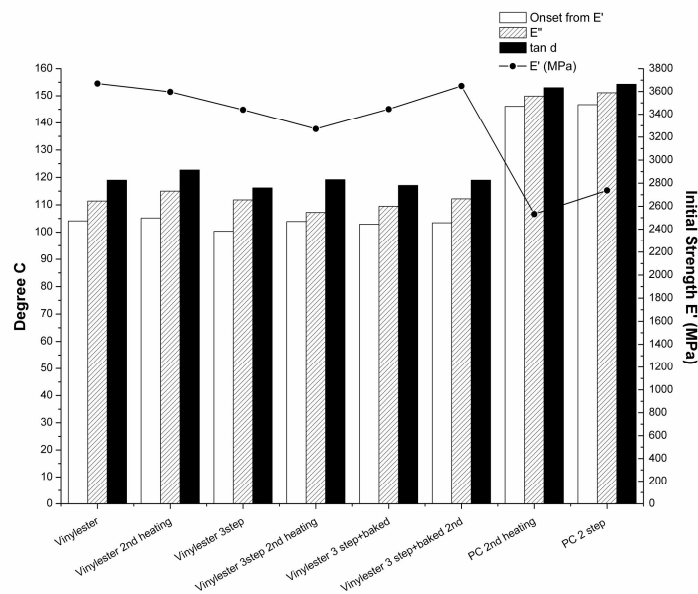


Figure 15. Initial strength and glass transition temperature determined from storage modulus, loss modulus and $\tan \delta$ for vinyl ester and PC after different pre-treatments.

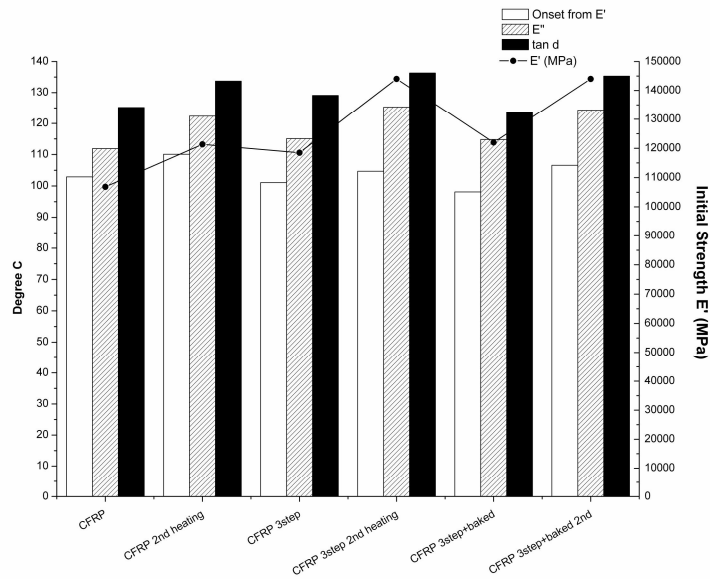


Figure 16. Initial strength and glass transition temperature determined from storage modulus, loss modulus and tan δ for CFRP after different pre-treatments.

9.2 Effect of in-situ substrate pre-treatment

Polymers are known for their low density, high flexibility and high chemical inertness, which make them find wide applications in automotive, semiconductor, optical, food packaging and biomedical industries. The polymers have been used as the matrix material for composites for a long time. The drawback of the polymers lies in their low hardness, high frictional coefficient, low resistance to scratch and abrasion properties and low surface energy, which makes the coating adhesion poor on polymer substrates. Several researchers have investigated coatings on polymers in terms of thermal barrier, antireflection, biocompatible, optical, wear resistance and protective properties and tried to improve the adhesion by several means [20,21,22,23].

Prior to deposition, pretreatments like chemical treatment, ion implantation, electron beam irradiation and plasma treatment with argon, helium, nitrogen and oxygen ions were done to modify the surface morphology, physical and chemical nature of the surface and hence the surface energy [24]. The chemical and plasma treatment of the polymers leads to formation of functional groups by chain scission followed by cross linking that improves the adhesion with increased hardness, wear resistance and low frictional coefficient. The above treatments also roughen the surface that affects the adhesion and is found to be different for different polymers [25].

The adhesion of the coating is significantly affected by ion cleaning with argon, nitrogen and mixture of argon/nitrogen. Without ion cleaning, the chromium nitride coating done on CFRP substrates flaked off showing poor adhesion.

9.2.1 Pre-treatment of substrates with different plasmas

The effect of argon, nitrogen and argon/nitrogen mixture plasma pre-treatment on chromium nitride coating on vinyl ester, polyamide, PMMA and PC was analyzed in this study. The deposition was carried out in Ganesh using a single chromium target with the substrate being scanned to avoid a rise in substrate temperature. Chromium was sputtered with 150 kHz pulse frequency and 2.6 μ s pulse off time applied to the target. The base pressure of the chamber was 2×10^{-2} Pa and operating pressure was 2 Pa. The substrates were wiped with ethanol and subjected to ion cleaning for about 1 minute with RF substrate bias of -75 V. Chromium was used as an adhesion layer and the substrate bias during deposition was -30 V. The target current density during deposition was on average 5.1 mA/cm². The flow of reactive gas nitrogen in to the chamber was controlled through piezo-valve using optical emission feedback signal from chromium emission

The substrates were cleaned with argon ions at different pressure. The variation of adhesion strength with argon pressure is shown in Fig. 17. The adhesion strength of coatings on all substrates was above 10 MPa. PC showed better adhesion at low pressure of Ar and vinyl ester at mid pressures but the difference was not significant at different argon pressures. PA too showed no significant difference. CrN on PMMA shows better adhesion at high pressure pretreatment with Ar and poor adhesion at low pressures.

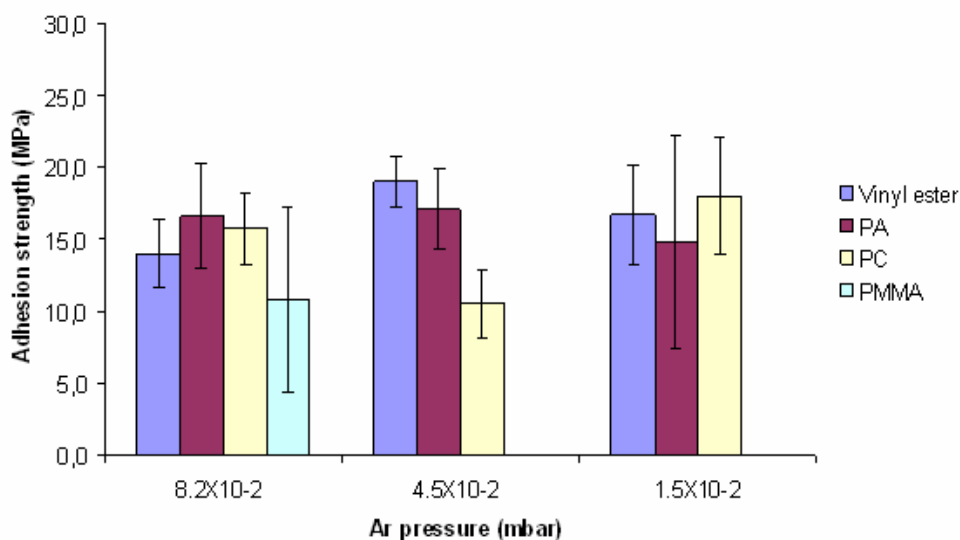


Figure 17. Variation of adhesion strength with argon pressure.

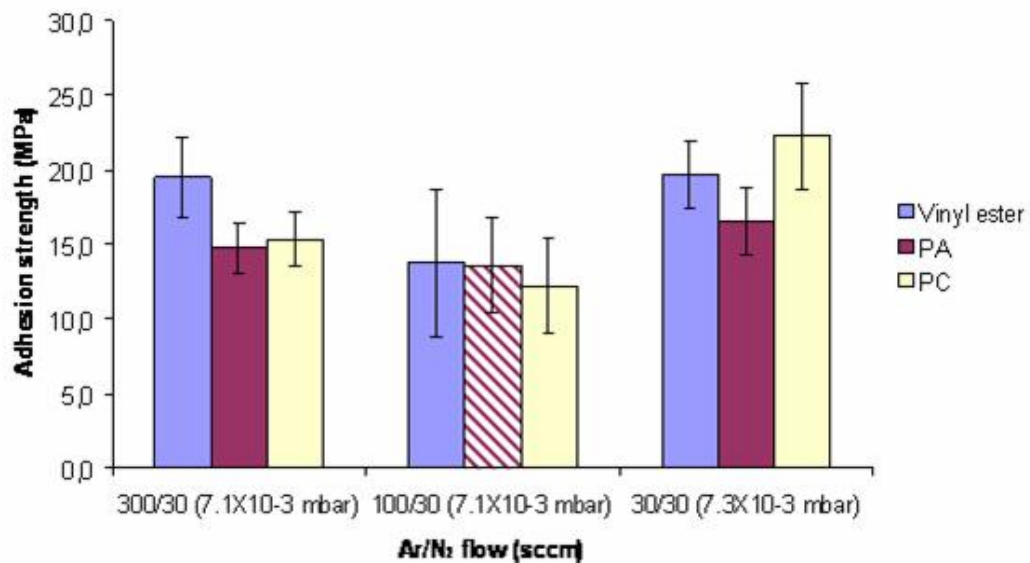


Figure 18. Variation of adhesion strength with argon/nitrogen pre-treatment.

Chromium nitride on polycarbonate and vinyl ester showed better adhesion for argon and nitrogen flow of 30 sccm. The glue failure occurred at 15MPa for polyamide at 100:30 Ar/N₂ (Fig. 18). Hence the adhesion strength on PA is not less than 15 MPa.

9.2.2 Ion cleaning and bias voltage

The effect of ion cleaning of the substrate by Ar plasma on contact angle was studied. The problem was the high variation between contact angles, perhaps due to fast oxidation of material between pre-treatment and measurement. Hence, different bias voltages were applied during ion cleaning, then 33 min Ti-layer was deposited and the adhesion strength was studied by pull-off adhesion tests. Parameters for ion cleaning were:

- Bias 200 V, pressure 30 μ , time 3 min, temperature < 37°
- Bias 400 V, pressure 14 μ , time 3 min, temperature < 37°
- Bias 600 V, pressure 14 μ , time 3 min, temperature < 37°

Fig. 19 shows measured adhesion strength values. All the materials wiped with ethanol achieved their highest adhesion strength after ion cleaning with bias 200 V. Only vinyl ester after 3-step pre-cleaning preferred bias 600 V, though the achieved adhesion strength value was similar as ethanol wiped vinyl ester. These tests showed that during the ion cleaning bias voltage should not go above 400 V.

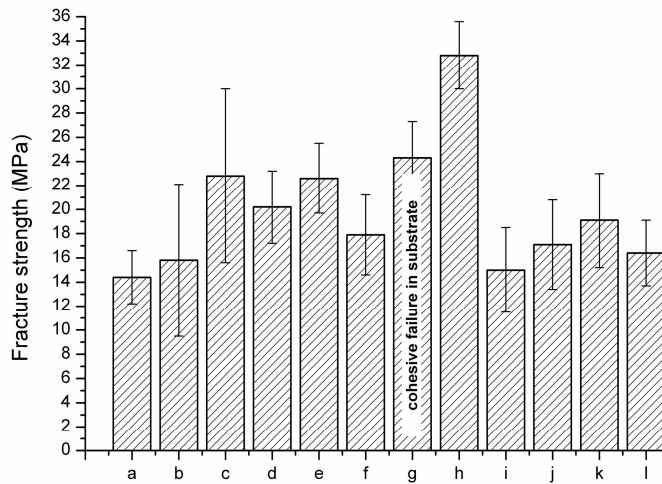


Figure 19. Adhesion strength after different ion cleaning process.

9.3 Effect of substrate temperature

The carbon fibre reinforced vinyl ester composites have the disadvantage of low glass transition temperature imposed by the vinyl ester polymer matrix that is around 100°C, as could be seen from the graph of DMA in Fig. 20. It is clear from the graph that the storage modulus of the material degrades significantly above this temperature range. This demands the deposition to be done below 100°C without affecting the mechanical properties.

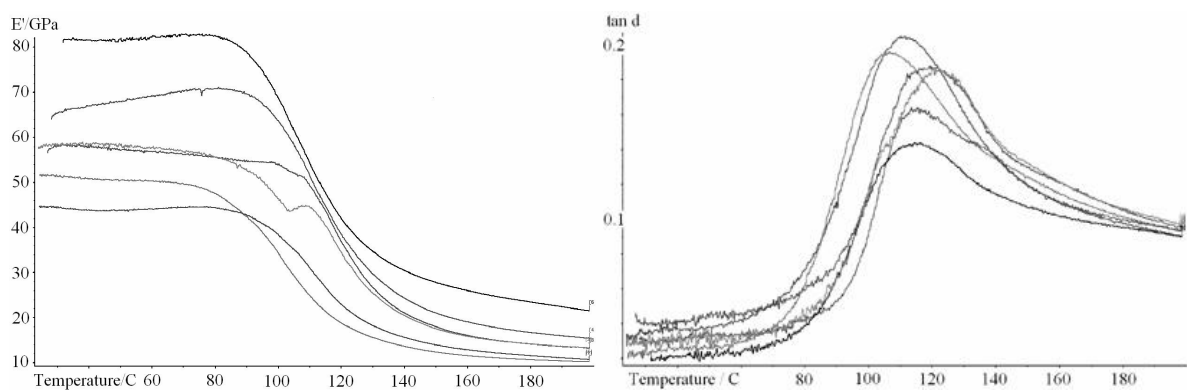


Figure 20. Storage modulus (a) and $\tan \delta$ (b) curves as a function of temperature for CFRP substrates

The variation in the storage modulus from different samples could also be clearly seen from the graph. This is due to poor binding between the fibres and the matrix as seen from the cross

sectional SEM micrograph of the material in Fig. 21. The micrograph also shows the presence of fibres on the surface.

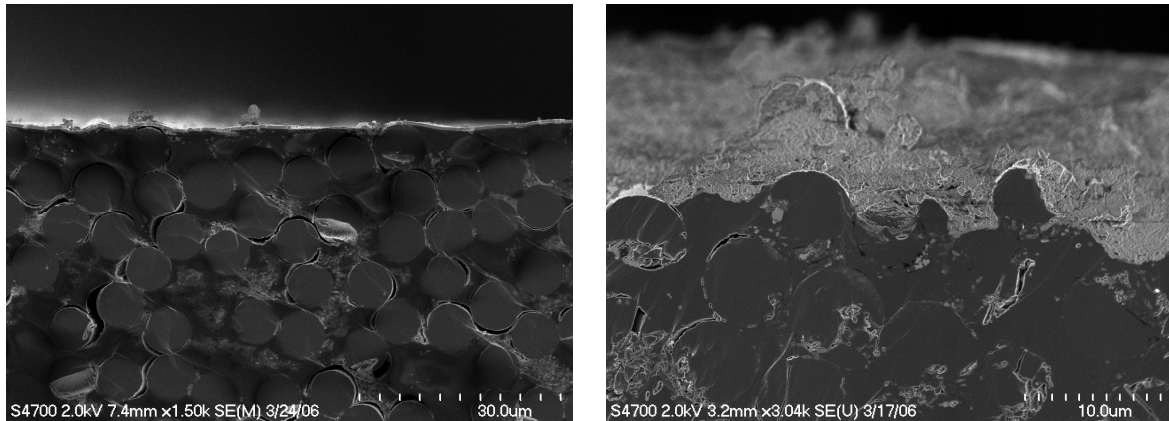


Figure 21. Cross sectional SEM micrographs of CrN coated CFRP substrate showing poor binding of carbon fibre to the matrix (a) and presence of fibre over the surface (b).

10 Effect of flux of ion energy bombardment on structure and mechanical properties of CrN

The DC pulse sputter deposition is known to produce high energetic particle bombardment on growing film, modifying the film properties significantly. The film quality was found to be improved with DC pulse by reduction of arc to a desired level [26]. With several effects of high energy particle bombardment like film crystallographic modification, removal of film defects, roughening of the surface, one of the main effects is densification of the film. These special features of DC pulse have remarkable influence on the film properties like adhesion, hardness, wear resistance, frictional resistance and corrosion resistance [27-32].

Having known the chromium nitride coating to be best suited for tribological applications, this film has been investigated in the present study to know the effect of varying pulse frequency on its microstructure and mechanical properties [33-37]. The film was deposited by reactive magnetron sputter deposition with argon as sputter gas and nitrogen as the reactive gas. High energetic bombarding ions are normally produced in overshoot phase of DC pulse due to very high positive target voltage phase that brings the plasma potential to a high positive value. This leads to sudden expansion of plasma sheath leaving behind uncovered ions that bombards the substrate/film with high energy [38,39]. Though it is known that DC pulse produces energetic bombarding ions, here specific studies has been done on the effect of varying pulse frequency from continuous DC to 350 kHz on the flux and energy of ions and neutrals of different species. The ions and neutrals of neutral gas, reactive and the metal species were investigated at different pulse frequencies and the influence of bombardment of these ions on structure and properties of the film was finally analyzed.

10.1 Experimental

Chromium nitride was sputter deposited on glass plates and silicon (100) wafers. The films were also deposited on thin glass plate of about 100 microns thickness to determine the film stress. The magnetron was of the type II unbalanced configuration. The base pressure before deposition was approximately 2×10^{-4} Pa. The sputtering gas was an argon/nitrogen mixture. The operating pressure during deposition of chromium, the adhesion layer, was 1.9 Pa and it was 2.1 Pa during chromium nitride deposition. The nitrogen gas flow was piezo valve controlled using optical emission monitor (OEM) feedback from the chromium emission line at 328 nm to control the film stoichiometry. The line intensity was set to 60% of the intensity during deposition of pure chromium. The target current density was ~ 21 mA/cm² and the deposition time for the chromium adhesion layer and chromium nitride coating was 5 minutes and 60 minutes respectively with the film thickness varying between 0.1 and 0.3 microns for Cr and from 1.2 to 2.4 microns for chromium nitride coating, depending on the pulse frequency. The thickness and stress of the films are measured by Dektak 6M stylus profilometer. Depositions were done for continuous DC and pulse frequency: 50, 100, 250 and 350 kHz at pulse-off time of 1.1 μ s. The substrates were unheated and not biased externally during deposition.

The energy of gas ions (argon- Ar⁺, Ar²⁺) and nitrogen- N₂⁺, N₂²⁺) and metal ions (Cr⁺) bombarding the substrate was monitored using a Hiden EQP 300 energy analyzer with grounded

orifice of 50 microns diameter. The energy resolution of the equipment was about 0.05 eV. The probe was not directly in front of the target but about 13 cm away from the centre of race track region (figure 22). The substrate was placed at the same position as the probe. This position was chosen to know the ion flux reaching the substrate away from the centre of Type-II magnetron. In Type-II magnetron, the outer magnets are much stronger than the centre magnet and this leads to increased ionization from the centre of the target and decreased ionization towards the end. In other words, the substrate placed directly in front of the target will receive more ion flux than the one placed away from the centre of the target. The study was done to know the effect of ion flux and energy on the film properties away from the centre. The neutrals were monitored in residual gas analysis mode reflecting away the positive and negative ions from the plasma and letting in only the neutrals from the plasma. The film structure and morphology was studied with Philips X-ray diffractometer (XRD) using Cu K_α radiation of wavelength 1.54 Å using an incident angle of 5° and scanning electron microscopy (SEM). The micro hardness and Young's modulus were determined using a nano-indenter with a Berkovich diamond tip. The average of nine points was taken for each sample. The indentation depth was approximately one-tenth of the coating thickness to minimize substrate effects. The film stress was measured on thin glass plate using Dektak 6M stylus. The stress was calculated by measuring the radius of curvature of substrate before and after deposition using Stoney's equation.

$$\sigma = \frac{1}{6} \left(\frac{1}{R_{post}} - \frac{1}{R_{pre}} \right) \frac{E t_s^2}{(1-\nu) t_f}$$

Where

σ = stress in the film after deposition

R_{pre} = substrate radius of curvature, before deposition

R_{post} = substrate radius of curvature, after deposition

E = Young's modulus of substrate

ν = Poisson's ratio of substrate

t_s = substrate thickness

t_f = film thickness

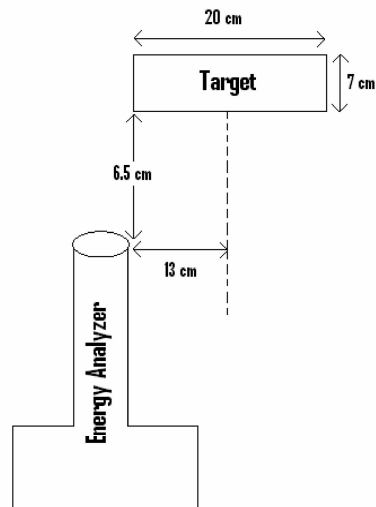


Figure 22. Schematic diagram showing the position of orifice of energy analyzer with respect to the target.

10.2 Energy and flux of ions

The DC voltage pulse applied to the target shows non-ideal behavior, which is shown schematically in figure 23. The normal ‘on’ voltage (A) is followed by a large positive overshoot (C) before settling to its normal ‘off’ value (B). (Note: Phase A will not be rectangular.) The highly energetic ions are produced in the overshoot phase, when the voltage quickly reaches very high positive value. This increases the plasma potential leading to sudden expansion of the plasma sheath at the substrate leaving behind uncovered ions that will be accelerated towards the substrate (or energy analyzer) with very high energy [25,37]. According to the different phases of pulse, the ion energy too varies widely. Continuous DC operation produces only low energy ions due to the absence of overshoot phase.

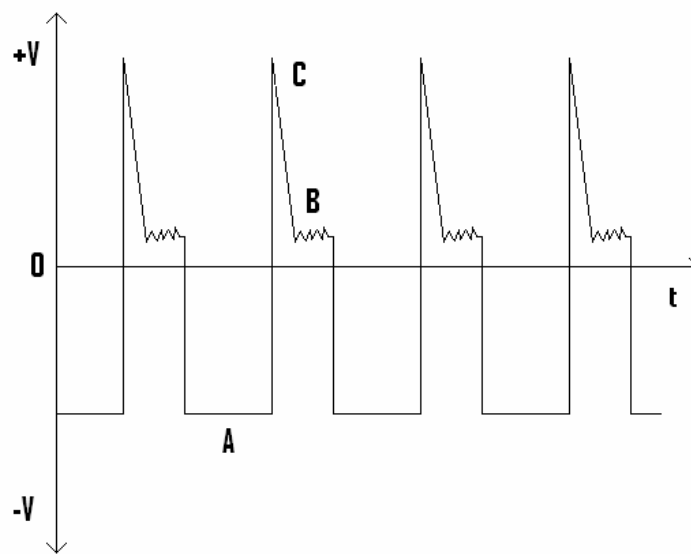


Figure 23. Schematic diagram of DC pulse showing different phases

The energy and flux of ions and neutrals of Ar^+ , Ar^{2+} , N^+ , N_2^+ and Cr^+ were determined for varying pulse frequency from continuous DC to 350 kHz at pulse off time of 1.1 μs . The typical energy spectra as obtained for Cr^+ , Ar^+ and N_2^+ at 350 kHz is shown in Figure 24. The neutrals of atomic nitrogen and chromium decrease with pulse frequency (Fig. 25). The duty cycle decreases with pulse frequency decreasing the chromium sputtering rate and so the chromium neutrals. As nitrogen flow is proportional to 60% of chromium emission, the nitrogen neutrals too decrease with chromium neutrals. Although the Ar flow should increase (and so are the neutrals) with decrease in nitrogen flow to keep the operating pressure constant, the total flux of argon and nitrogen neutrals are not constant but increasing with the pulse frequency. The ratio of nitrogen and metal neutrals to argon neutrals can be seen decreasing with the pulse frequency. The ratio of Cr to N_2 and N flux was found to be decreasing at 350 kHz while at 100 kHz, Cr/N flux was at maximum. This relative metal and reactive gas neutral might have an effect on film stoichiometry.

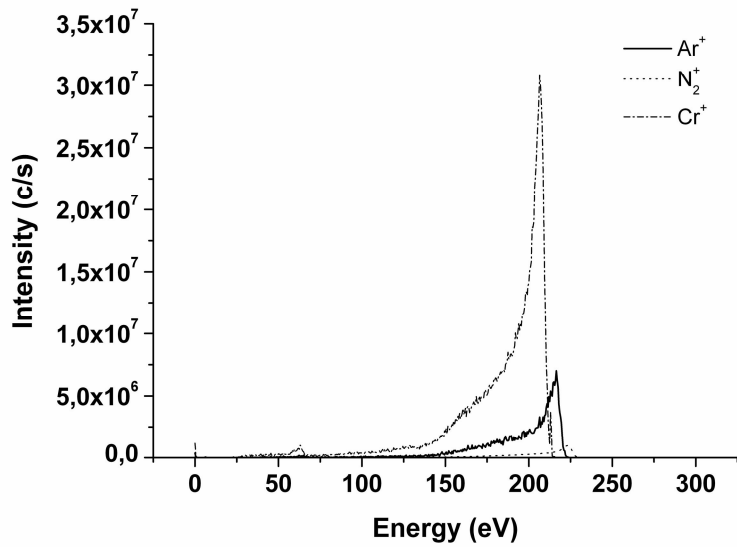


Figure 24. Energy spectrums of chromium and gas ions at pulse frequency of 350 kHz and pulse off time of 1.1 μ s

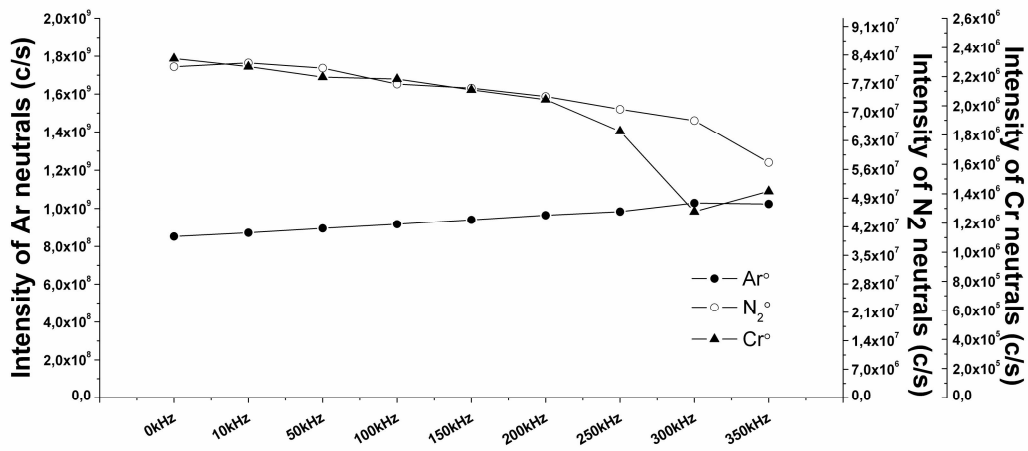


Figure 25. Variation of metal and gas neutrals with pulse frequency at 1.1 μ s

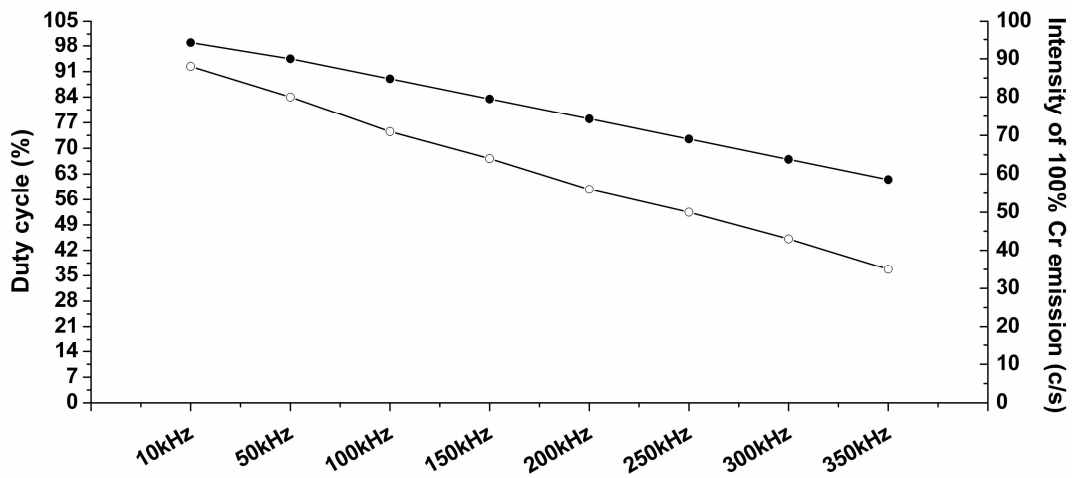


Figure 26. Variation of duty cycle and 100% Cr emission intensity at 328nm with pulse frequency at 1.1 μ s

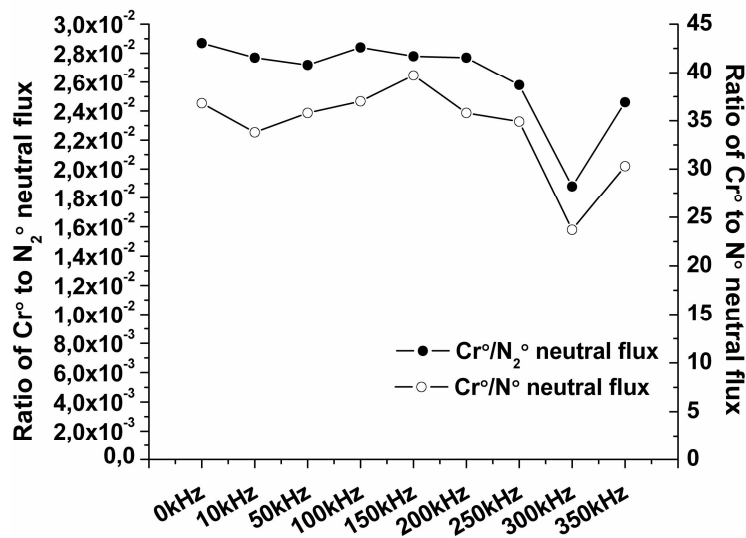


Figure 27. Variation of ratio of metal and reactive gas neutrals with pulse frequency at 1.1 μ s

The general level of ion bombardment was found to increase with the pulse frequency but shows a tremendous increase at higher frequencies. This might be due to high positive overshoot at 350 kHz, when the plasma reaches high positive value when the plasma sheath extends suddenly leading to high energetic flux of bombarding ions. This is the normal case expected, as at higher frequencies, the number of overshoot per unit time increases resulting in increased ion energy flux. In figure 26, the flux of ions were put in various energy bins and can be seen that at higher frequencies, the energy of ions reaches above 250 eV even without any substrate bias.

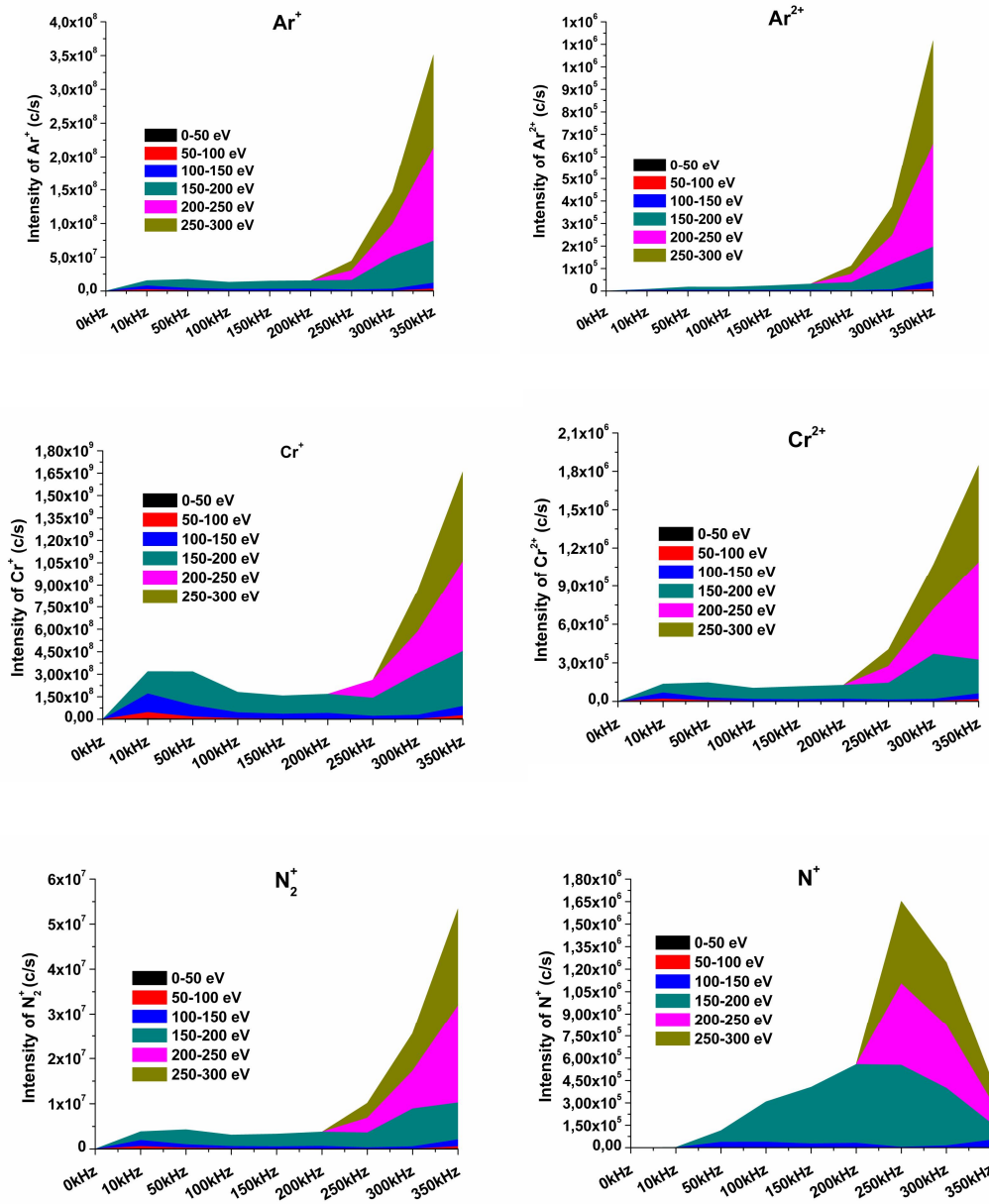


Figure 28. Variation of integrated intensity of gas and metal ions with pulse frequency at 1.1 μs

The Ar⁺ flux is found to increase at higher rate than Cr⁺ and N₂⁺ as can be seen from the ratio of flux of metal and reactive ions to that of Ar⁺. This might be due to the fact that the Ar atoms are more in number than the other atoms being residual gas and so the probability of ionization is more for Ar atoms. The doubly charged ions of metal and argon gas follows similar increment as that of single charged ions but the N⁺ ion is found to decrease at higher frequencies for reason not known. The ratio of reactive and metal ions to Ar ions decreases with pulse frequency. This is expected as the Ar neutrals increase at faster rate than Cr and N₂.

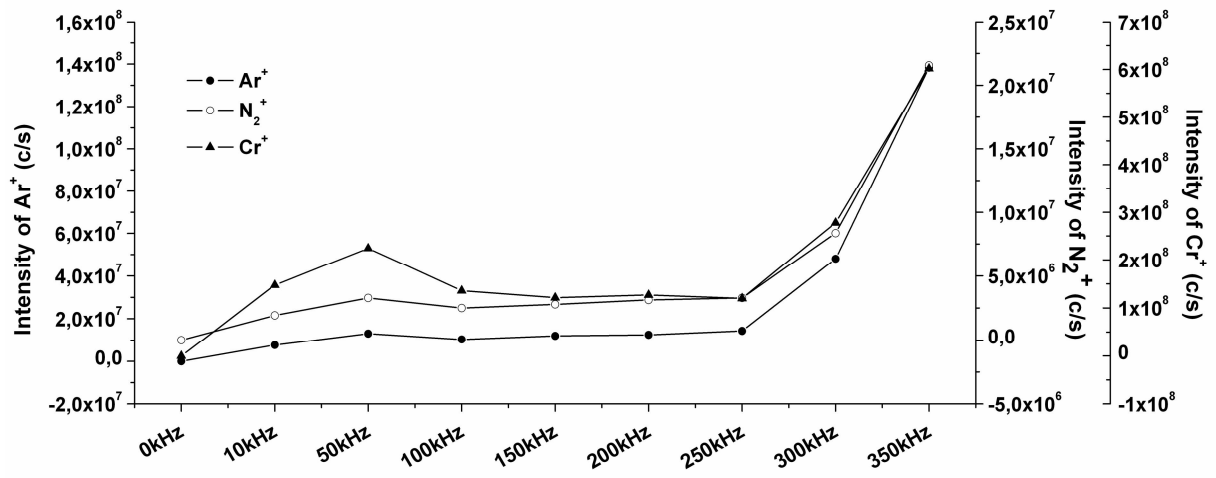


Figure 29. Variation metal and gas ions with pulse frequency at 1.1 μs

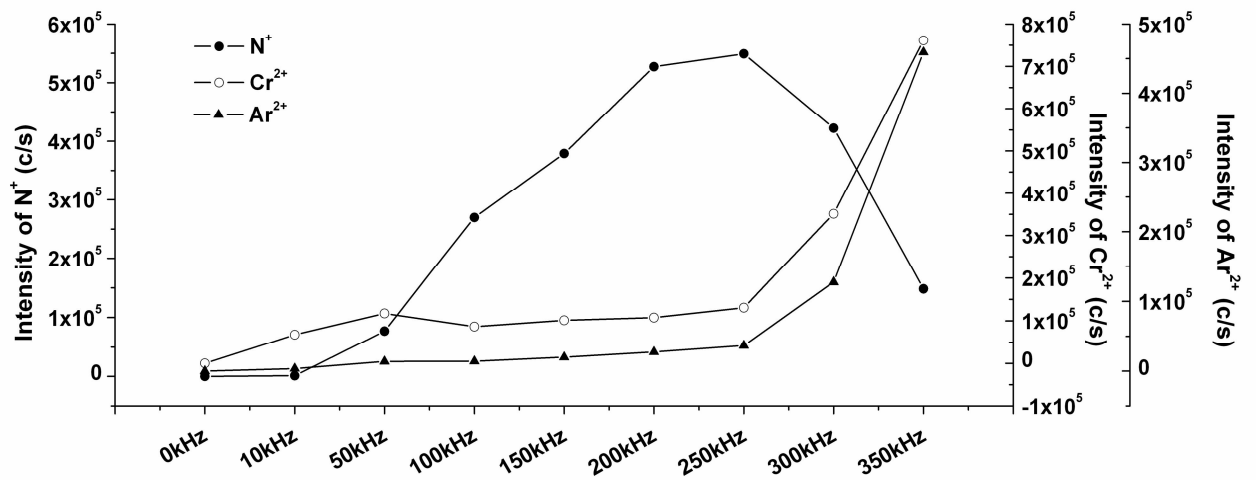


Figure 30. Variation of ionized nitrogen and doubly ionized argon and chromium with pulse frequency at 1.1 μs

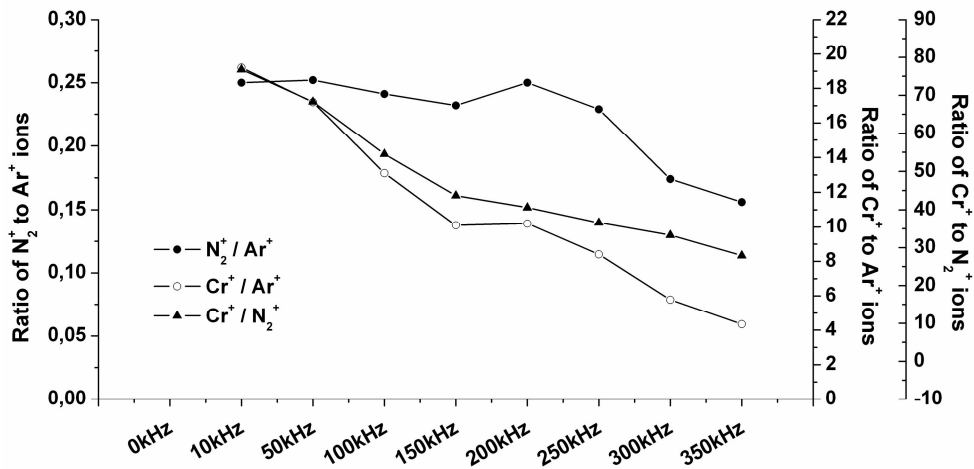


Figure 31. Variation of ratio of metal and reactive gas ions to argon ions with pulse frequency at 1.1 μ s

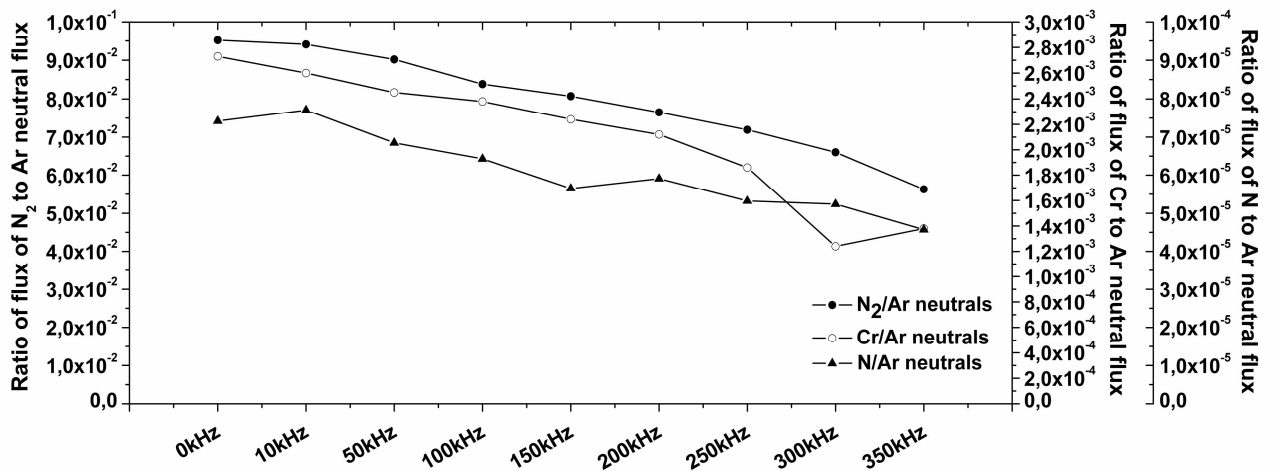


Figure 32. Variation of ratio of metal and reactive gas neutrals to argon neutrals with pulse frequency at 1.1 μ s

10.3 Film structure and morphology

The effect of the variations in ion bombardment on the crystal structure and morphology of the chromium nitride films have been investigated. The films deposited on glass plates were studied for the structural properties and on (100) Si, for mechanical properties. The coatings deposited over the range of pulse frequency were predominantly cubic CrN with a preferential (111) orientation, but a small amount of the Cr₂N phase was also observed. From thermodynamic point of view, the texture of the film is determined based on minimization of the energy comprising mainly of surface energy, strain energy, stopping energy and interface energy. The contribution of interface energy is less when there is large lattice mismatch between the film and substrate as between glass plate and chromium nitride. In spite of thermodynamic effects, kinetic effects are found to play a vital role in determining the film texture and found to be dependent on many deposition parameters like substrate temperature, substrate biasing, ion energy

bombardment, ion to neutral ratio and nitrogen partial pressure [40-45]. The (111) plane is found to have lowest strain energy and the growth is promoted when the energy is dominated by strain energy. As the CrN films deposited at all frequencies showed (111) orientation, the strain energy might be the dominating factor. The kinetic effects like ion energy bombardment and ion to neutral ratio has also been found to have major role in film crystallography and explained in the following section.

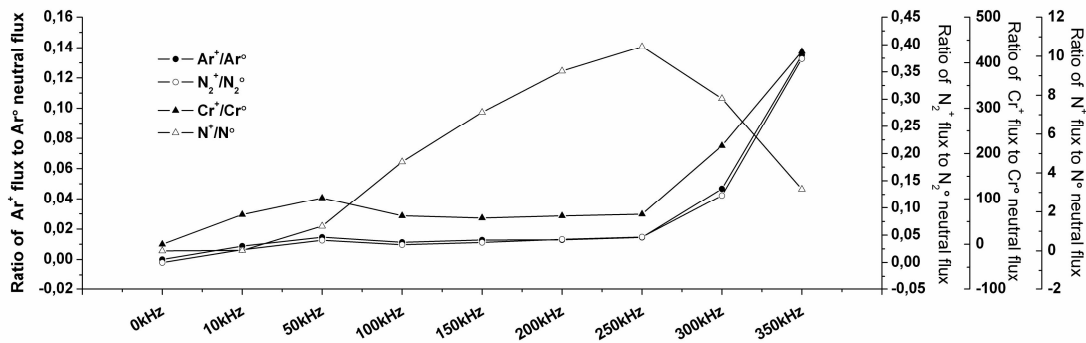
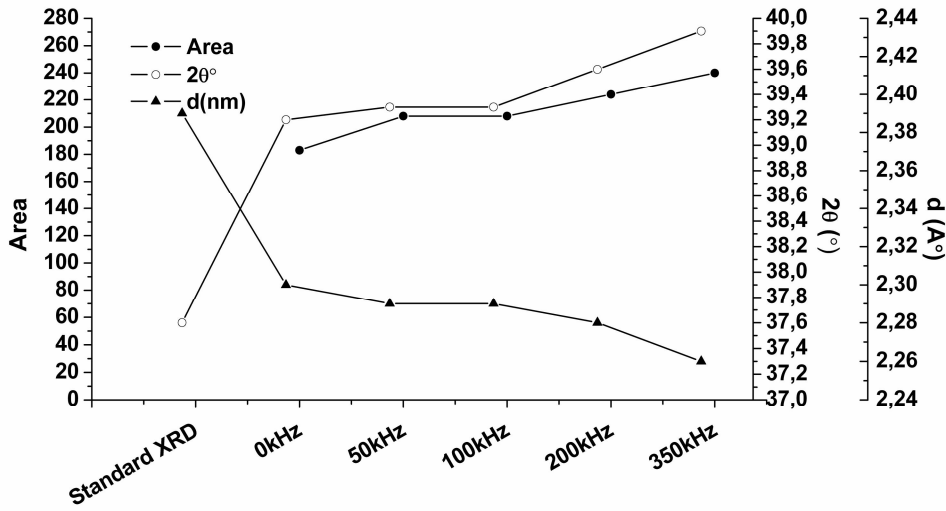
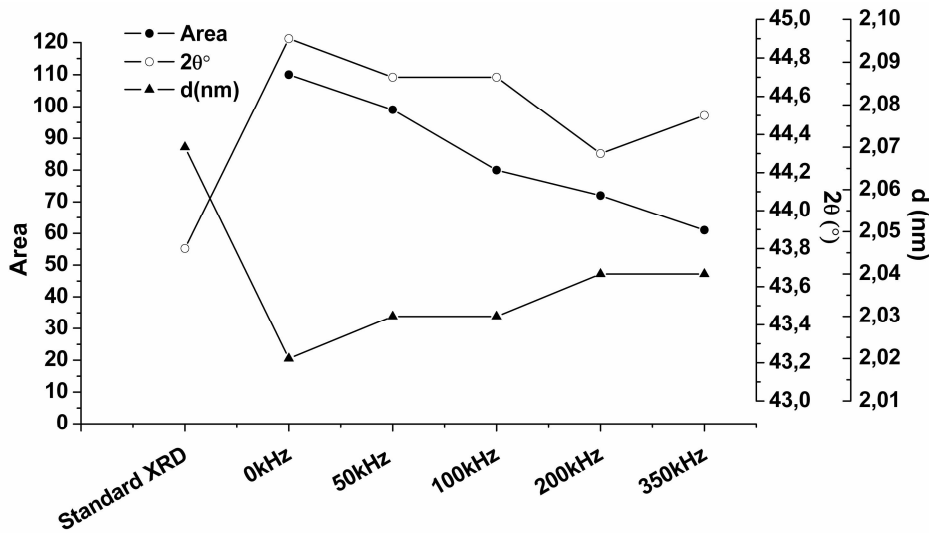


Figure 33. Variation of ratio of ions to neutrals with pulse frequency at 1.1 μ s



34 a



34 b

Figure 34a and 34b. The variation of d-spacing of CrN (111) and CrN (200) planes at different DC pulse frequency

The position, full width at half maximum (FWHM) and area of the peaks were found by a Gaussian fit. The relative orientation of the CrN was measured by comparing the peak areas, and the lattice parameters were calculated. The inter-planar distance of CrN planes of films, deposited at continuous DC and different pulse frequencies is clearly smaller than that of the bulk compound (JCPDS file no. 11-0065). With the increase in frequency, the d-spacing of CrN (111) is decreasing i.e., the plane is shrinking with increase in frequency but that of the CrN (200) plane is expanding with the frequency (figure 34.) These two apparently contradictory results can be reconciled, if the cubic CrN becomes somewhat more tetragonal as frequency is increased. If the 'a' and 'c' lattice parameters are calculated, there is consistent behavior as

shown in figure 14. Parameter 'a' is almost constant whereas 'c' shows a gradual decrease with increasing pulse frequency. The distortion is probably due to the bombardment of energetic ions, which increase with the pulse frequency. At 350 kHz, the distortion is at the maximum of about 11%. The films also become more preferentially (111) oriented as pulse frequency increases. The ratio of area of peaks of CrN (111) to CrN (200) increases from 1.7 under DC conditions to 3.9 at 350 kHz. The strain energy layers with thickness but in the present study, the films deposited at 350 kHz had the lowest thickness. This might be due to continuous increase in strain energy with increase in ion energy bombardment, which increases with pulse frequency.

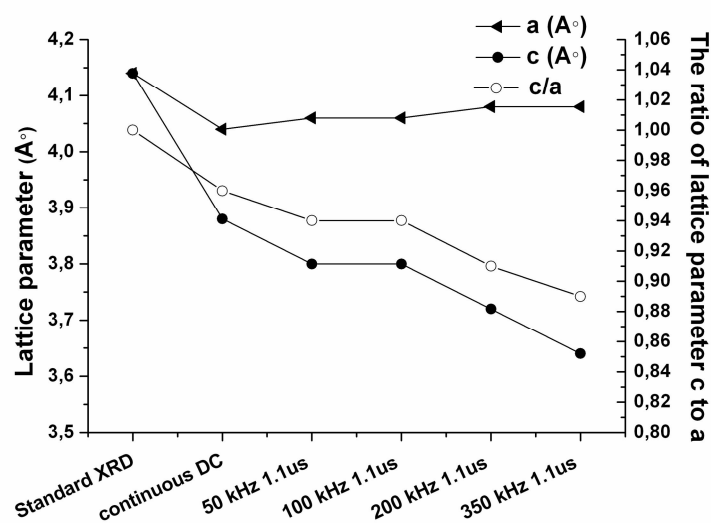


Figure 35 The variation of lattice constants of CrN at different DC pulse frequency

The cross-section of CrN film at different frequencies by SEM does not show much difference but the film deposited at 350 kHz can be found to be denser than at lower frequencies due to high energetic particle bombardment. The decrease of the film thickness with pulse frequency can also be seen clearly. The thickness of the film is about 2.4 micron under DC conditions and gets reduced to about 50% at 350 kHz, which is about 1.2 microns. This is due to decrease in sputtering rate as can be seen from the decrement of 100% Cr emission line at 328 nm due to decrease in duty cycle with the pulse frequency.

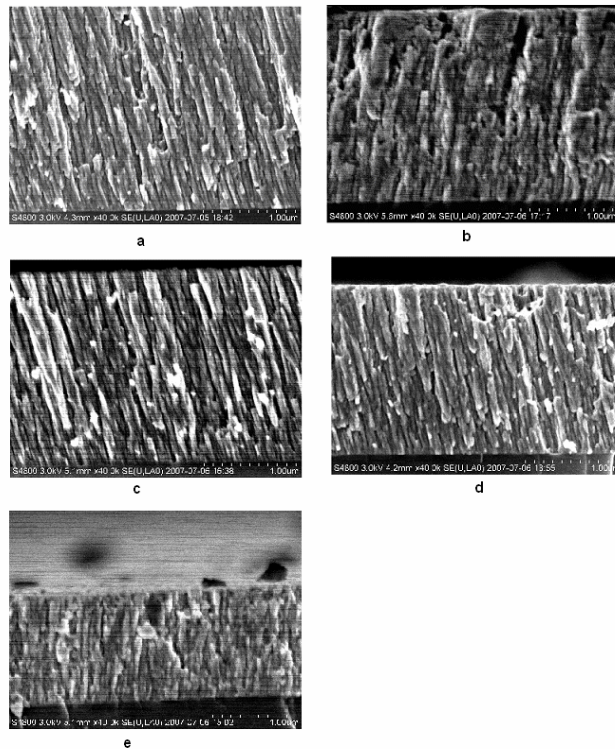


Figure 36. SEM cross-section of CrN deposited at a) 0 kHz, b) 50 kHz, c) 100 kHz, d) 200 kHz and e) 350 kHz

10.4 Film stress and mechanical properties

The measured stress was found to be tensile for all the films deposited at continuous DC and different pulse frequencies. The stress was found to be at maximum for 100 kHz and minimum for continuous DC and 350 kHz. It is known that magnetron sputtered films deposited above 7.5 mTorr exhibit tensile stress [46]. At high pressure, the particles bombarding the substrate will lose energy through collisions and bombard the substrate at oblique angle of incidence increasing the atomic self shadowing effect. With these effects, the film exhibit tensile stress and this can be interpreted in terms of Grain Boundary Relaxation (GBR) model [47]. In addition, the deposition temperature was low about 77°C when the surface mobility of atoms is low and so the self-shadowing effect might have increased.

The hardness and Young's modulus were found to be high for films for minimum tensile stress and low for maximum stress. This is consistent with the results obtained by several researchers that hardness decreases with increase in tensile stress and increases with increase in compressive stress [48]. This is explained by simple principle of plasticity. It is known that the stress imposed by indentation, normal to the film surface is compressive. During indentation, the tensile residual stress parallel to the surface increases the local von Mises stress, enhancing the plastic deformation and hence reducing the hardness. The stress of the film does not scale with total ion energy bombardment with the frequency. At high frequencies, the tensile stress might have decreased due to the high energetic particle bombardment inducing compressive stress. At continuous DC, the tensile stress might be low due to small lattice distortion. As the distortion

increases with ion energy bombardment, the film stress might have increased. After certain frequency, the high energetic bombardment might have relaxed the stress reducing the stress magnitude. The building up of stress and its relaxation is found by other researchers too [49].

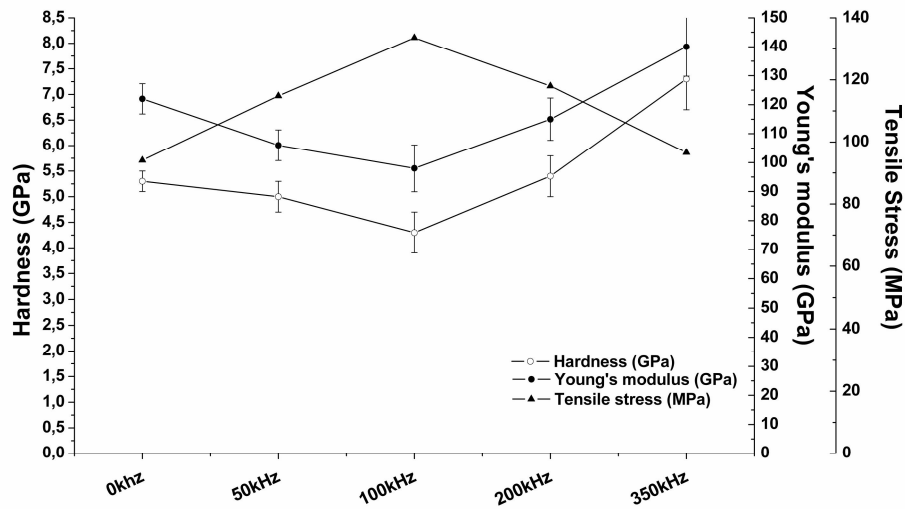


Figure 37. Variation of stress, hardness and Young's modulus with pulse frequency

11 Characterization of films

11.1 Chromium nitride Coating on CFRP

The deposition was carried out in a Teer coatings Ltd cylindrical closed field magnetron deposition system. One single rectangular chromium target of 99.5% purity with a dimension of $145 \times 350 \text{ mm}^2$ was used. The substrate materials used are CFRP-2 and CFRP-5. Prior to coating, the CFRP samples were pre-cleaned by ultrasonic waves with detergent solution, isopropyl alcohol and acetone for about ten minutes in each solution. The samples were then baked in an oven for eighteen hours at a temperature of 80°C .

The sputtering gas was Ar or an Ar/N₂ mixture and the stoichiometry was controlled using optical emission monitor (OEM) feedback from the Cr emission line at 426 nm. The OEM setting was 60%, 65% or 70% of the maximum chromium emission to discover the effect of film stoichiometry on the coating behavior. The samples were ion cleaned using argon plasma at a substrate bias of -400 V and the deposition was done with substrate bias voltage of -30 V. The ion cleaning was done at different time intervals of 10, 15, 20 and 30 minutes. Pulsed DC power was applied to the chromium target at a frequency of 250 kHz and a pulse off time of 1600 ns. The target was operated in the controlled current mode, fixed at 2 A. The background pressure in the chamber was 5×10^{-5} mbar and the sputtering pressure during chromium deposition was between 4.2×10^{-3} and 5.5×10^{-3} mbar and for chromium nitride deposition was between 3.6×10^{-3} mbar and 4×10^{-3} mbar. The initial deposition was chromium for about 5, 30 and 60 minutes to enhance the adhesion of coating on to the substrate prior to the deposition of chromium nitride for 1 hour. The thickness of the deposited films was approximately 0.8 microns. X-ray diffraction measurements showed that in all cases, the deposited material was cubic CrN. The temperature of the substrate during deposition was monitored by means of temperature-sensitive tapes attached to their surface. The structure of films was determined using two and four targets and the deposition temperature was measured.

The structure of the coating was studied by X-ray diffraction (XRD) using Philips diffractometer with Cu K α radiation of wavelength 1.54056 Å in 2 θ - Ω mode. The grain size was calculated using the Scherrer formula [21].

The micro-hardness and Young's modulus was determined using the nano-indenter XP with a Berkovich diamond. Measurement was done at ten points for each sample. The indentation depth was set at 80 nm, which is about one-tenth of the coating thickness.

The microstructure of the film was analyzed with a scanning electron microscope (SEM).

11.2 Structural analysis

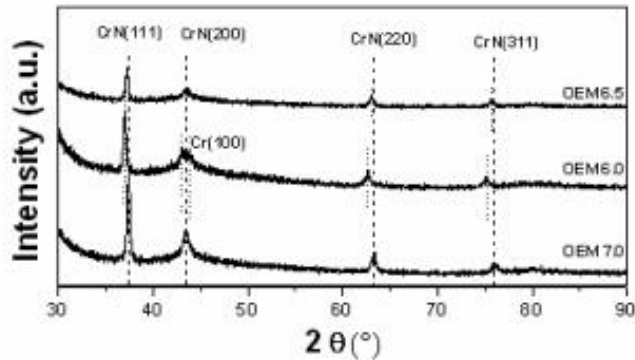


Figure 38. X-ray diffractograms of CrN films.

Figure 38 shows the X-ray diffractograms of chromium nitride films coated with different OEM values. The samples for X-ray diffraction were pre-cleaned, baked for 18 hours and ion-cleaned for 10 minutes followed by deposition of chromium for 5 minutes and then chromium nitride. Cubic CrN is observed in all the diffractograms with preferential (111) orientation. The variation in OEM setting gave only a variation in stoichiometry without a major effect on the crystal structure. The grain size was found to be 29, 25 and 27 nm for samples of OEM 60 %, 65 % and 70 % respectively.

The cross sectional view of SEM micrograph in Figure 39 shows chromium nitride and underlying chromium layers, the thicknesses of which are found to be 0.7 and 0.1 microns respectively. The surface roughness could be clearly observed from the micrograph. The film has columnar structure with inter-granular voids and it is not fully dense. This could be due to the low deposition temperature.

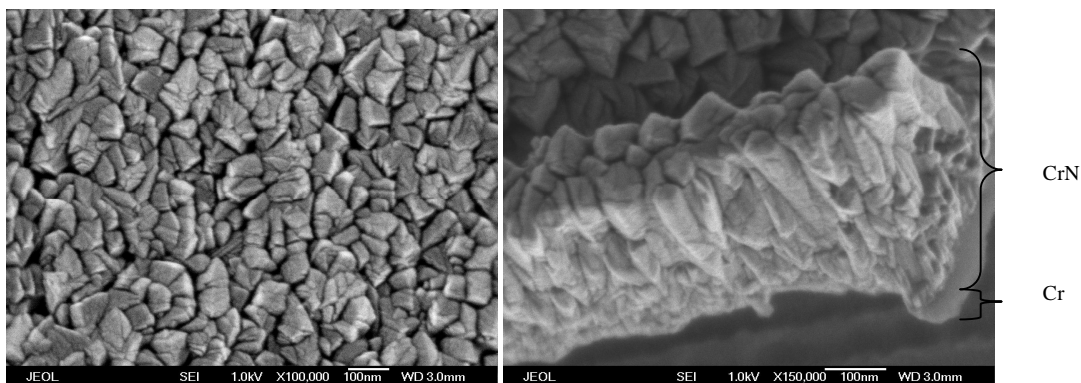


Figure 39. SEM micrographs of CrN film on CFRP substrate showing the surface (a) and cross section (b) of the film.

The temperature of the samples coated widely varied for number of targets used. The deposition temperature for four targets was above 155°C, two targets were about 143°C and one target was about 90°C, which is in the safer level. The substrate being a polymer composite could withstand maximum temperature of about 100°C. When the substrate exceeds this temperature, the structure of the substrate material will change.

11.3 Determination of mechanical properties

The values of micro hardness and Young's modulus measured for the samples deposited with OEM 60 %, 65% and 70% are shown in Table 3. The hardness and modulus are found to be higher for OEM of 65 %. This could be attributed to more stoichiometric CrN film deposited with OEM 65% than that of OEM 60% and 70 %, where higher concentration of N₂ and Cr respectively might have affected the stoichiometry. Note that even though the indentation depth is restricted to 10% of the film thickness, the hardness values are strongly influenced by the soft substrate. These measurements only represent a comparison between samples, not an accurate value.

Table 3. Micro hardness and Young's modulus of CrN films on CFRP substrate determined by nano-indentation.

<i>OEM</i>	<i>Hardness [GPa]</i>		<i>Modulus [GPa]</i>	
	<i>Average</i>	<i>Standard deviation</i>	<i>Average</i>	<i>Standard deviation</i>
<i>60 %</i>	<i>4.3</i>	<i>1.25</i>	<i>28.0</i>	<i>11.71</i>
<i>65 %</i>	<i>5.5</i>	<i>1.97</i>	<i>37.9</i>	<i>9.23</i>
<i>70 %</i>	<i>5.1</i>	<i>1.34</i>	<i>27.1</i>	<i>5.88</i>

11.4 Chromium nitride coating on polymers

The CrN coating is observed with (200) preferential orientation on vinyl ester irrespective of OEM set point of Cr emission (Figure 40). (222) plane of CrN on polycarbonate is strongly oriented for the OEM set point of 60% and 70% of Cr emission. CrN deposited with OEM set point of 60% of Cr emission shows preferential orientation of (200) (Figure 41). The film on polyamide showed mixture of cubic and hexagonal phases of chromium nitride (Figure 42). The peak at 2θ angle of around 35 degree might be that of oxinitrides formed due to out gassing of polyamide substrate. This peak reduced at OEM set point of 50%. The texture of the films deposited on different polymers at same conditions found to vary significantly. This might be because of the different surface mobility of atoms on the substrates that differs with surface energy. The texture is also determined by nitrogen partial pressure which has been found to affect certain substrates. Cubic plane with (200) orientation is preferred where the surface mobility is high. From this point of view, it might be said that atoms have more surface mobility on vinyl ester giving (200) texture. In case of PC, only films deposited with 60% of Cr emission showed (200) orientation whereas those deposited with 60% and 70% are of (222) orientation. It has been known that the texture is also determined by other experimental factors like nitrogen partial pressure, thickness, substrate bias, substrate temperature etc. In PC, the texture might have been determined by nitrogen partial pressure.

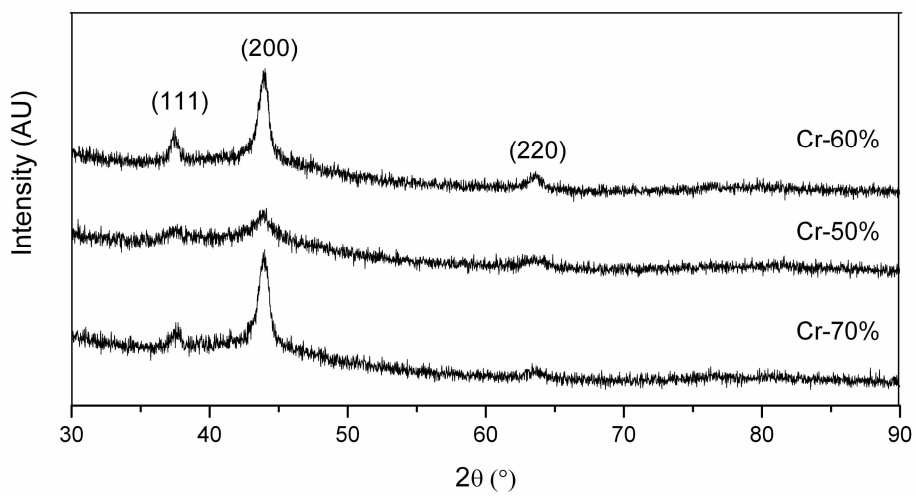


Figure 40. X-ray diffractograms of chromium nitride on vinyl ester at different set point of chromium emission.

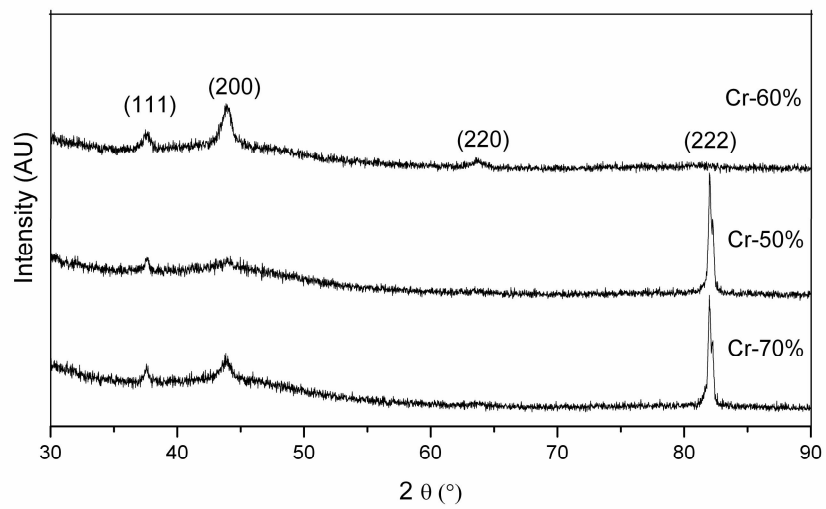


Figure 41. X-ray diffractograms of chromium nitride on polycarbonate different set point of chromium emission.

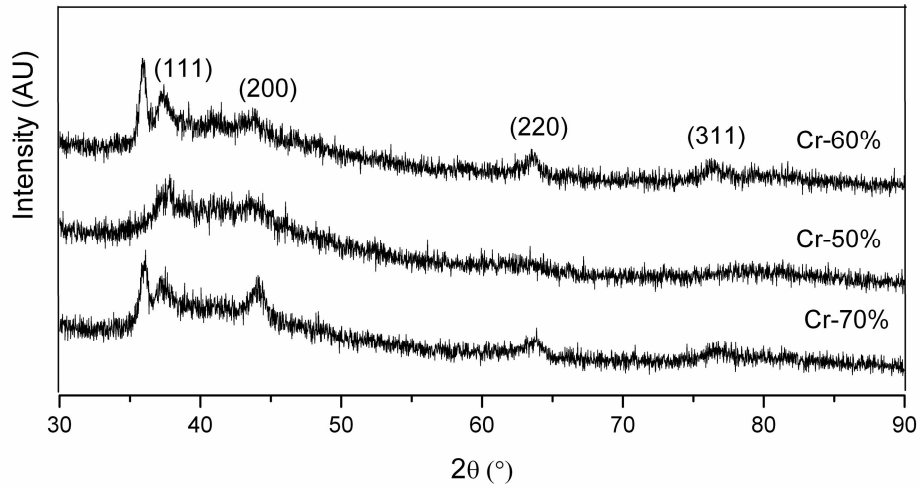


Figure 42. X-ray diffractograms of chromium nitride on polyamide at different set point of chromium emission.

11.4.1 Determination of Hardness and Young's modulus

The hardness and Young's modulus was constant for films deposited on polyamide irrespective of the OEM setting (in Fig.43). The vinyl ester deposited with 60% Cr emission set point showed high hardness and Young's modulus. The films deposited with 50% Cr emission showed lower hardness and Young's modulus (fig 43). This might to be due to low orientation of (111) and (200) cubic chromium nitride planes which is comparatively less than that of other two set points.

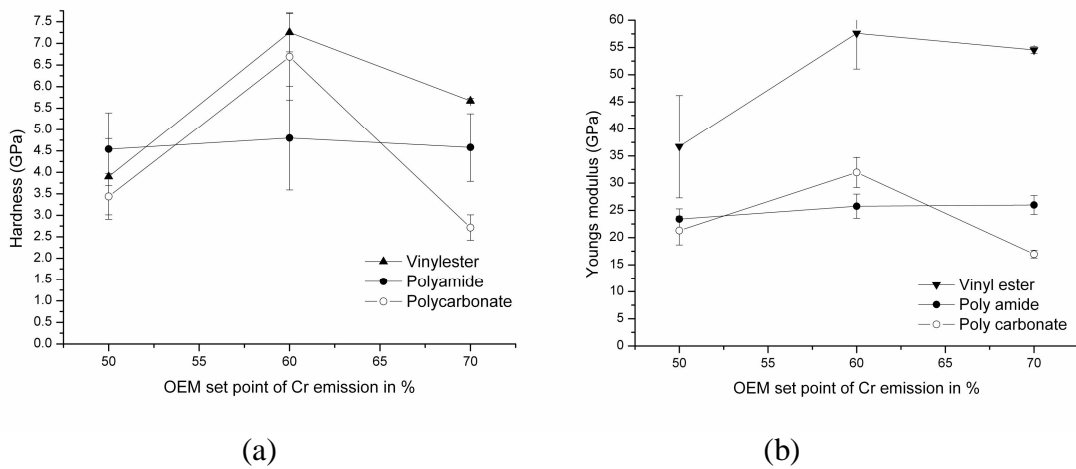


Figure 43. Variation of Hardness (a) and Young's modulus (b) with different OEM setting for vinyl ester and polyamide

11.5 DLC and Ti doped DLC coatings

11.5.1 Deposition Parameters – Frequency and Off-time of Pulse

The basic studies concerning of the film thickness were carried out by depositing plain titanium metal layer by pulsed d.c. magnetron sputtering. As a power source, the Advanced Energy Pinnacle plus d.c. power supply was used. The titanium layer was deposited on silicon wafers and glass plates. In the initial stage the parameters under interest were frequency and pulse off-time which were applied to the titanium target by pulsed DC power.

The studied combinations:

350 kHz	1.1 us	1.1 us (max)
250 kHz	1.1 us	1.6 us (max)
150 kHz	1.1 us	2.6 us (max)
50 kHz	1.1 us	4.0 us (max)

The measured thicknesses are shown in Figure 44. The thicker film was obtained with lower frequency value. In addition, the behavior with 150 and 250 kHz leads to the assumption that short off-times have deposit thicker films. Also the graph in Figure45 points out that the increased duty cycle during pulse results in thicker film. Although there is significant scatter, a trend line can be clearly seen.

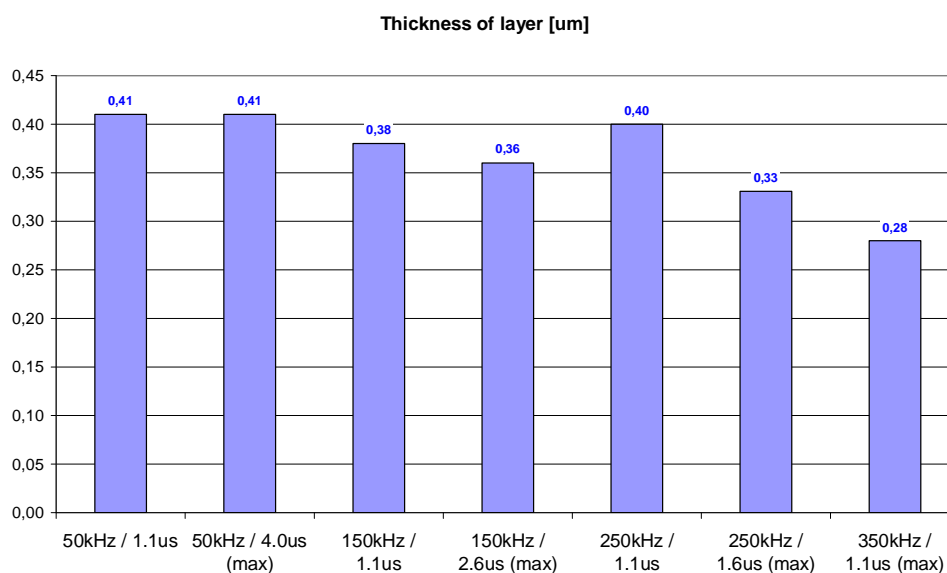


Figure 44. Thickness as a function of frequency and off-time of pulse.

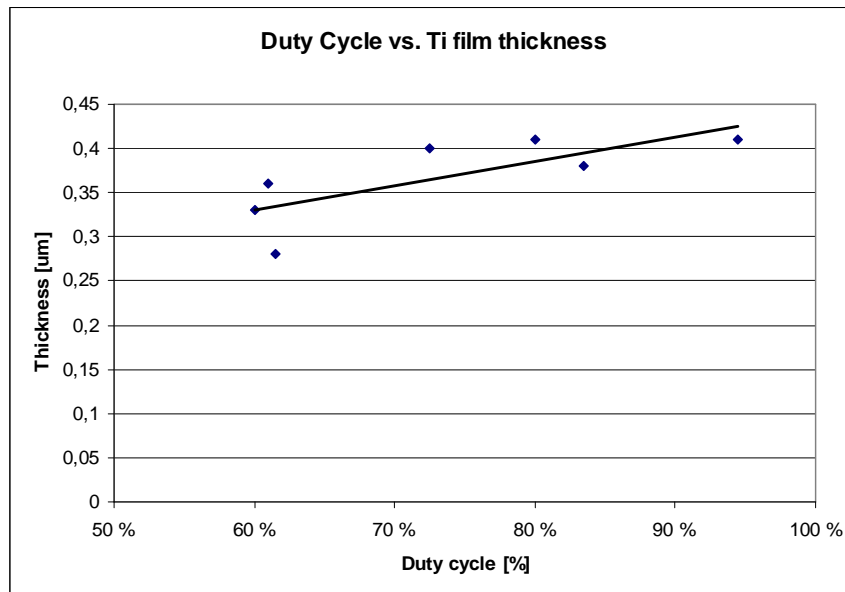


Figure 45. Film thickness as a function of duty cycle of DC pulse.

11.5.2 Deposition Parameters – BIAS Voltage and Titanium Proportion

In order to develop the properties of DLC films, modifications to films have been made by metal doping. The metallic Ti with relatively good plasticity can give a stress relaxation at the expense of a hardness decrease [6]. A relatively thin Ti interlayer can considerably change the mechanical properties of the coating. It was expected that the addition of titanium into the diamond-like carbon films could significantly reduce the internal stress and in addition, improve the adhesion properties of these films.

It has been reported that by using the bias voltage, which affects on the TiC grain size and structure, improved hardness and elastic modulus values are achieved [50]. It is assumed that ion bombardment during deposition disturbs the columnar growth and decreases the grain size as the ion energy is increased [51].

The sputtering gas was Ar or an Ar/CH₄ mixture and optical emission monitor (OEM) feedback from the titanium emission line at 501 nm was used to control the proportion of titanium. The OEM setting was 30%, 60%, 70%, 80% or 90% to discover the influence on film structure. The deposition was done with substrate bias voltage off, 100 V, 300 V or 500 V.

Figure 46 a and b, 324.9 nm and 632.9 nm respectively, are shown the graphs between different OEM percentages in depositions when the bias was off. The Raman spectra with 632.9 nm laser display two strong peaks at approximately 1320 and 1590 cm⁻¹, which are associated with the A_{1g} and E_{2g} vibrational modes of graphite [52, 53]. However, with 324.9 laser the Raman spectra display the peak at approximately 605 cm⁻¹ correspond to titanium carbide [52]. Also X-ray diffraction measurements revealed strong peaks corresponding to cubic TiC. It should be noticed that TiC is an interstitial carbide and it is essentially a non-stoichiometric compound with carbon

vacancies. Hence, all the Raman peaks observed are disorder-induced Raman peaks due to the carbon vacancies because stoichiometric TiC has no Raman active vibration modes [54].

Raman spectra showed only difference in intensities. Again with different wavelengths of laser DLC and titanium carbide peaks are observed. The height of cubic TiC peaks as a function of bias voltage was plotted in Figure 48. The trend is clearly seen, higher bias voltage gave higher peak intensities.

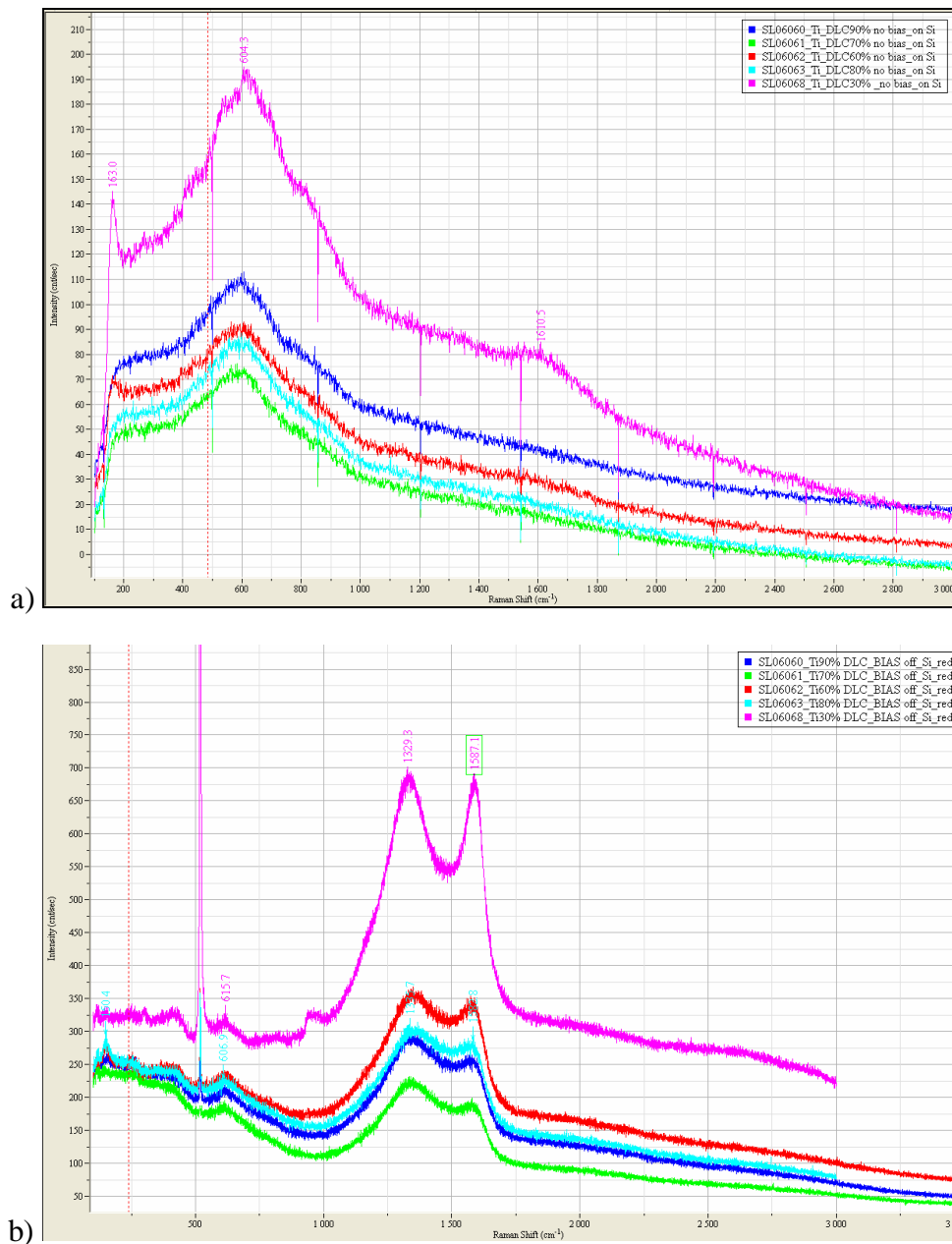


Figure 46. Raman spectra of Ti-DLC films with different OEM values and bias off.

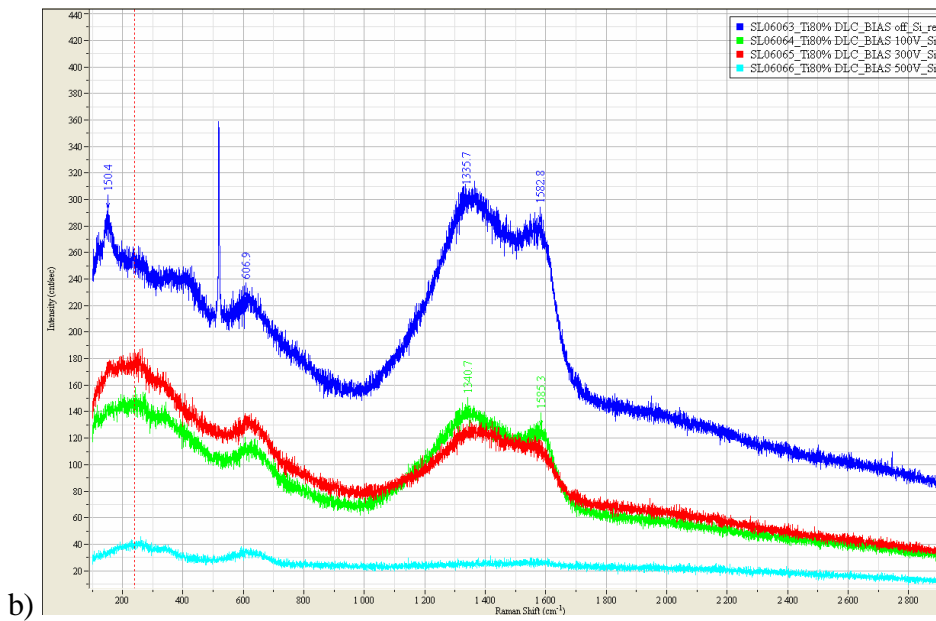
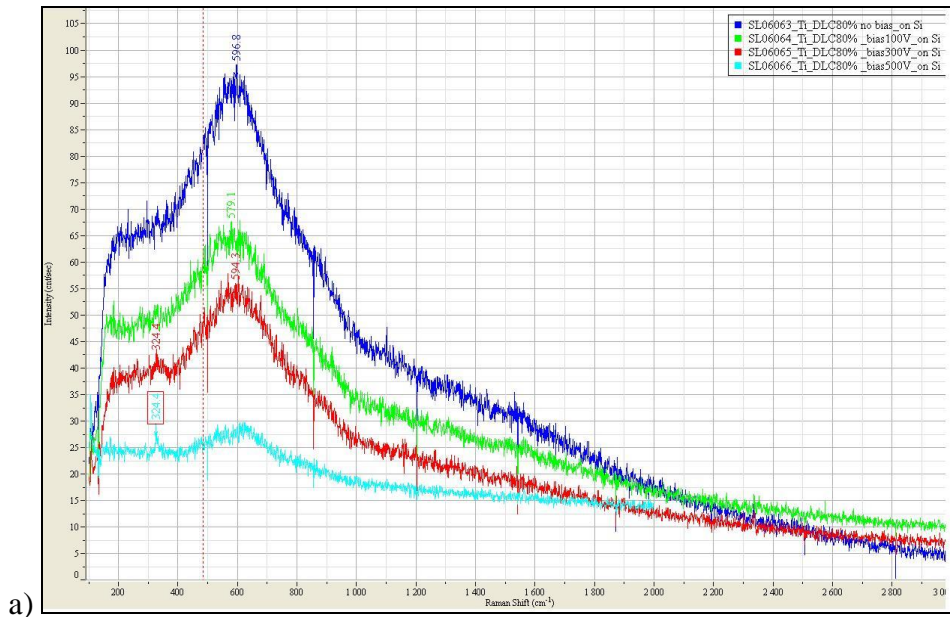


Figure 47. Raman spectra of Ti-DLC films with different bias voltages and OEM 80%.

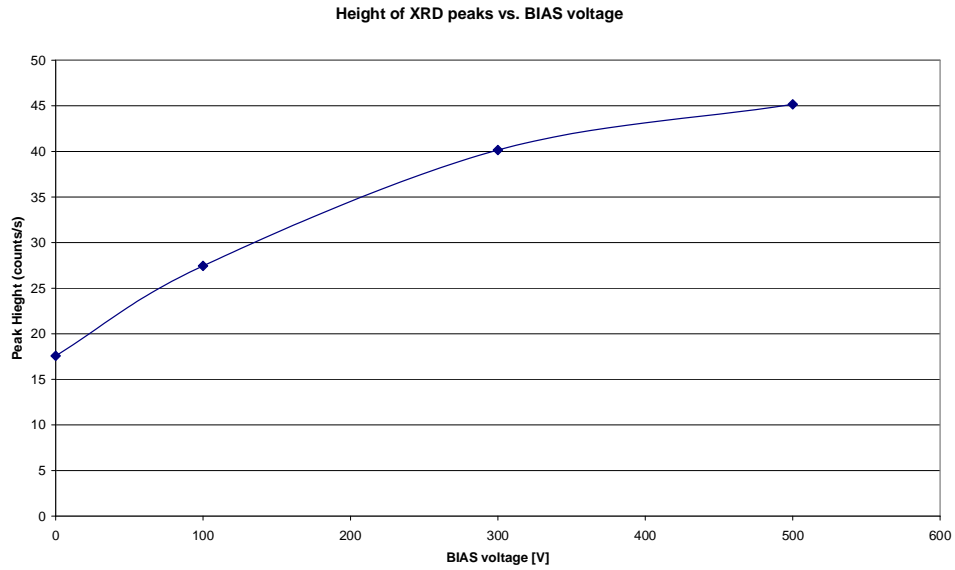


Figure 48. The peak height of cubic TiC as a function of BIAS voltage.

It was known beforehand that the disadvantage with the used deposition technique is low deposition rate. Hence, some depositions were made without drum rotation to achieve thicker films and the position of the substrates was in the front of target. The thickness of the films that were deposited without rotation of substrate was approximately four times greater than those that were deposited with sample rotation. Although the films were thicker, the surface morphology and cross section of the films by SEM showed that the films were not dense like the thinner samples (Figure 49 and Figure 50).

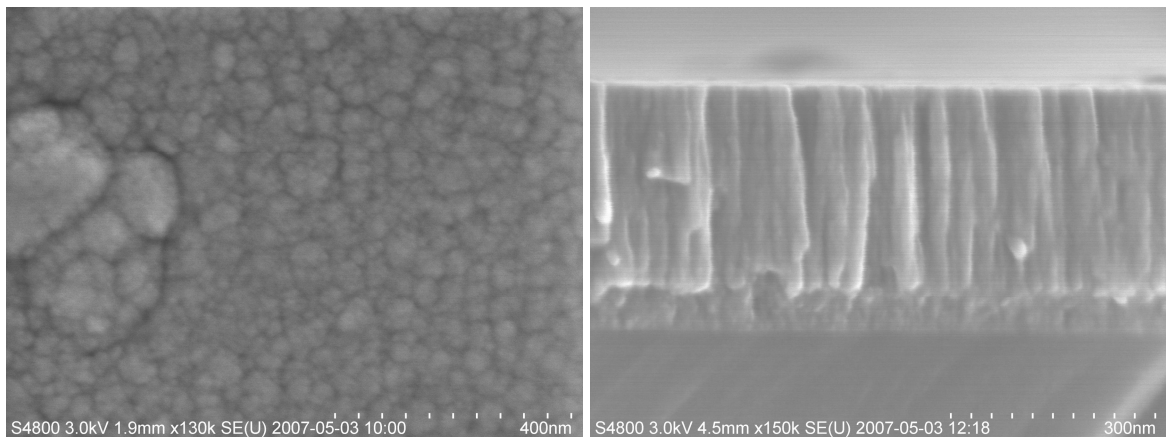


Figure 49. SEM micrographs of microstructure of Ti-DLC film deposited with rotation.

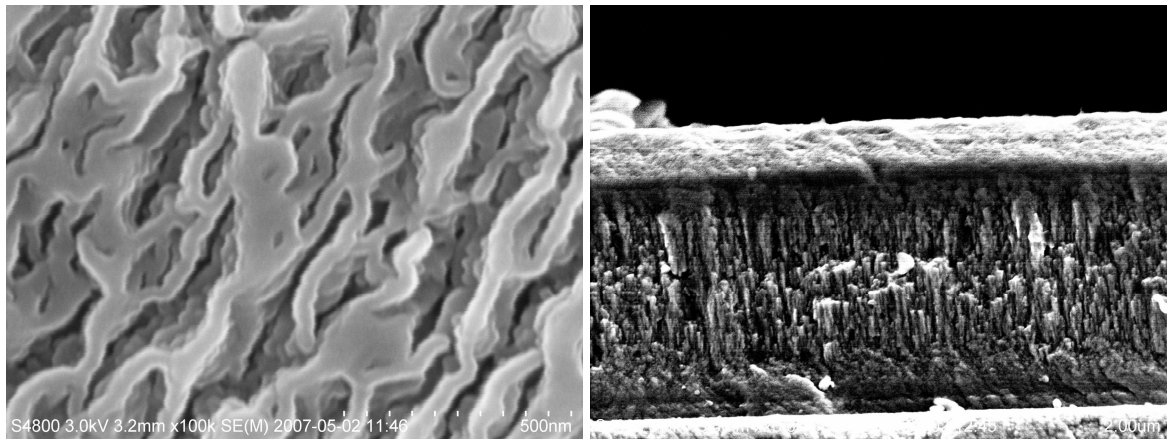


Figure 50. SEM micrographs of microstructure of Ti-DLC film deposited without rotation.

12 Wear-resistant behaviour of coating-composite combination

12.1 Abrasive wear performance of coated composites

The ball cratering technique is routinely used and is commercially available for the measurement of coating thickness. In this study the same method was used as a small-scale abrasive wear test [55]. This is achieved by grinding a small crater in a coating with a ball of known geometry to provide a tapered cross-section of the film when viewed under an optical microscope. A schematic representation of the crater is shown in Figure 51.

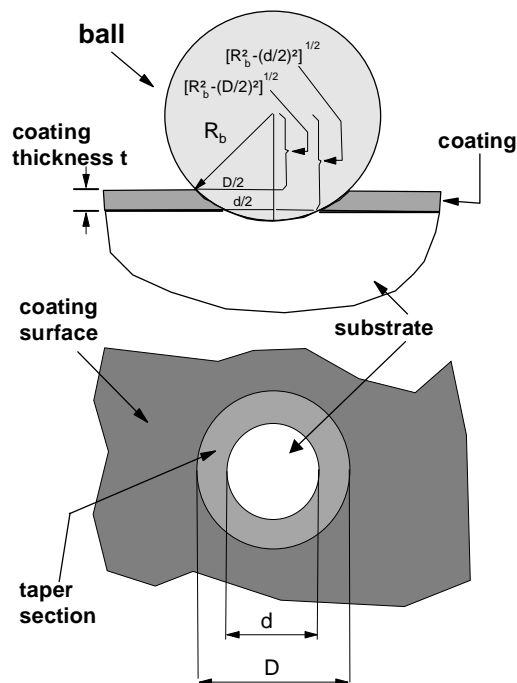


Figure 51. A schematic diagram of the crater and the geometry used for calotest.

The wear measurement done on chromium nitride coated composite and vinyl ester substrates by ball cratering is shown in Figure 5. The fibres coming out of the composite surface makes the wear measurement difficult whereas vinyl ester itself did not get affected. Thus, in order to get fibre free surface, a thick polymer layer could be coated over CFRP. The wear measurement of vinyl ester gave the wear scar diameter of $1200 \mu\text{m}$ and crater depth of $12 \mu\text{m}$, which is more than the thickness of the coating ($0.8 \mu\text{m}$). Deforming with the substrate, the coating is found to adhere strongly to the surface. Thus, in spite of being soft, the substrate could be protected strongly.

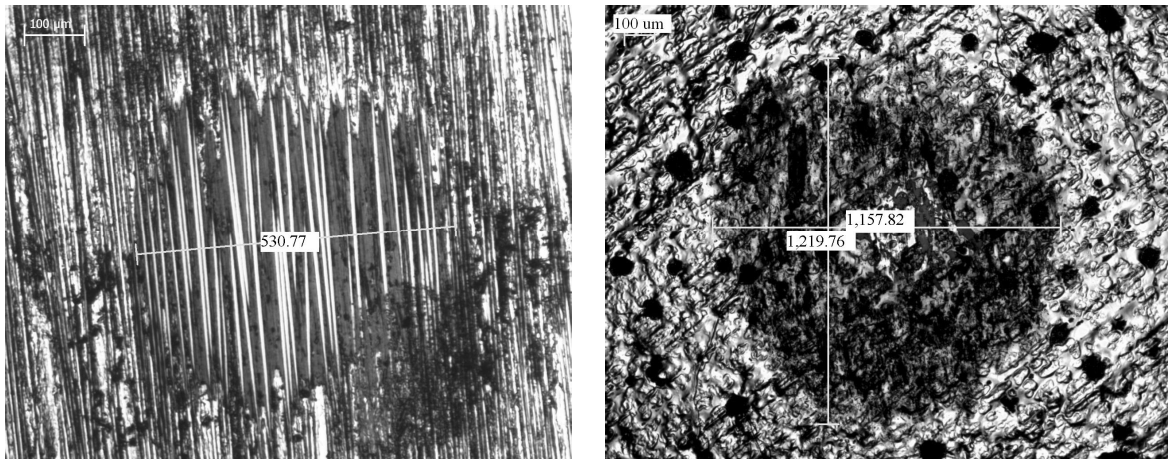


Figure 52. CrN on CFRP (a) and on vinyl ester (b) subjected to calotest.

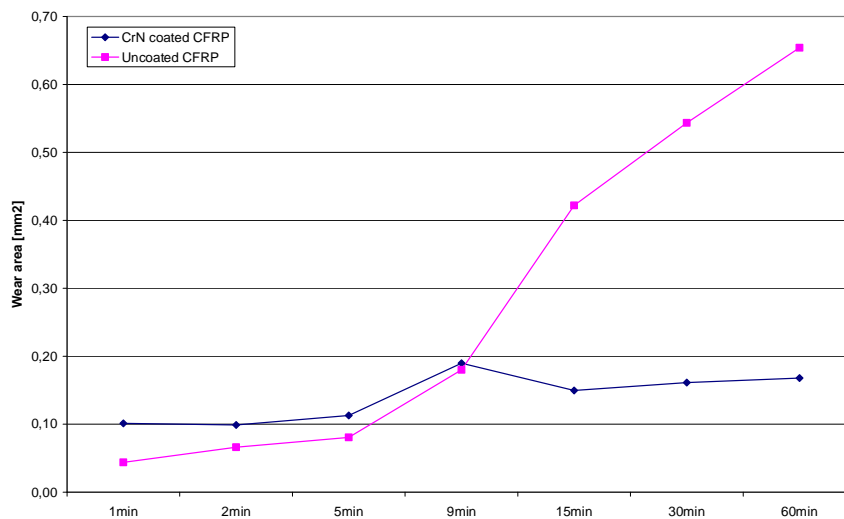


Figure 53. The wear measurement done on CrN coated and uncoated composite plate. The y axis shows the area of the wear scar.

The graph of wear measurements done on composite plate is shown in Figure 53. The wear rate of both the coated and the uncoated samples is low but the uncoated sample has a lower rate. After a time, the wear rate of the uncoated CFRP increases at a much higher rate. This can be explained in the following way: The wear of the uncoated CFRP, after an initial low wear rate then increases approximately proportional to the area of coating exposed to the ball as might be expected. For the coated CFRP, in the initial stages, the contact area is smaller therefore the pressure on the surface is higher. With high pressure applied, the CFRP substrate cannot support the coating therefore it deforms and perhaps cracks and small particles of coating act as an abrasive to give initially a higher rate. However, once this stage is past, the wear rate will be determined by the coating and remain low-the ball is largely supported higher and more wear resistant coating.

12.2 Wear performance of polymers

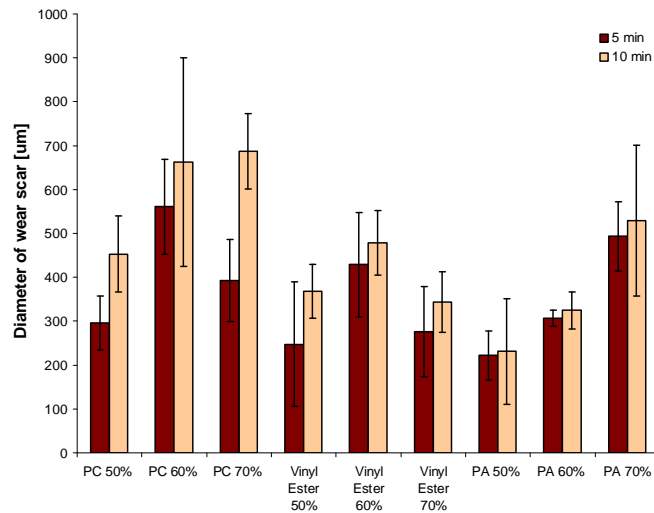


Figure 54. The wear performance of CrN on polymers with different OEM set points.

The wear resistance of chromium nitride is found to be increasing for polyamide and polycarbonate when the Cr content in the film increases. The results are not reliable for vinyl ester due to the rough surface (Figure 54).

12.3 Wear performance of single side coated CFRP component

The wear measurements were done using wear tester for CFRP components. In the initial tests chromium nitride coated composite and hard chrome plated composite were tested. Rotation speed was 1500 m/min and wear time 40 h. Chromium nitride coating was only on the upper side of component. Chromium layer covered the whole component.

Worn areas of sputtered CrN and hard chrome plated CFRP components are shown in Figure 55 and 56. In both cases the film covers the component without peeling. The amount of wear as a percentage change in a length, mass and volume is shown in Fig. 58 and Fig. 59. It was not clear if there was any reduction in wear with CrN thin film because the most of the mass loss was from the component itself. With all over plated hard chrome film both component and also the drum of the tester wore. Wear of the drum could be due to high hardness and roughness of hard chrome film and also the long pre-wearing time before the correct shape was achieved.

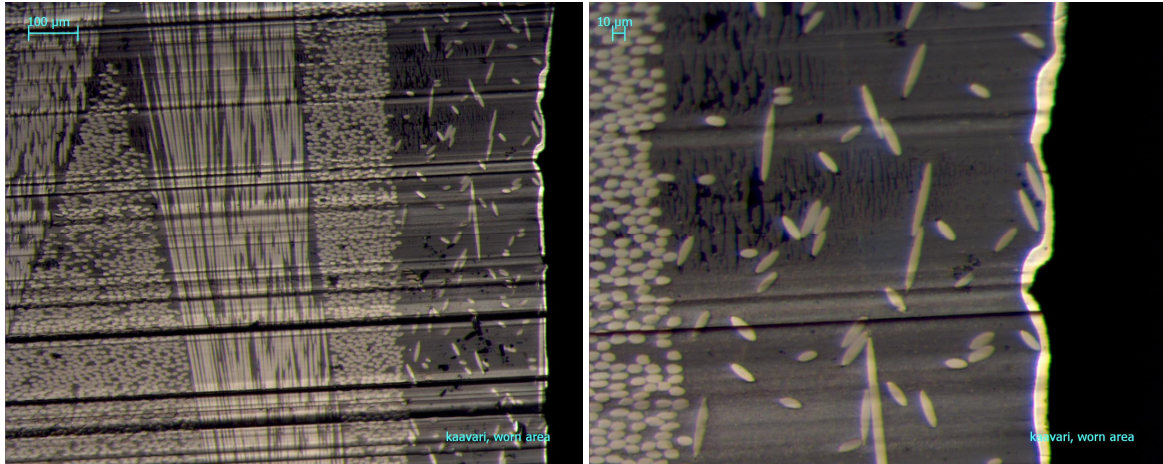


Figure 55. Worn area of CFRP component coated by sputtered CrN film.

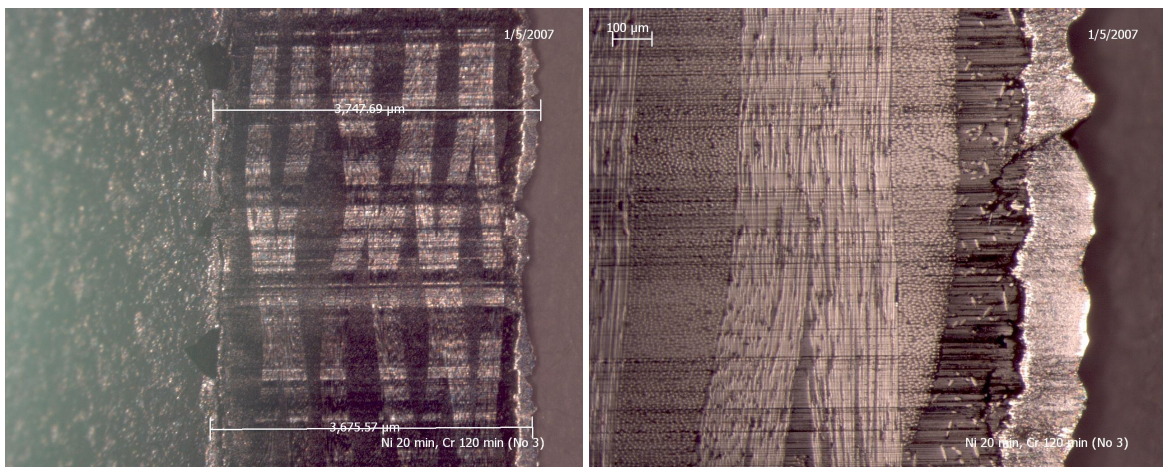


Figure 56. Worn area of hard chrome plated CFRP component. Both side coated by nickel as an adhesion layer and chrome.

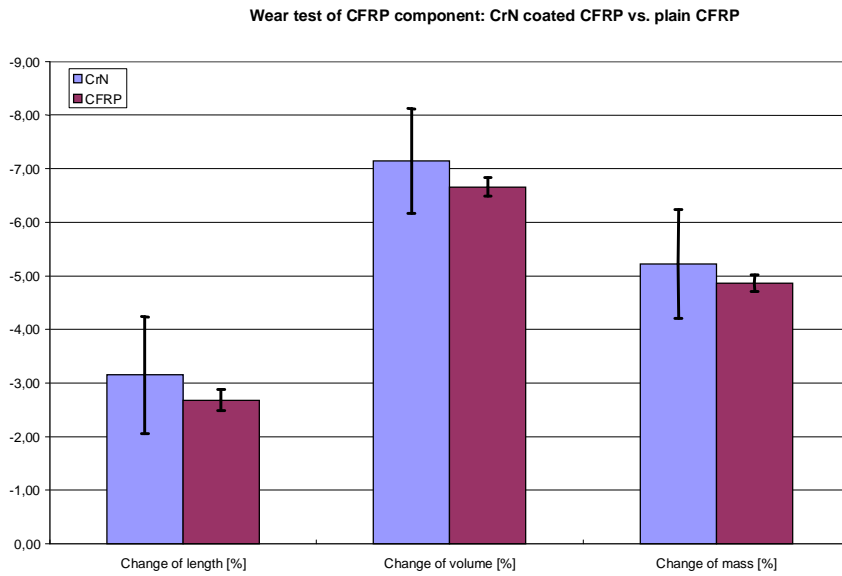


Figure 58. Wear behavior for CrN coated composites and plain CFRP.

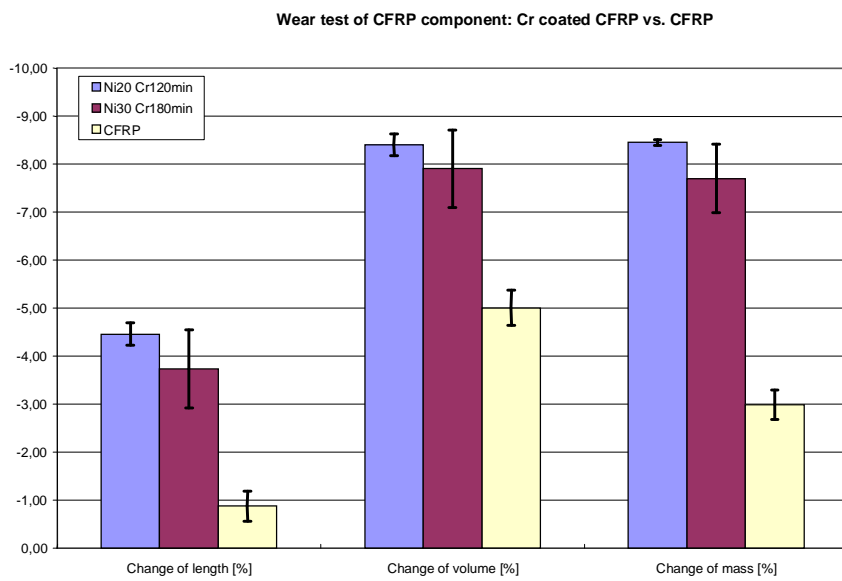


Figure 59. Wear behavior for hard chrome plated composites and plain CFRP.

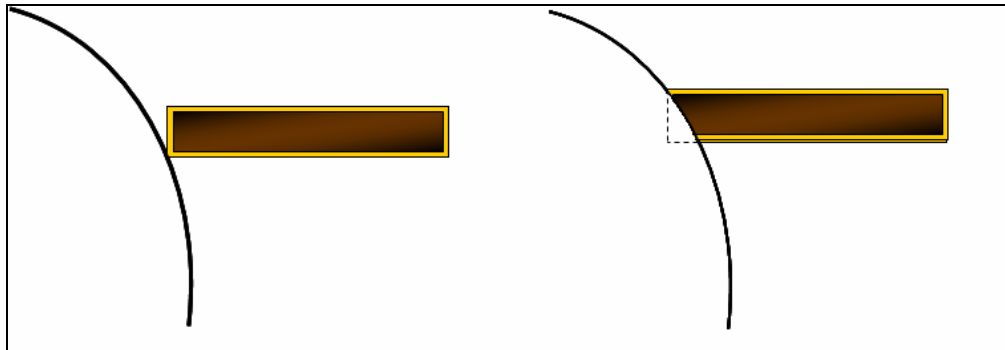


Figure 60. Schematic view of initial stage of wear test and after certain time.

The disadvantage of the tester is the required long time before the upper layer start to wear. Schematic view of phenomena is in Figure60. Hence, after these initial tests already worn reference CFRP components were used. Worn components were deposited with the specified film and then tested them. The time for the test was shorten to 5 h and rotation speed was kept the same, 1500 m/min.

The graph of wear behaviour as a percentage change in a length and mass after two different runs is shown in Figure61. CrN film could give a slight better performance against the wear compared to plain CFRP component. However, with Ti-DLC coating no improvement was seen and with hard chrome plated samples the wear was much higher than without coating. It could be that with plain CFRP and CrN the fibres act as a sort of lubricant whereas with the Ti-DLC and hard chrome plated component the worn film behaved as an abrasive particles and accelerated the wear.

The measured pull-off adhesion values gave Ti-DLC deposited component 22 MPa fracture strength. With CrN coated component the achieved pull-off strength was 13 MPa, but the film was not totally removed, thus it was concluded that the strength is higher than the measured value. As the adhesion was observed to be poor between epoxy glue and the hard chrome plated component, the pull-off adhesion strength could not be measured. The value of the glue failure was 16 MPa.

It was expected that even if the film on pre-worn sample will not give the improvement in wear resistance the sharper edge for the component could be achieved. The edges of components are seen in Figure62, Figure63, Figure64 and Figure65. With CrN and Ti-DLC coated samples the edge is fractionally sharper and more uniform than with plain CFRP sample. Nevertheless, the edge of hard chrome plated sample became much rougher than the plain composite.

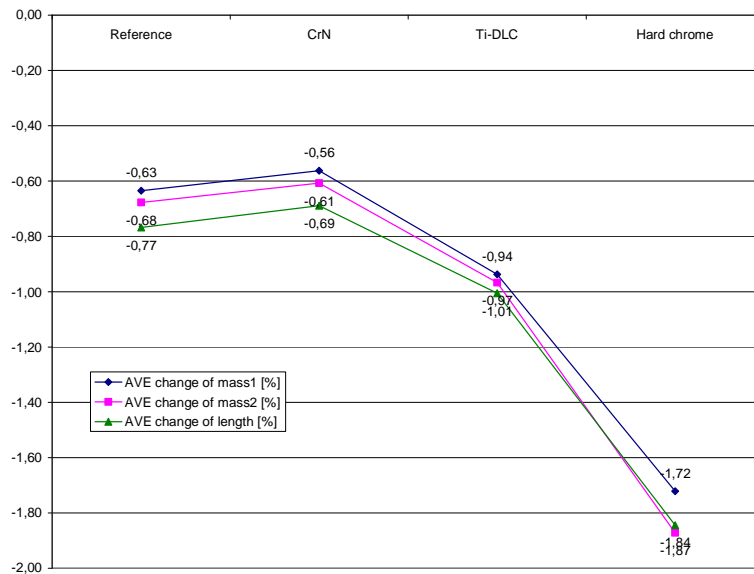


Figure 61. Wear behavior for deposited and plain CFRP component.

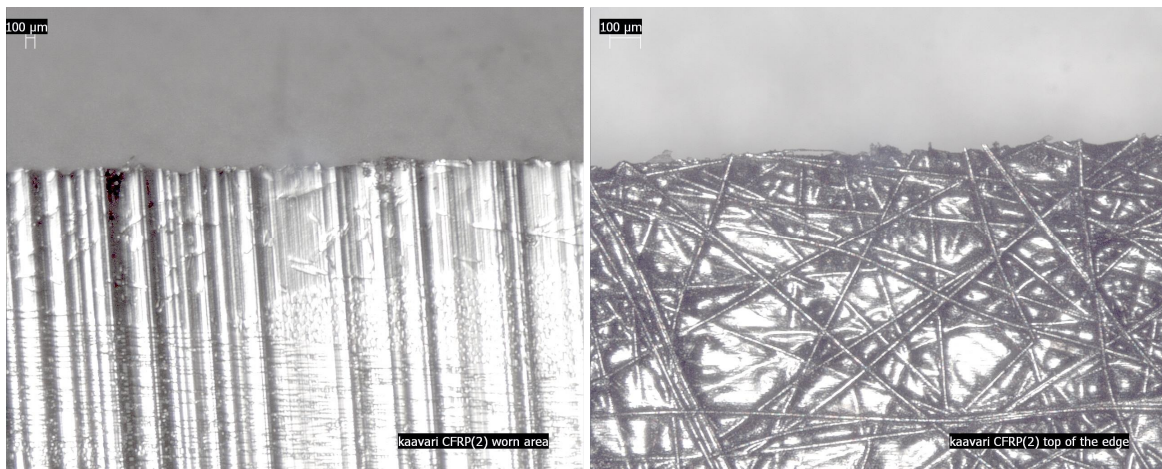


Figure 62. Worn area and edge of CFRP component.

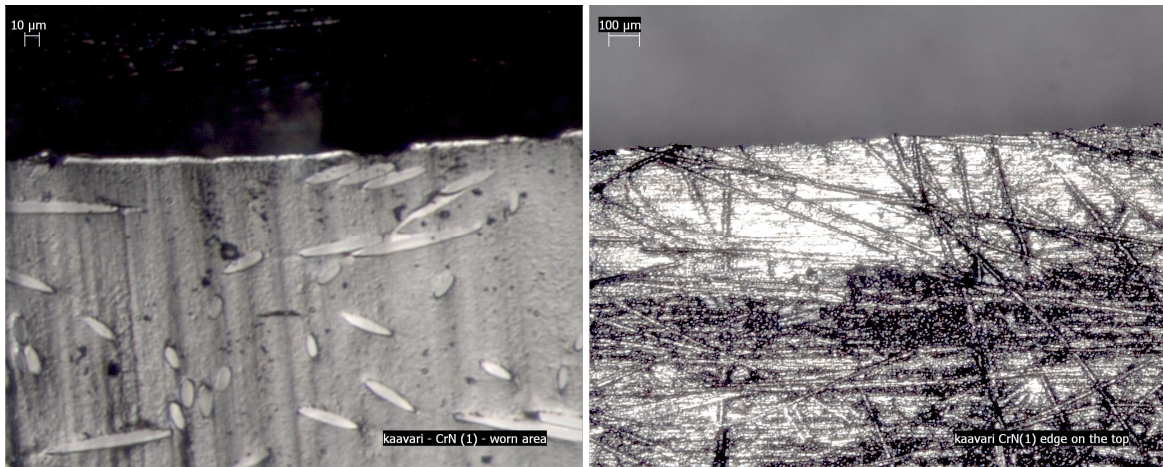


Figure 63. Worn area and edge of the component coated by CrN film.

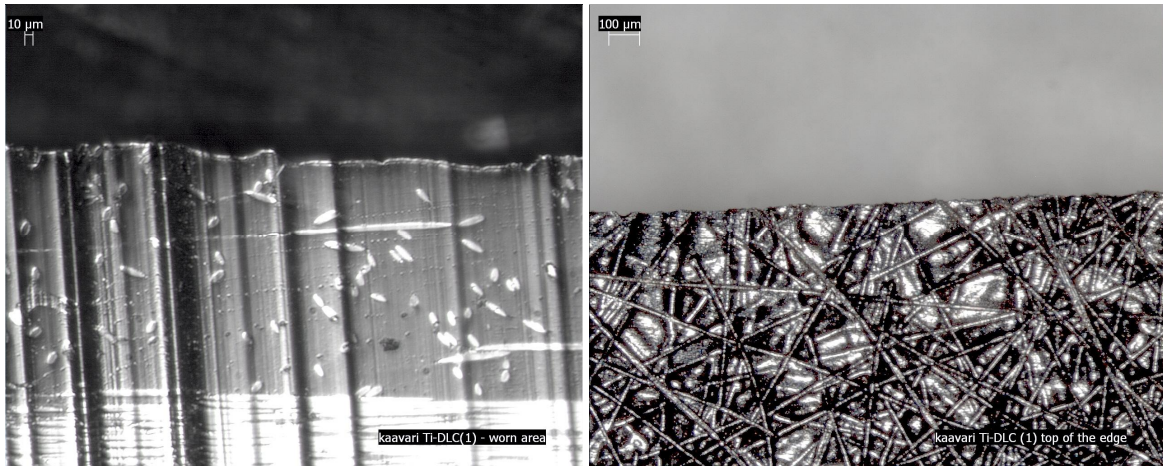


Figure 64. Worn area and edge of the component coated by Ti-DLC film.

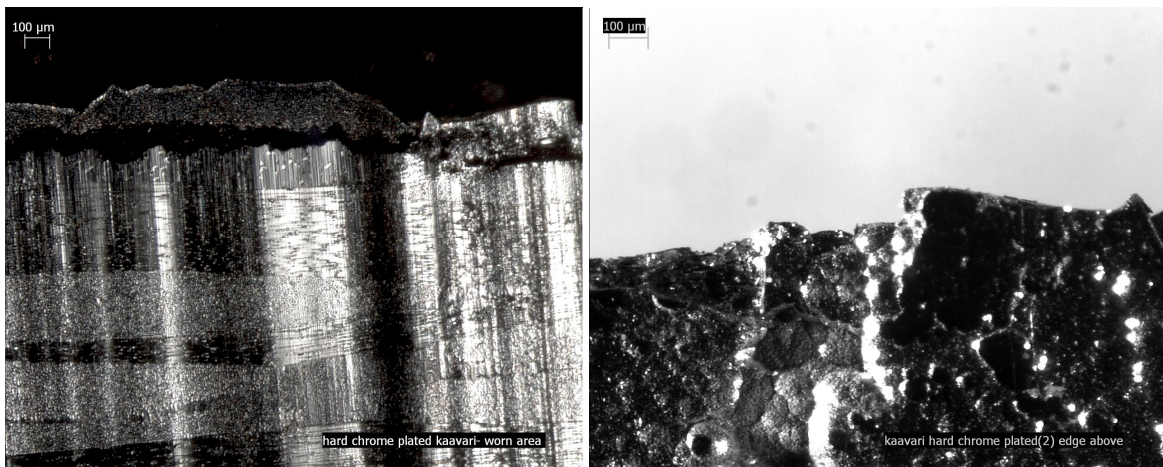


Figure 65. Worn area and edge of hard chrome plated component.

13 Summary

Hard thin film coatings can be successfully deposited on polymer based composites at low temperatures, ≤ 100 °C by reactive magnetron sputtering. In general the adhesion of the coatings is good. For improving wear resistance the fiber free surface region is needed to avoid fibre particles being pulled from the surface taking the wear resistant coating with them and taking part in to the wear process.

Based on the adhesion tests on plain carbon fibre reinforced plastic substrates, the strength values over 20 MPa is needed to reach cohesive failure of substrate or adhesive failure as substrate/coating interface. The variation of breaking strength value of CrN films on CFRP substrates varies between 19.6 – 22.4 MPa. The fractures in our studies took place in the bulk material and it gives the assumption that the adhesive forces acting between coating and substrate are stronger than the cohesive forces of the substrate.

In general the pretreatment procedure for polymers prior to thin film deposition is critical to achieve good coating adhesion. In this study both ex-situ and in-situ pretreatments were studied. Chemical cleaning tends to remove possible crease and other impurities from the surface but can also be seen as a surface modification method. Among PC, carbon fibre reinforced plastic and vinyl ester the three steps cleaning procedure in ultrasonic bath increased surface energy only for the vinyl ester. For other polymers only ethanol wiping is enough to increase the surface energy. Acetone as a strong solvent used in chemical cleaning was noticed to have unfavorable effect on surface properties of PC and vinyl ester together with baking after cleaning. Baking after cleaning in chemical solution is necessary to remove the moisture from the substrate. Effect of baking time and temperature in suitable range for polymers did not show to have significant effect on substrate properties.

Ion cleaning prior to sputtering is commonly used in-situ cleaning procedure. In this project the effect of argon and argon/nitrogen mixture plasmas were studied. Argon pressure did not show significant difference on adhesion strength of CrN film on vinyl ester, PC and PA. CrN on PMMA shows better adhesion at high pressure pretreatment with Ar and poor adhesion at low pressures. CrN on polycarbonate and vinyl ester showed better adhesion for argon and nitrogen flow of 30 sccm. The glue failure occurred at 15 MPa for polyamide at 100:30 Ar/N₂. Hence the adhesion strength on PA is not less than 15 MPa.

The flux of ions and neutrals showed significant variation with the pulse frequency. The flux of metal and gaseous ions increased with pulse frequency with Ar ion at higher rate. The chromium and nitrogen neutrals decreased with frequency while Ar neutrals increased with frequency. The energy of ions reached above 250 eV at higher frequency even without any substrate bias. The ion energy bombardment with pulse frequency is found to have significant effect on structure and mechanical properties. The films showed preferential orientation of cubic CrN (111) at all frequencies. The lattice was distorted from cubic to tetragonal with increased ion energy bombardment with the pulse frequency. The deposition rate decreased with pulse frequency due to decrease in duty cycle. The film stress was found to be tensile which might be due to high operating pressure and low deposition temperature. The tensile stress was found building up with pulse frequency up to 100 kHz and getting relaxed at high frequencies. The stress can be found

to be controlled by ion energy bombardment. The hardness and Young's modulus found to be inversely proportional to tensile stress.

Wear testing of hard wear resistant coating on soft polymer and polymer composite was found to be complicated. Test results are strongly depended on substrate surface properties such as smoothness. This was shown for example in the wear resistance of chromium nitride that was found to be increasing for smooth polyamide and polycarbonate when the Cr content in the film was increased whereas rough surface of vinyl ester made adhesion results unreliable. Wear resistance of sputtered CrN and Ti-DLC and electrolytic hard chrome plating was compared in one specific application. When deposited on specific CFRP component the CrN showed slightly better wear resistance than composite without coating. Ti-DLC and hard chrome plating showed no improvement on wear resistance. It is suggested that CFRP and CrN the fibres act as a sort of lubricant whereas with the Ti-DLC and hard chrome plated CFRP component the worn film behaved as an abrasive particles and accelerated the wear.

References

- 1 R. Suchentrunk, Metallizing of plastics – A Handbook of theory and practice, Finishing Publications Ltd., 1993.
- 2 A.P. Harsha and U.S. Tewari, Tribological studies on glass fiber reinforced polyetherketone composites Journal of Reinforced Plastics and Composites, 23, 65-82, 2004.
- 3 <http://www.teercoatings.co.uk/index.php?page=cfubmsip>.
- 4 A. Grill, Plasma-deposited diamondlike carbon and related materials, IBM Journal of Research and Development, 43, 147-161, 1999.
- 5 A. Grill, Tribology of diamondlike carbon and related materials, Surface and Coatings Technology, 94-95, 507-513, 1997.
- 6 J. Bulíř, M. Novotný, M. Jelínek, T. Kocourek, V. Studnička, Plasma study and deposition of DLC/TiC/Ti multilayer structures using technique combining pulsed lase deposition and magnetron sputtering, Surface and Coatings Tecdhnology, 200, 708-711, 2005.
- 7 A.A. Voevodin, J.S. Zabinski, Diamond and Related Materials, 7, 463, 1998.
- 8 K. Baba, R. Hatada, Deposition and characterization of Ti- and W-containing diamond-like carbon films by plasma source ion implantation, Surface and Coatings Technology, 169-170, 287-290, 2003.
- 9 H. Dimigen and C.-P. Klages, Microstructure and wear behaviour of metal-containing diamon-like coatings, Surface and Coating Technology 49, 543-547, 1991.
- 10 V.M. Elinson, V.v. Sleptsov, A.N. Laymin, V.V. Potrayasay, L.N. Kostuychenko, S.D. Mousinna, Diamond Relat, Mater. 8, 2103, 1999.
- 11 K. Donnelly, D.P. Dowling, M.L. McConnell, R.V. Flood, Diamond Relat. Mater. 8, 538, 1999.
- 12 S. Miyake, T. Saito, S. Watanabe, E. Hayashi, T. Nakamaru, Hyomen Gizyutsu 52 (12), 82 2001.
- 13 H. Meerkamm, W. Fruth, T. Krumpiegl, C.Schauffer, Mechanical and tribological properties of PVD and PACVD wear resistant coatings, International Journal of Refractory Metals and Hard Materials 17, 201-208, 1999.
- 14 http://en.wikipedia.org/wiki/Raman_spectroscopy
- 15 Donald M. Mattox, “Handbook of Physical Vapor Deposition (PVD) Processing”, Noyes Publivations, USA, 1998
- 16 PAT Automatic Adhesion Tester Instruction Manual, DFD Instruments, Norway
- 17 <http://www.dfdinstruments.co.uk/topics/Study5-ASTM-D4541.htm>
- 18 Standard ASTM D4541
- 19 Standard ISO 4624
- 20 B.B. Straumal, N.F. Vershinin, A. Cantarero-Saez, M. Friesel, P. Zieba, W. Gust, Vacuum arc deposition of protective layers on glass and polymer substrates, Thin Solid Films 383, 224-226, 2001.
- 21 C.H. Su, C.R. Lin, C.Y. Chang, H.C. Hung, T.Y. Lin, Mechanical and optical properties of diamond-like carbon thin films deposited by low temperature process, Thin Solid Films 498, 220 – 223, 2006.

- 22 Jin-Wook Seong , Dai Won Choi, K.H. Yoon, Effect of oxygen content on barrier properties of silicon oxide thin film deposited by dual ion-beam sputtering, *Journal of Non-Crystalline Solids*, 352, 84–91, 2006.
- 23 T. Schmauder , K.-D. Nauenburg, K. Kruse, G. Ickes, Hard coatings by plasma CVD on polycarbonate for automotive and optical applications, *Thin Solid Films* 502, 270 – 274, 2006.
- 24 S. Dahl, D. Rats, J. von Stebut, L. Martinu, J.E. Klemberg-Sapieha, Micromechanical characterisation of plasma treated polymer surfaces, *Thin Solid Films* 355-356, 290-294, 1999.
- 25 K. De Bruyn , M. Van Stappen , H. De Deurwaerder , L. Rouxhet , J.P. Celis, Study of pretreatment methods for vacuum metallization of plastics, *Surface and Coatings Technology* 163 –164, 710–715, 2003.
- 26 P. J. Kelly and R. D. Arnell, “Control of the structure and properties of aluminum oxide coatings deposited by pulsed magnetron sputtering”, *J. Vac. Sci. Technol. A* 17(3), 945, May/June 1999.
- 27 Jung W. Lee and Jerome J. Cuomo, “Plasma characteristics in pulsed direct current reactive magnetron sputtering of aluminum nitride thin films”, *J. Vac. Sci. Technol. A* 22(2), 260, Mar/Apr 2004.
- 28 M. Audronisa, P.J. Kelly, R.D. Arnell, A.V. Valiulis, “Pulsed magnetron sputtering of chromium boride films from loose powder targets”, *Surface & Coatings Technology*, 200, 4166– 4173, 2006.
- 29 Mei-Ling Wu, Xi-Wei Lin, Vinayak P. Dravid, and Yip-Wah Chung, “Preparation and characterization of superhard CN_x /ZrN multilayers”, *J. Vac. Sci. Technol. A* 15(3), 946, May/June 1997.
- 30 P.J. Kelly, C.F. Beevers, P.S. Henderson, R.D. Arnell, J.W. Bradley, H. Baicker, “A comparison of the properties of titanium-based films produced by pulsed and continuous DC magnetron sputtering” *Surface and Coatings Technology*, 174 –175, 795–800, 2003.
- 31 M. Audronis , P.J. Kelly, R.D. Arnell, A. Leyland, A. Matthews, “The structure and properties of chromium diboride coatings deposited by pulsed magnetron sputtering of powder targets”, *Surface & Coatings Technology* 200, 1366 – 1371, 2005.
- 32 P.S. Henderson, P.J. Kelly, R.D. Arnell, H. Backer, J.W. Bradley, “Investigation into the properties of titanium based films deposited using pulsed magnetron sputtering”, *Surface and Coatings Technology*, 174 –175, 779–783, 2003.
- 33 Y.L. Su, S.H. Yao, “On the performance and application of CrN coating”, *Wear*, 205, 112-119, 1997.
- 34 I. Milosev, H.-H. Strehblow, B. Navinsek, “Comparision of TiN, ZrN and CrN hard nitride coatings, “Electrochemical and thermal oxidation”, *Thin Solid Films*, 303, 246-254, 1997.
- 35 J. Pitter, F. Cerny, J. Cizner, J. Suchanek, D. Tischler, “High temperature corrosion properties of SiN_x, and CrN_x coatings deposited by IBAD method”, *Surface & Coatings Technology* 200, 73 – 76, 2005.
- 36 H:Chen, P.Q. Wu, C. Quaeys, K.W. Xu, L.M. Stals, J.W. He, J.-P. Celis, “Comparision of fretting wear of Cr-rich CrN and TiN coatings in air of different relative humidities”, *Wear* 253, 527-532, 2002.
- 37 J.Kaminski, J. Rudnicki, C. Nouveau, A. Savan, P. Beer, ”Resistance to electrochemical corrosion of Cr_xN_y- and DLC-coated steel tools in the environment of wet wood”, *Surface & Coatings Technology* 200, 83 – 86, 2005.

- 38 T. Moiseev and D. C. Cameron, "Pulsed dc operation of a penning-type opposed target magnetron", *J. Vac. Sci. Technol. A* 23(1), 66, Jan/Feb 2005.
- 39 J. W. Bradley, H. Bäcker, Y. Aranda-Gonzalvo, P. J. Kelly and R. D. Arnell, "The distribution of ion energies at the substrate in an asymmetric bi-polar pulsed DC magnetron discharge" *Plasma Sources Sci. Technol.* 11, 165-174, 2002.
- 40 S.Mahieu, P.Ghekiere, G.De Winter et al, 'Biaxially aligned titanium nitride films deposited by reactive unbalanced magnetron sputtering', *Surface and Coatings Technology*, 200, 2764-2768, 2006.
- 41 Jyh-Wei ee, Shih-Kang Tien and Yu-Chu Kuo, *Journal of Electronic materials*, 34,12,2005.
- 42 G. Q. Yu, B. K. Tay, S. P. Lau, K. Prasad, L. K. Pan, J. W. Chai and D. Lai, *Chemical Physics Letters*, 374, 264-270, 2003.
- 43 G. Wei, A. Rar and J. A. Barnard, *Thin Solid Films*, 398-399, 460-464, 2001.
- 44 W. Ensinger, K. Volz and M. Kiuchi, *Surface and Coatings Technology*, 128-129, 81-84, 2000.
- 45 Z. B. Zhao, Z. U. Rek, S. M. Yalisove and J. C. Bilello, *Thin Solid Films*, 472, 96-104.
- 46 D.W.Hoffman, J.A. Thornton, *Thin Solid Films* 40 (1977) 355.
- 47 Windischmann, H., *Intrinsic stress in sputtered-deposited thin films*, *Critical Reviews in Solid State and Material Science*, 17(6): 547-596 (1992).
- 48 X.Zhang, A. Misra, H.Wang, A.L. Lima, et al, "Effects of deposition parameters on residual stresses, hardness and electrical resistivity of nanoscale twinned 330 stainless steel thin films", *J. App. Physics*, 97, 094302 (2005).
- 49 K.F. Chiu, Z.H. Barber, R.E. Somekh, *Thin Solid Films*, 343-344 (1999) 39-42.
- 50 Yawei Hu, Liuhe Li, Xun Cai, Qiulong Chen, Paul K. Chu, *Mechanical and tribological properties of TiC/amorphous hydrogenated carbon composite coatings fabricated by DC magnetron sputterin with and without sample bias*, *Diamond and Related Materials*, In Press.
- 51 W. Ensinger, *Low energy ion assist during deposition - an effective tool for controlling thin film microstructure*, *Nuclear Instruments and Methods in Physics Research Section B: Beam Interactions with Materials and Atoms*, Volumes 127-128, (1997), 796-808.
- 52 B.H. Lohse, A. Calka, D. Wexler, "Raman spectroscopy sheds new light on TiC formation during the controlled milling of titanium and carbon", *Journal of Alloys and Compounds*, In Press.
- 53 Andrea Carlo Ferrari, "Determination of bonding in diamond-likea varbon by Raman spectroscopy", *Diamond and Related Materials* 11, 1053-1061, 2002.
- 54 Xing-zhao Ding, B.K. Tay, S.P. Lau, P. Zhang, X.T. Zeng, "Structural and mechanical properties of Ti-containing diamond-like carbon films deposited by filtered cathodic vacuum arc", *Thin Solid Films*, 408, 183-187, 2002.
- 55 K.L. Rutherford, I.M. Hutchings, "A micro-abrasive wear test, with particular application to coated systems", *Surface and Coatings Technology* 79, 231-239, 1996.



SURFACE COATINGS ON COMPOSITE MATERIALS

Literature study - COATCOM project

By

Tommi Kääriäinen, ASTRaL

TABLE OF CONTENTS

Background	3
Definition	3
1 Carbon and glass fibre reinforced pastics	4
1.1 Chemical structure of composite materials	4
1.1.1 Polymers	4
1.1.2 Fibers and semi-manufactured products	5
1.1.3 Other constituents in composites (Fillers and additives)	6
2 Important properties of thermosetting plastics	7
2.1 Thermal stability and conductivity	7
2.2 Electrical conductivity	8
3 Wear resistant coatings on composites (polymers)	8
3.1 Coating methods	8
3.2 Different types of coatings and their characteristics on composite materials (literature review)	9
3.2.1 Properties of coatings at lower temperatures	10
3.3 Wear classification	10
3.4 Wear testing	11
3.5 Wear in coated polymers (literature review)	12
4 Characteristics affecting coating performance	13
4.1 Adhesion	14
4.1.1 Adhesion in general	14
4.1.2 Adhesion of atomistically deposited coatings on composite materials (polymers)	14
4.1.3 Adhesion testing	15
4.2 Surface properties and modification of composites (and polymers) for enhancing the adhesion	18
4.3 Interface formation between coating and substrate (near surface) material	19
4.4 Coating materials and composition	21
REFERENCES	23

Background

Carbon and glass fibre composites are used for a wide range of industrial products. These materials can be fabricated into complex components but their performance in terms of abrasion and impact resistance is limited. In recent study has been noticed that adding the fibers to the polymer matrix will even deteriorate the tribological properties of parent polymer [25]. In order to enhance their performance and thus extend their use into more products and other fields of use, their surface properties need to be enhanced.

Current technology for wear resistant components typically uses hard chrome plating for the surface layer. This material must be phased out by EU instruction due the carcinogenic properties of the chemicals involved.

Magnetron sputtering of wear and erosion resistant thin surface coatings is a technique which has widespread application to a range of products [1]. However deposition on to composite materials brings with it a number of new problems. In particular, the adhesion of the coating on to the resin-bound fibrous composite brings challenges in the mechanical and chemical mismatch between them.

Definition

In this literature study we look at the characteristics that are effecting to the composite-coating system through the current state of knowledge in the discipline. The aim of this study is to give valuable starting point and information for the research work which two themes are described hereafter. The report itself covers the basic chemistry, structure and properties of composite materials, coating methods available for the polymers, the most important characteristics present in the composite-coating system, essential evaluation methods for the coating performance, and substantial coatings that have been deposited on polymer based materials.

Project outline:

Theme 1: Research into the general characteristics of magnetron sputtered coatings on composites. This will be a three year project which will study the fundamental aspects of adhesion between surface coatings and composite substrates and the wear-resistant properties of the composite/coating combination. Increased knowledge and understanding from this work will open new product areas where the use of composites are not yet possible and give Finnish industry a lead in the marketplace.

Theme 2: Study of coatings for application to specific composite products. These will be relatively short term in nature and will focus on particular surface coatings which are known to have excellent properties on metal substrates with the intention of obtaining fast improvements in product performance. Success here will allow a quick transition to the product development phase. These short projects will draw from the knowledge obtained from the more fundamental studies. This theme will include the characterisation of hard chrome plated composite materials to give a benchmark for comparison with sputtered coatings.

1 Carbon and glass fibre reinforced plastics

Carbon Fibre Reinforced Plastics (CFRP) and Glass Fibre Reinforced Plastics (GFRP) are the composite materials where the thermoplastics such as polyamide, polypropylene and polycarbonate and thermosetting plastics such as epoxy, polyester, vinyl ester and phenol have been reinforced by carbon and glass fibres (reinforcements) in order to improve their properties such as mechanical strength and stiffness. Furthermore the small particles so called additives are added to the composites for further improvements of their properties and facilitate their manufacturing. Usually the total amount of reinforcements and additives in composite is between the 30-70 weight percent [2].

1.1 Chemical structure of composite materials

1.1.1 Polymers

Composites that are investigated in this project consist mainly of vinyl ester and epoxy matrices. Vinyl ester and epoxy resins belong to the group of thermosetting polymers that are formed by an irreversible chemical reaction in situ from epoxy or vinyl ester and a hardener. During the curing they form a rigid crystalline structure. Above T_g (glass transition temperature) the polymer becomes amorphous which changes its mechanical properties drastically: resin modulus (stiffness) decreases, compressive and shear strength drop. Different vinyl ester and epoxy resins are available. The final resulting thermosetting plastic depends on the chemical nature of the hardener and the conditions. Vinyl esters are cured with a catalyst. The most common epoxy resin is formed with the reaction of bisphenol A and epichlorohydrin. Epoxy resins are usually cured with an amine or anhydride hardeners. In the Figure 2 and 3 typical vinyl ester and epoxy molecules are presented.

Vinyl ester is an unsaturated resin formed by the reaction of methacrylic or acrylic acid with a bisphenol diepoxide. This polymer is then mixed with an unsaturated monomer such as styrene as in the polyesters. The cure of the vinyl ester is same as for conventional polyesters so that a free radical initiator such as organic peroxide is used as a hardener. The structures of vinyl ester and polyester differ in the placement of unsaturated sites on polymer chain. The vinyl ester contains unsaturated vinyl groups only in the terminal positions when those groups in the polyester are in the middle [3].

Vinyl esters have very high chemical and environmental resistance. Based on the different functional groups vinyl esters are less hydrophobic than epoxies (ester group is more hydrophilic than epoxy group). Still the amount of the ester groups is not big and the C-C bonds and aromatic groups make the vinyl ester resin mostly hydrophobic. Hence vinyl esters possess good water resistance as composites. Epoxies have good mechanical and thermal properties, they are also good insulators and they are hydrophobic. Chemically modified epoxies that have an even higher hydrophobicity are also available.

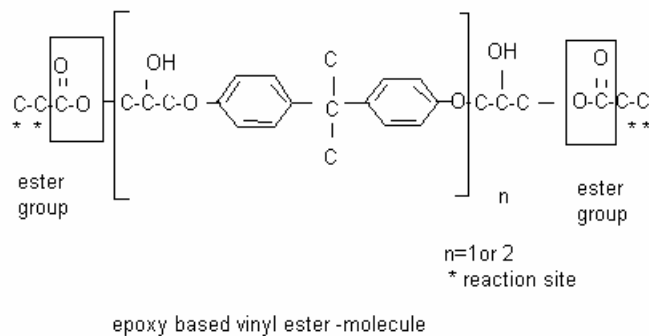


Figure 2. Chemical structure of a vinyl ester molecule

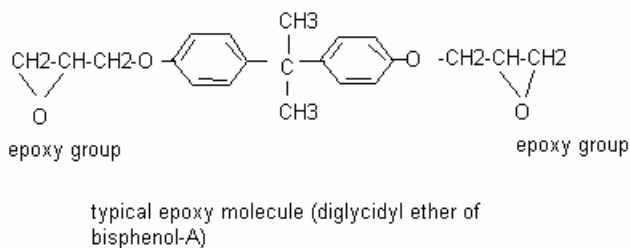


Figure 3. Chemical structure of an epoxy molecule

1.1.2 Fibers and semi-manufactured products

In this section, a short presentation is given of glass and carbon fibers based on their use in composites scrutinized in this project. There are several glass fibre types and forms to be added to the composite materials. Glass fibres can be divided to different groups according to their use.

E-glass is a composition of calcium aluminoborosilicate and its alkali content is less than 2 %. E-glass is used as a general-purpose fibre and it represents 99% of all the glass fibres manufactured. E-glass fibre has good strength and high electrical resistivity [2,3].

S-glass stands for high strength and it is used in the applications where very high tensile strength is required. S-glass has a magnesium aluminosilicate composition [3].

C-glass fibres have a soda-lime-borosilicate composition and they are used in corrosive environments and in the applications where chemical stability is required [3].

Carbon fibres have very high carbon content which is usually 95-99 %. They can be manufactured many ways and using different precursors. The most used carbon fibre is based on polyacrylonitrile (PAN). The other precursors are for example rayon and isotropic and liquid pitches [3].

Fibers can be used as a continuous fibers, discontinuous fibers or as a semi-manufactured products such as woven fabrics. Fibers can also be treated or sized prior to use. Sizing has an effect on the interactions between matrix material and reinforcements in the composites [19].

1.1.3 Other constituents in composites (Fillers and additives)

Fillers and additives are used in polymer systems to increase mechanical properties: strength, stiffness, and toughness, to enhance barrier properties and their resistance to heat and fire, to enhance electromagnetic properties, or simply to lower the cost. Some additives are also used to improve the behaviour of composite in the manufacturing process. Other additives than fiber itself are catalysts, fillers, thickeners, mold release agents, pigments, thermoplastic polymers, polyethylene powders, flame retardants, and ultraviolet absorbers [3].

Silane is used in the composite as a coupling agent or adhesion promoter. Silane is also used for sizing the fibers.

Thermoplastics such as PVAc are used for sizing of the fibres and to have low polymerization shrinkage during composite processing. Here the content of the thermoplastic in resin system is less than 5%.

The amount of curing agent in the resin varies in the range of 1...4 w% depending on which type of composite it will be used for. For laminating, the content is between 1 and 2 w% and in surface resin it varies between 2 and 4 w%.

Internal release agents are used in composite to prevent the adhesion between the mold and composite during processing. Typical release agents are zinc stearate, calcium stearate and stearic acid. The concentration of internal release agent is less than 2 w% of the resin.

Pigment concentration is generally 1 to 5 w% of the resin. Pigments can affect the cure time and shelf life stability of composite and can also accelerate or inhibit the reactivity of the catalyst-resin system [3].

Different fillers can be added to the polymer systems. There are hundreds of fillers available but the most commonly used are calcium carbonate, magnesium carbonate, silicon dioxide, hydrated alumina, and clays like kaolin and talc. The term filler is sometimes used specifically to mean particulate additives. Fillers can be divided by their sizes and shapes. Calcium carbonates reduce the shrinkage of the molded parts and enhance the strength uniformity. Hydrated alumina in composite provides flame retardancy and enhance the electrical properties. Kaolin clays when used together with calcium carbonate improve resistance to cracking in molded parts [3]. Silicon dioxide in thermosets will enhance the electrical insulating properties, dimension stability and thermal conductivity [2]. Carbon black is used as a pigment but also to protect the composite from UV- and thermal radiation and to enhance the electrical conductivity and formability [2].

Different type of non woven fabrics can be added to the composite mainly for enhancing the surface properties of molded products. Non woven fabrics are also used to improve the chemical-, thermal-, flame-, and wear resistance and electrical conductivity and shock resistance. Some non woven fabrics will absorb microwaves and reflect the radiation from different sources [2]. For instance steel and carbon tissues are commercially available non woven fabrics.

2 Important properties of thermosetting plastics

2.1 Thermal stability and conductivity

The important process parameter when coating thermosetting plastics is temperature. The temperature of substrate material during the coating process should be maintained so low that no damage to the substrate occurs. Polyester resins are commonly used in elevated-temperature applications. Vinyl ester and epoxy resins have good thermal stability. Table 1 shows the temperature resistance range of these resins. Although the matrix plastics used in composite materials are usually thermosetting plastics, the usage of thermoplastics in composites has been predicted to increase [2]. Table 2 shows some general properties such thermal conductivity and glass transition temperature of plastics and some metals.

Table 1. Temperature resistance of thermosets when cured[2].

Thermosetting plastic	Temperature resistance (°C)
Vinyl ester	120-180
Epoxy	120-180
Polyester	120-180
Phenol	180-300

Table 2. Some general properties of materials [53].

Material	Density (kg/m ³)	Thermal conductivity (W/m/K)	Glass transition temperature T _g	Max. operating temperature (°C)
ABS	1040	0.25	115	50
Epoxy	1200	0.23	-	130
PEEK	1300	-	143	204
PEEK (30% carbon)	1400	-	-	255
PET	1360	0.2	75	110
PET (36% glass)	1630	-	-	150
Phenolic (glass filled)	1700	0.5	-	185
Polyamide-imide	1400	0.25	260	210
Polycarbonate	1150	0.2	149	125
Polyimide	1420	-	400	260
PTFE	2100	0.25	-113	250
Polysulfone S2010 + 30% GF reinforced *	1490	-	-	183
Stainless steel	7855	90	-	800
Nickel chrome alloy	7950	12	-	900

* [56]

2.2 Electrical conductivity

Electrical conductivity of the substrate is an important factor particularly in electrolytic/electroless deposition processes. In composites, the electrical conductivity of the polymer matrix is poor but can be enhanced with fillers during the molding process and by surface modification such as chemically nickelizing as a part of the electrolytic hard chrome plating.

3 Wear resistant coatings on composites (polymers)

Polymer based composite materials have relatively low temperature resistance. Due to this there are only a few suitable coating methods that can be used for metal and ceramic deposition on composite materials. The size and the shape of the product will also put a limitation on the coating methods. The functional parts in the paper machine which need tribological improvements can be over 10 meters long and might have very complex shapes (scraper blade holder). The coating methods mainly used for the composite materials are lamination and profiling (adhesive bonding), lacquering, thermal spraying, physical vapor deposition and electroless-electrolytic plating [4]. All of these methods can be divided to the sub categories where the coating methods have their own features and effects on the substrate and coating performance. Different coating methods are presented in the following.

3.1 Coating methods

Mattox [1] has divided the coating processes to the following categories:

Atomistic/Molecular deposition

- Electrolytic coating environment (Electroplating, Electroless plating), used for ABS
- Vacuum Environment (Vacuum evaporation, Ion beam sputter deposition)
- Plasma Environment (Sputtering deposition, PECVD, Arc vaporization)
- Chemical Vapor Environment (CVD)
- Chemical Solution (Spray pyrolysis)

Particulate deposition

- Thermal spraying (Flame spray, Plasma spray, HVOF)
- Impact Plating

Bulk coatings

- Wetting Processes (Painting, topcoat-surface resin, gelcoat-surface resin)
- Fusion Coatings (Sol-gel, weld overlay, *prepregs such as non woven carbon tissue, plastic overlay, other glued surface layers*)

Surface modification

- Chemical conversion
- Electrolytic environment
- Mechanical (Work hardening)
- Thermal treatment
- Ion Implantation
- Roughening and Smoothing (Chemical-mechanical polishing)
- Enrichment and depletion

3.2 Different types of coatings and their characteristics on composite materials (literature review)

The sputtering process has been widely used to deposited hard wear resistant coatings on polymer substrates [11, 16-18, 20-24, 33-36, 38, 41, 51]. Deposition with substrate surface temperature of lower than 100°C is possible, which allows sputtering process to be used for temperature sensitive materials.

Ion plating or ion beam assisted deposition (IBAD) has also been used for polymer substrates. One of the advantages is that complex shaped substrates can be coated with conformal coatings [1]. Relatively high pull off strength and peel strength of metal films can be achieved by IBAD [40, 52].

Plasma-enhanced chemical vapor deposition (PECVD) is applicable method to deposit hard wear resistant coatings such as diamond-like carbon films on polymers [39, 41]. When plasmas are used in CVD process to activate and partially decompose the precursor species, the deposition can be done at lower temperature than in conventional CVD [1].

Development work has been done for the thermal spray coatings on carbon fibre reinforced polymers. Coatings with composition of WC/10Co/4Cr, NiCrBSi, Chromium oxide, Alumina /3% titania has been thermally sprayed on to the carbon fibre reinforced polymer tubes. Coating thickness of 370 µm has been achieved [7].

Beydon et al [ref] used thermal sprayed copper to evaluate the coating adhesion with the three point bending test and the double cantilever beam test. A thermoplastic bond coat was used between the CFRP substrate and thermal sprayed copper to enhance the adhesion of the coating. In the same study they also determined that 100 µm is the optimum coating thickness with regard to the coating adhesion [13].

Vacuum arc deposition has been used to deposit wear resistant coatings on insulating and temperature sensitive materials such as polymers [29-32]. Typical feature of arc deposition is a droplet formation which produces macro- and microparticles to the substrate surface. This puts some limitations for its use especially when depositing on polymers [34].

Electroless/electrolytic plating is widely used to deposited metals and alloys to polymer substrates. Hard chrome plating has been used to improve wear and corrosion resistance of polymer surfaces and for decorative purposes. Menningen et al studied hard chrome plating on carbon fibre reinforced plastics to improve their wear resistance [26].

One of the suitable coating methods for polymers is the sol-gel technique [43]. With the sol-gel technique it is possible to deposit uniform coatings on complex-shaped substrates. Inorganic sol-gel coatings are generally porous without heat-treatment at temperatures over 400 °C, which will limit its usage. Porous coatings will not perform well in the application where aqueous and wet solutions exist.

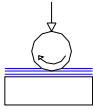
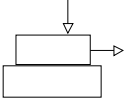
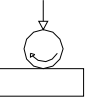
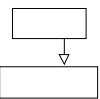
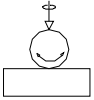
3.2.1 Properties of coatings at lower temperatures

Restricted process temperature and consequently low substrate temperature might effect the coating properties. Meerkamm [41] suggested the low temperature was the reason for the low hardness of DLC coating on PA polymer. The process temperature in their experiment was of 120 °C.

Some coatings might need annealing after deposition to perform as expected. Chou [43] reported this to be case with inorganic sol-gel coatings. Without heat-treatment the pores remain in the coating.

3.3 Wear classification

Wear behavior of materials will depend on the material characteristics but also the wear mechanisms involved in real wearing situation. When choosing the standardized laboratory wear tests for representing the particular wear situation in real wearing conditions, it is important to identify the wear mechanisms in particular environment. The figure 1 shows one approach to the wear mechanisms in different type of situations and system structures. The figure 1 also shows how complex phenomenon wear is. Corrosion will furthermore increase the complexity of wear. When corrosion and mechanical wear are both presented they will cause the synergic wear component to the overall wear. This synergic component is identified as a wear which is not causing only from the mechanical wear or corrosion.

System structure	Type of force causing the wear		Type of wear	Wear mechanism			
				Adhesion	Abrasion	Fatigue of surface	Tribo-chemical
Lubrication between solid surfaces	Sliding Rolling Shock Impacts					x	x
Solid surfaces against each other	Sliding		Sliding wear	x	x	x	x
	Rolling		Rolling wear	x	x	x	x
	Shock-loading		Shock wear	x	x	x	x
	Vibration		Vibration wear	x	x	x	x

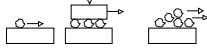
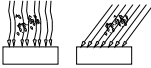
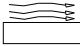
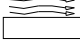
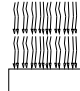
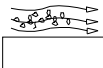
Solid surfaces and wearing particles	Grinding				x		
Solid surfaces and particles	Particle jet		Erosion		x	x	x
Solid surface and gas	Flow		Gas erosion				x
Solid surface and liquid	Flowing vibration		Cavitation			x	x
	Flowing Shock		Drop erosion			x	x
Solid surface and wearing particles in the liquid	Flow		Erosion		x	x	
			Corrosion-Erosion		x	x	x

Figure 1. Wear classification according to the stress and wear mechanism [55].

3.4 Wear testing

One of the main purposes for wear testing is to evaluate and mimic the coating performance under real usage conditions. Wear testing can also be run to achieve more information of fundamentals of specific type of wear. A reliable testing method for each processing condition in laboratory scale is often difficult to arrange and hard to find. However there are several standardized wear testing methods which allows researchers and engineers to compare the results to the work of others and enables the receive better understanding of fundamental nature of wear phenomenon. The results of standardized wear tests are highly dependent on variable parameters in the test. Even if the same standard is used for wear testing but the test procedure has been run with two different facilities, the results of these two tests might differ. Therefore it is more sensible to compare the wear behavior of different materials inside the same test procedure. Eventually, the real wear resistance of coated components can only be tested in the real usage environment. The field test procedure is also valuable way to get supporting information for the laboratory tests and therefore it should be planned and executed carefully. Table 3 lists several ASTM wear testing methods.

Table 3. ASTM standards for wear testing [45].

Wear type	ASTM Standard	Name/Description
Adhesive sliding	G99-04a	“Standard Test Method for Wear Testing with a Pin-on-Disk Apparatus”.
Adhesive sliding	G77-98	“Standard Test Method for Ranking Resistance of Materials to Sliding Wear Using Block-on-Ring Wear Test”.

Adhesive sliding	G83-96	"Standard Test Method for Wear Testing with a Crossed-Cylinder Apparatus".
2-body abrasion	G132-96(2001)	"Standard Test Method for Pin Abrasion Testing".
2-& 3-body abrasion	G65-04	"Standard Test Method for Measuring Abrasion Using the Dry Sand/Rubber Wheel Apparatus".
2-& 3-body abrasion	G105-02	"Standard Test Method for Conducting Wet Sand/Rubber Wheel Abrasion Tests".
Solid particle erosion	G76-04	"Standard Test Method for Conducting Erosion Tests by Solid Particle Impingement Using Gas Jets".
Galling	G98-02	"Standard Test Method for Galling Resistance of Materials".
Liquid droplet erosion	G73-04	"Standard Practice for Liquid Impingement Erosion Testing".
Abrasion	D1044	"Standard Test Method for Resistance of Transparent Plastics to Surface Abrasion".
Abrasion	D4060-01 [35, 54]	"Standard Test Method for Abrasion Resistance of Organic Coatings by the Taber Abraser".
Cavitation erosion	G134-95(2001)e1	"Standard Test Method for Erosion of Solid Materials by a Cavitating Liquid Jet".

Widely used wear testing method for thin films is also CALOTEST (CSEM, Switzerland) [23].

3.5 Wear in coated polymers (literature review)

The wear results of different wear tests are not comparable if there is any divergence between the test methods and procedures. The most reliable is to compare the results inside the same test run. In the following the wear data of hard coatings on polymer substrates in general is presented. More detailed information can be found from the refereed articles.

Grimberg et al [29] studied vacuum arc metal coatings of Ti, Zr, Cu and multilayer metal-nitride coatings of Ti/TiN and Ti/ZrN on polysulfone substrates. The friction and wear of the coated samples were evaluated with reciprocating wear tester where AISI 52100 steel ball was used against the coated surface. In general most of the coated samples had poorer tribological performance, basically wear resistance, than the polymer itself. According to the author this was mostly attributed to the generation of hard abrasive particles due to the delamination of poorly adherent coating. Good results among the different coatings achieved with Ti/ZrN which friction coefficient was lower than the polysulfone substrate but the wear rate was still reported to be the same after 500 testing cycles. Cu coatings which also had good adhesion similar to Ti/ZrN achieved low friction coefficient and wear rate. Ti and Ti/TiN coatings mainly received higher friction coefficient values and wear rates than Cu and Ti/ZrN. No correlation between the friction coefficient and wear could be observed.

Zhitomirsky et al [30, 31] continued the previous study [29] of hard vacuum arc coatings on polysulfone substrate where process parameters were optimized. In the later studies the enhancement of adhesion of Ti layer was attributed to the formation of carbide between the polymer

surface and Ti intermediate layer. They achieved lower wear rates with Ti/TiN coatings than Ti/ZrN coatings which was opposite in the previous study. Furthermore the friction coefficient of Ti/ZrN was higher than in the previous study. The wear was measured with reciprocating wear measurement device similar to previous study but steel ball diameter was different. No correlation between the friction coefficient and wear could be observed from the results. It could be seen that when adhesion is enhanced the wear resistance is also be improved. It can be also seen that wear results of different studies are not reliably comparable. The crystal structure of the coating has major effect on its wear resistance. The Ti/TiN coating in their study was observed to have nanocrystalline structure to which was attributed the good wear resistance [30].

Riester et al [35] used a modified Taber abraser to evaluate the sliding wear resistance of magnetron sputtered TiN and TiC coatings on glass fibre and glass bead filled PBT (Polybutyleneterephthalate) and PA (Polyamide) substrates. The wear volume was calculated using the results from the liquid particle count analysis where the size range and composition of the particles removed from the surface was collected. Reportedly the major impact for the wear of the hard coated samples is not the adhesion of the coating to the substrate material, but the surface roughness of the polymer and also the produced coating since applying the thin hard film to the plastic substrate does not change the roughness of the surface. Surface roughness varies with different polymers and reinforced polymers. Lower surface roughness leads to the lower wear rate when adhesion is not the major wear mechanism in the wear process. The smooth surface in PBT was achieved with GB as a filling material.

Kälber et al [23] used a CALOTEST device to evaluate abrasive wear behavior of gas flow sputtered Ti-C:H films on PA substrate. They observed that wear resistance, measured as a volumetric loss, of this hard film strongly depends on the film structure when using ethine as a reactive gas. With lower titanium content the wear rate was higher, an effect which was not observed when methane was used as a reactive gas. Much lower wear rates were achieved with methane gas instead of ethine gas. The wear rate was the same with methane gas even though the titanium content of the film was varied between 20 to 60 at.%. Kälber et a also observed that high wear resistance of hard coating on PA substrate could be achieved without applying a substrate bias.

4 Characteristics affecting coating performance

There are many factors that have to be considered when producing a coating on polymers and polymer composites. The adhesion between the deposited film and substrate material is the most important characteristic when the coating is used to enhance the properties such as wear and corrosion resistance. Adhesion is a very complicated phenomenon and it will be handled here only in its basics. Real polymer-coating systems can be considered to form between three different layers which are the substrate surface, interface layer between the substrate and film, and film or coating layer. All of these have their effects on the performance of the polymer-coating system on their own and through the interactions between them.

4.1 Adhesion

4.1.1 Adhesion in general

Adhesion is very complex phenomena and there is no single theory which explains adhesion in comprehensive way. There are a number of different theories to explain adhesion by a purely mechanistic approach. Several physical and physico-chemical theories have been developed to include electrostatic theory, the diffusion theory, the adsorption and wetting theory and the theory of the Weak Boundary Layer (WBL) [4]. In the real polymer – metallic coating system, the understanding of bonding can be based on all of the above mentioned ideas.

Mechanical bonding

In mechanical bonding two surfaces are joined together so that one phase interlocks mechanically into another. Interlocking takes place in the pores and the uneven parts of the surface.

Chemical bonding

Chemical bonding can be divided to the following types:

- Metallic (homopolar) bonding
- Covalent (homopolar) bonding
- Ionic (heteropolar) bonding

In addition to above mentioned primary interatomic bond types there are secondary bond types which exist between the two interacting material:

- Hydrogen bonds
- Dipole – dipole interactions
- Dipole – induced dipole interactions
- Dispersion forces

In general these secondary bond forces are grouped and named as van der Waals forces. Van der Waals forces are generally much weaker than forces between primary bond types. Furthermore van der Waals forces are electrostatic in their nature [4]. Adhesion is also related to the distance between the two interacting materials. Intermolecular forces act over distances from 0.1 to 0.5 nm. If the nature of these forces is chemical the resulting energies range from 40 to 800 kJ/mol and if they are van der Waals forces the energies are limited to 40 kJ/mol or less [4].

4.1.2 Adhesion of atomistically deposited coatings on composite materials (polymers)

There are many factors that have to be considered for achieving good adhesion. In general good adhesion requires strong chemical bonding between the dissimilar atoms, a high fracture toughness of the materials in contact, low residual stress in the interfacial region and no degradation mechanism operating [1,p.594]. In sputtering deposition the depositing particles are having very high kinetic energy which is advantageous for adhesion [4]. Ion bombardment can also be used to build up charge sites to the surface of electrically insulating substrates which enhances nucleation of

adatoms (mobile atoms). Good adhesion to polymers can be achieved by using the film material that forms organo-metallic bonds with the substrate. These type of materials are Al, Cr or Ti [1,p.621].

Menningen et al. [6 ,26] reported that adhesion of electroless/electrolytic hard chrome coating system on CFRP (Carbon Fibre Reinforced Plastic) is mainly based on mechanical interlocking and van der Waals bonding. Mechanical roughening will produce interlocking surface sites and thus enhance adhesion of the electroless/electrolytic plated coating. It has also been reported that sand blasting of carbon fibre reinforced plastics improves the coating adhesion in sputtering deposition. This pretreatment must still proceed carefully so that carbon fibers are not exposed [4, p.163, 11]. Menningen et al were able to achieve over 20 MPa adhesive strength of the coating measured with pull-off test.

Ge et al. [10] studied adhesion strength of sputtered deposited copper on an epoxy substrate. They were able to achieve the pull strength of 5.6 MPa without any surface pre-treatment. In the same study the sputtered copper on a chemically etched epoxy surface achieved adhesion strength of 8.3 MPa and plasma pretreated with oxygen the strength of 11.5 MPa.

Martin [20] reported that main adhesion mechanism of sputtered Cr and NiCr on epoxy substrate is chemical adhesion. XPS study in the surface showed oxide formation between the epoxy and Cr. In the study adhesion was measured as a peel strength. Kraatz et al [24] noticed also that oxide formation is part of the adhesion mechanism for sputtered Cr and Ti on graphite-epoxy composites. They measured pull-off adhesion strength values for the Cr, Ti and Ni films on graphite-epoxy composite substrate 23.3 Mpa, 30.3 MPa and 25.5 MPa respectively. In the same study multilayer coating adhesion for Ni/Cr and Ni/Ti films were 13.6 MPa and 30.6 MPa respectively.

Kälber and Jung [23] studied hollow cathode type reactive gas flow sputtering on various types of polymers including polyamide (PA), polyetheretherketone (PEEK), epoxy resin (EP) and phenol formaldehyde resin (PF). The coatings successfully deposited were metallic, oxidic, nitridic, and carbidic films of titanium and chromium. Due to the relatively high coefficient of friction and counterbody wear, they focused on the deposition of metal containing amorphous hydrocarbon films (Me-C:H). Adhesion of Ti-C:H films on PA and PEEK measured with pull off test gave the values in range of 8 to 20 MPa.

Li et al [42] found out in their study where Ar, O₂ and O₂/CF₄ plasmas were used for the surface pretreatment prior to coating of Au films on polysiloxane based polymer, that pull of strength of Au films also increased respectively. The increased adhesion strength was attributed to increased surface roughness and wettability of the polymer surface.

4.1.3 Adhesion testing

There are a number of standardized adhesion testing methods that can be used to evaluate adhesive strength between coatings and substrates. Generally tests can be divided to quantitative and qualitative testing methods. In literature the terms practical adhesion and fundamental adhesion are also used to define nature of adhesion strength in concern. Usually the testing methods are destructive but also non-destructive methods are used. One of the non-destructive testing methods that gives information from the substrate-coating interface layer is acoustic emission. Mattox [1] stated "The best test of adhesion is functionality under processing, storage and service conditions", which is also true with other coating performance tests such as wear and corrosion tests. Table 4 describes most common standards for adhesion testing of thin films.

Table 4. Standard testing methods for adhesion testing of thin films [45-46].

Tets method	Standard	Description
Cross cut test	– SFS-EN ISO 2409	“Specifies a test method for assessing the resistance of paint coatings to separation from substrates when a right-angle lattice pattern is cut into the coating, penetrating through to the substrate. The method may be carried out as a "pass/fail" test or as a six-step classification test. Hard and soft substrates need a different test procedure. The property measured depends, among other factors, on the adhesion of the coating to either the preceding coat or the substrate.”[46]
Bend test	– ASTM D 4145-83 (2002)	“This test method describes a procedure for determining the flexibility and adhesion of organic coatings (paints) on metallic substrates that are deformed by bending when the sheet is fabricated into building panels or other products.” [45]
Pull-off test	– SFS-EN ISO 4624 (Description) – IEC68-2-14N [44], – ASTM D4541-02	“This International Standard describes methods for determining the adhesion by carrying out a pull-off test on a single coating or a multi-coat system of paint, varnish or related product. These test methods have been found useful in comparing the adhesion behaviour of different coatings. It is most useful in providing relative ratings for a series of coated panels exhibiting significant differences in adhesion.” [46]
Knife test	– ASTM D6677-01 [45]	“1.1 This test method covers the procedure for assessing the adhesion of coating films to substrate by using a knife. 1.2 This test method is used to establish whether the adhesion of a coating to a substrate or to another coating (in multi-coat systems) is at a generally adequate level.” [45]
Tape test	– ASTM D3359-02	“1.1 These test methods cover procedures for assessing the adhesion of coating films to metallic substrates by applying and removing pressure-sensitive tape over cuts made in the film. 1.2 Test Method A is primarily intended for use at job sites while Test Method B is more suitable for use in the laboratory. Also, Test Method B is not considered suitable for films thicker than 5 mils (125µm). “ [45]
Peel test	– ASTM B533-85 * (2004) (Description) – DIN 53494	“This test method gives two procedures for measuring the force required to peel a metallic coating from a plastic substrate. One procedure (Procedure A) utilizes a universal testing machine and yields reproducible measurements that can be used in research and development, in quality control and product acceptance, in the description of material and process characteristics, and in communications. The other procedure (Procedure B) utilizes an indicating force instrument that is less accurate and that is sensitive to operator technique. It is suitable for process control use.” [45].

Scratch adhesion test	<ul style="list-style-type: none"> - (G171-03) ** (Description), - prEN 1071-3:2000, - ASTM D2197-98 *** 	<p>“This standard describes laboratory procedures for determining the scratch hardness of the surfaces of solid materials. Within certain limitations, as described in this guide, this test method is applicable to metals, ceramics, polymers, and coated surfaces. The scratch hardness test, as described herein, is not intended to be used as a means to determine coating adhesion, nor is it intended for use with other than specific hemispherically-tipped, conical styli “ [45].</p>
--------------------------	---	--

*B533-85(2004) Standard Test Method for Peel Strength of Metal Electroplated Plastics [45].

**G171-03 Standard Test Method for Scratch Hardness of Materials Using a Diamond Stylus [45].

***ASTM D2197-98 (Reapproved 2002); Standard Test Method for Adhesion of Organic Coatings by Scrape Adhesion [45].

4.1.3.1 Other adhesion tests

Most of the wear test methods can also be used to evaluate adhesion at a practical level. Wear tests are discussed in Chapter 4.3.

4.2 Surface properties and modification of composites (and polymers) for enhancing the adhesion

Initial substrate surface is almost always pretreated prior to coating process. The purpose of pretreatment is to change the surface characteristics to be more favourable for the coating. The nature of change in the surface due to pretreatment can be chemical, morphological or physical. Surface cleaning is a critical procedure to remove the surface oil and solvent soluble contaminants like waxes and silicones before the coating procedure. This can be seen as a pretreatment of the surface at the most basic level. There are number of different pretreatment methods in use. The surface can be treated mechanically or chemically. The surface can be ground or sand blasted. Chemical etching in different solutions is used to roughen the surfaces as well. Surface activation can be used to increase the chemical reactivity of the surface. In general surface activation methods include plasma, wet chemical, corona, UV / ozone, flame, laser and activation pretreatments, and sputter cleaning [1,11,12, 14, 15, 16, 37, 42].

For good adhesion it is important that the interface material and near-surface material have high fracture toughness and no flaws that could act as a crack starting points under stress [1,p.594]. These factors should be considered when substrate materials are pretreated prior to deposition process.

Mechanical properties of the substrate are important for the coating performance in wear resistant films. Particularly with thin films the external load in certain application should be carried by substrate material. If the substrate material is brittle and fractures easily the adhesion between the film and the substrate could be low [1,p.59]. Hard coating on a soft substrate will not perform well if the support of the substrate does not exceed the external load.

Plasma treatment or plasma activation of polymers has shown improvements in coating adhesion strength. Plasma treatment can modify the surface by changing the surface chemistry causing texturing. This surface texturing can then improve the adhesion strength through mechanical interlocking [1,p.81]. Plasma treatment of polymer will also make the surface more chemically reactive which enhances the bonding and nucleation density by increasing the surface energy. The oxygen plasma is used for activating the polymer surfaces by oxidation. It forms carbonyl groups on the surface which make the surface more reactive with oxidizing metal atoms such as titanium, chromium and zirconium. Plasma treatment in nitrogen or ammonia turns polymer surface more basic and the surface is not conducive to reaction with oxidizing metals but will react with aluminum which is amphoteric [1,pp.62, 80]. Ge et al [10] also noticed in their study where plasma with oxygen was used that there is a certain treatment time after which the adhesion of sputtered deposited copper on epoxy will decrease. Reduced adhesion was explained to the formation of a weak boundary layer as a result of excessive treatment. Martin [20] noticed that O₂ plasma compared to Ar plasma used prior to sputtering deposition of Cu and Cr on epoxy gave better adhesion values.

Li et al [42] observed that there is no obvious change in surface topography after the Ar and O₂ plasma treatment of polysiloxane based polymer. However the surface roughness was significantly increased after plasma treatment in O₂/CF₄. The wettability of the polymer surface was improved by all of these plasmas. Ar plasma reduced the contact angle at the beginning but after 2 minutes treatment it remained in the same level whereas with O₂ plasma the contact angle dropped lower. The best result was carried out with O₂/CF₄ plasma which reduced contact angle from 81° to near 0° only in after 1 minute treatment.

Checchetto et al have studied hexagonal boron nitride (BN) on polycarbonate (PC) substrates. They observed significant improvement in adhesion by using N⁺- ion etching of the PC substrate prior to BN sputtering [21,22].

Ion implantation by ion beam as a pre-treatment method for polycarbonate has shown improvements in adhesion of Cr deposited layers. Ion irradiation will strengthen the polymer substrate surface to the level of the coating which will provide better stress distribution from the bulk material to the surface and avoid delamination [9]. Improvement in adhesion with sputtering cleaning of argon ions, also based on ion irradiation, was attributed to the change of the interfacial morphology [16].

Ge et al [10] used wet chemical etching and plasma treatment to enhance the coating adhesion on epoxy substrate. They found out that electrolessly deposited copper required sufficiently roughened surface for having good adhesion where sputtered copper achieved best adhesion on relatively smooth but oxygen-rich surface.

Adhesion can be increased by roughening the surface for having mechanical interlocking between the film and substrate [1,p.622]. In the atomistically deposited films mechanical treatment such as blasting might also weaken the adhesion due to the lowered contact area and increased amount of voids in the roughened surface. Therefore the control of surface roughness and the characteristics of deposition process to reduce this roughness and voids are very important to the development of good adhesion. It is essential to notify that for achieving the maximum film adhesion through the mechanical interlocking the deposited film must fill-in the surface roughness [1,p.67].

4.3 Interface formation between coating and substrate (near surface) material

In real polymer-metallic or alloy coating systems the interface formation between the substrate (near surface) and depositing film is important in order to achieve good adhesion and furthermore good performance of coating. In this interfacial region the material can be called interface material which has different characteristics from substrate and coating. In literature the interfacial regions are categorized as follows depending on interactions between substrate and depositing film material; *Abrupt and mechanical interlocking, diffusion, compound, pseudodiffusion, reactively graded and a combination of these* [1,p.459]. Abrupt and mechanical interlocking interfaces differ with the nature of substrate surface. An abrupt interface is formed in smooth surfaces where mechanical interlocking exists in rough surfaces. In a diffusion interface, substrate and the film material are lightly mixed without having any compound formation whereas a compound interface consists of a chemical compound of the substrate and the film material due to the chemical reaction between them [1,p.459-464].

Interfacial region composition of sputtered Titanium nitride films on polymers (PBT) has been studied due to its importance in adhesion. Riester et al studied in their work the effects of plasma pretreatment and r.f. etching plasma bias power to the interface composition. It was found that in the deposited film without any presputtering etching, the chemistry of titanium changes across the film layer and the amount of oxidized titanium is higher in the interface than in the coating. This was ascribed to result from the oxygen coming from the substrate. Riester et al [ref] also found that when using Ar and O₂ plasma for pretreatment of polymer substrate, there is only small dependence on etching bias power of the elemental composition of the interface. Nevertheless a remarkable change between in the elemental concentrations can be found when using N₂ plasma with different bias powers for pretreatment. Oxygen concentration in the coating is mainly releasing from the substrate and the concentration can be modified with plasma etching [17,18].

Knaatz et al studied metal films on graphite-epoxy composites. Auger electron spectroscopy (AES) profiling indicated that adhesion mechanism for Cr and Ti might involve oxidation of these metals [24]. The adhesion will be formed partly due to covalent bonding.

Zhitomirsky and Grimberg et al observed also carbide formation in addition of oxide formation of Ti on polysulfone substrate. Titanium was vacuum arc deposited on to a polysulfone substrate prior to ZrN and TiN films. Carbide formation in the interface layer with Ti and Nb was suggested to improve the adhesion of complete coating system [29-31].

4.4 Coating materials and composition

There is large variety of wear and corrosion resistant films that can be deposited on polymers. In the following some of these materials deposited on polymers are presented. The materials mentioned here covers the films that has been deposited by PVD, PACVD, ion plating (IBAD), electroless/electrolytic plating, thermal spraying, Sol-gel technique, and vacuum arc deposition.

Metal coatings

Metals: Ag, Al, Au, Cu, Cr, Ti, Ni, Pd, Pt, Ta, V, [9 -13 15, 16, 20, 24, 36]

Multilayer metal coatings: Ni/Cr, Ni/Ti, Ni(EP)/Ni/Cr, Ni(EP), TaCr [24]

Electroless/electrolytic plating: Cu, Ni, Cr [6, 26, 37, 49]

Low friction wear resistant coatings:

Diamond-like carbon (DLC) coatings, a-C, Me-C:H, a-C:H, [23, 32, 39, 41]

- a-C (amorphous hydrogen free hard carbon)
- a-C:H (amorphous DLC films)
- Me-C:H (Metal-containing hydrocarbon), Me can be Ti, W, Cr

Lubricating coatings

MoS₂ [41, 48]

Hard coatings / Ceramic coatings

h-BN (hexagonal boron nitride) [22]

TiN, Ti/TiN, TiO₂ [17, 18, 32-34, 36, 51]

TiAlN, TiCN [41]

Cr-Al-N [47]

Bilayers Ti/TiN, Ti/ZrN, Al/ZrN, Al/TiN, Zr/TiN, Zr/ZrN [29, 30,32]

Multilayer ceramic coatings: Ti_{0.5}Al_{0.5}N/CrN [28].

WC/10Co/4Cr, NiCrBSi, [7]

Chromium oxide [7]

REFERENCES

- [1] D. M. Mattox, Handbook of PVD Processing, Noyes Publications, 1998
- [2] Olli Saarela, et al. Komposiittirakenteet, Muoviyhdistys ry, 2003 Helsinki.
- [3] ASM, Engineered materials handbook, Vol. 1, Composites, 1987
- [4] R. Suchentrunk, Metallizing of plastics – A Handbook of theory and practice, Finishing Publications Ltd., 1993.
- [5] Larry Rupprecht, Conductive Polymers and Plastics in Industrial Applications, Plastics Design Library, 1999. ISBN 1-884207-77-4.
- [6] M. Menningen, et al. Application of fracture mechanism to the adhesion of metal coatings on CFRP, Surface and Coatings Technology, 1995, vol. 77-78, p.835-840.
- [7] Gordon England website, <http://www.gordonengland.co.uk/frpapp.htm>, accessed 31.12.2004.
- [8] William D. Callister, Material Science and Engineering, An Introduction, 2003. ISBN 0-471-22471-5.
- [9] L. Guzman, et al. Hard coating adhesion on ion implanted polymer surfaces, Thin Solid Films, 2000, vol.377-378, p.760-765.
- [10] J. Ge, et al. Surface modification and characterization of photodefinable epoxy/copper systems, Thin Solid Film, 2003, vol.440, p.198-207.
- [11] K. De Bruyn, et al. Study of pretreatment methods for vacuum metallization of plastics, Surface and Coatings Technology, 2003, vol.163-164, p.710-715.
- [12] D. Schröer, et al. Pretreatment of polymer surfaces – the crucial step prior to metal deposition, Electrochimica Acta, 1995, vol.40, no.10, pp.1487-1494.
- [13] R. Beydon, et al. Measurement of metallic coatings adhesion on fibre reinforced plastic materials, Surface and Coatings Technology, 2000, vol.126, pp.39-47.
- [14] W. Petasch, et al. Improvement of the adhesion of low-energy polymers by a short-time plasma treatment, Surface and Coatings Technology, 1995, vol.74-75, pp.682-688.
- [15] R. Weichenhain, et al. KrF-excimer laser pretreatment and metallization of polymers, Applied Surface Science, 1997, vol.109/110, pp. 264-269.
- [16] Yasushi Fujinami, et al. Effect of sputtering-cleaning on adhesion of the metallic films to polymer substrates, Journal of Materials Chemistry and Physics, 1998, vol. 54, pp. 102-105.
- [17] M. Riester, et al. Composition of the interface region of sputtered titanium nitride thin films on thermoplastic polymers, Surface and Coatings Technology, 1999, vol. 116-119, pp. 1179-1182.
- [18] M. Neuhäuser, et al. Optical emission spectroscopy studies of titanium nitride sputtering on thermoplastic polymers, Surface and Coatings Technology, 1999, vol. 116-119, pp.981-985.

- [19] A. Pegoretti, et al. Thermomechanical behavior of interfacial region in carbon fibre/epoxy composites, *Journal of Composites*, 1996, part A 27 A, pp.1067-1074.
- [20] Lara j. Martin and C. P. Wong. Chemical and mechanical adhesion mechanisms of sputter-deposited metal on epoxy dielectric for high density interconnect printed circuit boards, *IEEE Transactions on components and packaging technologies*, 2001, vol. 24, no.3, pp. 416-424.
- [21] R. Checchetto, et al. Structure and optical properties of boron nitride thin films deposited by radio-frequency sputtering on polycarbonate, *Journal of Physics Condensed Matter*, 2000, vol. 12, no.44,pp.9215-9220.
- [22] R. Checchetto, et al. BN coating adhesion on ion-implanted polymer surfaces, *Thin Solid Films*, 2001 vol.398-399, pp. 222-227.
- [23] T. Kälber, T. Jung. A novel low-cost process for the deposition of metallic and compound thin films on plastics, *Surface and Coatings Technology*, 1998, vol. 98, pp. 1116.1120.
- [24] P. Kraatz, et al. Auger depth profiles and stud pull adhesion of metal films on graphite-epoxy composites, *Thin Solid Films*, 1997, vol. 308-309, pp. 375-381.
- [25] A.P. Harsha and U.S. Tewari. Tribological studies on glass fiber reinforced polyetherketone composites, *Journal of Reinforced Plastics and Composites*, 2004, vol. 23, pp. 65-82.
- [26] M. Menningen, et al. Metallic wear resistant coatings for carbon fibre epoxy composite rolls, *Surface and Coatings Technology*, 1995, vol. 71, pp. 208-214.
- [27] Corrosion doctors website, <http://www.corrosion-doctors.org>., accessed 9.1.2005.
- [28] Peter Panjan, et al. Deposition and characterization of Ti_{0.5}Al_{0.5}N/CrN multilayer coatings sputtered at low temperature, *Journal of Materiali in Tehnologije (Slovenia)*, 2003, vol. 37(3-4), pp. 123-128.
- [29] I. Grimberg, et al. Structure and tribological properties of thin vacuum arc coatings on polysulfone, *J Surface and Coatings Technology*, 1997, v. 94-95, pp. 213-219.
- [30] V.N. Zhitomirsky, et al. Vacuum arc deposition of metal/ceramic coatings on polymer substrates, *Surface and Coatings Technology*, 1998, vol. 108-109, pp. 160-165.
- [31] V.N. Zhitomirsky, et al. Vacuum arc deposition of conductive wear resistant coatings on polymer substrates, *Surface and Coatings Technology*, 1999, vol. 120-121, pp. 373-377.
- [32] B.B. Straumal, et al. Vacuum arc deposition of protective layers on glass and polymer substrates, *Thin Solid Films*, 2001, vol. 383, pp. 224-226.
- [33] E. Lugscheider, et al. Magnetron-sputtered hard material coatings on thermoplastic polymers for clean room applications, *Surface and Coatings Technology*, 1998, vol. 108-109, pp. 398-402.
- [34] E. Lugscheider, et al. Magnetron sputtered titanium nitride thin films on thermoplastic polymers, *Surface and Coatings Technology*, 1999, vol. 116-119, pp. 1172-1178.

- [35] M. Riester, et al. Taber abraser/liquid particle count coupling for the determination of sliding wear of metallized plastics, *Surface and Coatings Technology*, 1997, vol. 97, pp. 649-655.
- [36] M. Riester, et al. Morphology of sputtered titanium nitride thin films on thermoplastic polymers, *Surface and Coatings Technology*, 1999, vol. 116-119, pp. 1001-1005.
- [37] M. Charbonnier and M. Romand. Polymer pretreatments for enhanced adhesion of metals deposited by the electroless process, *Journal of Adhesion and Adhesives*, 2003, vol. 23, pp. 277-285.
- [38] M. Riester, et al. Physical vapor deposited thin hard films on polymers: sample preparation for SEM analysis, *Journal of Adhesion Science and Technology*, 1999, vol. 13, pp. 963-971.
- [39] N.K. Cuong, et al. Diamond-like carbon films deposited on polymers by plasma-enhanced chemical vapor deposition, *Surface and Coatings Technology*, 2003, v. 173-174, pp. 1024-1028.
- [40] H. Kupfer and G.K. Wolf. Plasma and ion beam assisted metallization of polymers and their application, *Nuclear Instruments and Methods in Physics Research*, 2000, vol. B 166-167, pp. 722-731.
- [41] H. Meerkamm, et al. Mechanical and tribological properties of PVD and PACVD wear resistant coatings, *Journal of Refractory Metals and Hard Materials*, 1999, vol. 17, pp. 201-208.
- [42] W.T. Li, et al. Significant improvement of adhesion between gold thin films and a polymer, *Journal of Applied Surface Science*, 2004, vol. 233, pp. 227-233.
- [43] T. P. Chou and G. Cao. Adhesion of sol-gel-derived organic-inorganic hybrid coatings on polyester, *Journal of Sol-Gel Science and Technology*, 2003, vol. 27, pp. 31-41.
- [44] M.P.K. Turunen, et al. Pull-off test in the assessment of adhesion at printed wiring board metallisation/epoxy interface, *Journal of Microelectronics Reliability*, 2004, vol. 44, pp. 993-1007.
- [45] ASTM website, www.astm.org, accessed 11.1.2005.
- [46] The Finnish Standards Association SFS website, www.sfs.fi, accessed 11.1.2005.
- [47] M. Brizuela, et al. Magnetron sputtering of CrN coatings with additions of aluminium: Mechanical and tribological study, Ninth International Conference on Plasma Surface Engineering, 2004, Poster presentation ThP18.
- [48] P. Tunturi. Metallien pinnoitteet ja pintakäsittelyt, MET 3/99, Metalliteollisuuden keskusliitto.
- [49] J. Siivinen and A. Mahiout. Hiilikuitukomposiittien pinnan ominaisuuksien parantaminen. Luottamuksellinen tutkimusraportti (Confidential Research Report), 2004, VTT.
- [50] K.L. Mittal, Editor. *Metallized Plastics 2: Fundamental and Applied Aspects*, 1991, Plenum Press, New York.
- [51] O. Knotek and F. Löffler. Magnetron sputtered TiN hard coatings on plastics, *Metallized Plastics 2. Symposium Proceeding*, 1991.

[52] Th. Flottmann and W. Lohmann. Ion beam assisted metallization of plastics, Metallized Plastics 2. Symposium Proceeding, 1991.

[53] R.J. Crawford. Plastics Engineering, third edition, 1998, Butterworth-Heinemann, Oxford. ISBN 0 7506 3764 1.

[54] A. Hozumi, et al. Two-layer hard coatings on transparent resin substrates for improvement of abrasion resistance, Surface and Coating Technology, 1996, vol. 82, pp. 16-22.

[55] Seppo Kivioja, et al. Tribologia – kitka, kuluminen ja voitelu. Kolmas korjattu painos, 1997, Helsinki. ISBN 951-672-307-1.

[56] MatWeb, Material property data website, www.matweb.com, accessed 19.1.2005.